Dissertation

submitted to the

Combined Faculties for the Natural Sciences and for Mathematics

of the Ruperto-Carola University of Heidelberg, Germany

for the degree of

Doctor of Natural Sciences

Presented by

MSc Arianna Lockhart

Born in: Milan, Italy

Oral examination: 20th February 2018

Investigating the role of RNase H enzymes in the regulation of telomeric R-loops during replicative senescence

Referees:

Prof. Dr. Michael Knop

Prof. Dr. Brian Luke

Table of Contents

Table of Contents

Table of Contents

Table of Contents

List of Publications

Lafuente-Barquero, J.*, Luke-Glaser, S.*, Graf, M.*, Silva S., Gómez-González, B., **Lockhart, A.**, Lisby, M., Aguilera, A., Luke, B. The Smc5/6 complex regulates the yeast Mph1 helicase at RNA-DNA hybrid-mediated DNA damage. *PLoS Genetics*, in press.

Graf, M.*, Bonetti, D.*, **Lockhart, A.***, Serhal, K., Kellner, V., Maicher, A., Jolivet, P., Teixeira, M.T., and Luke, B. (2017). Telomere Length Determines TERRA and R-Loop Regulation through the Cell Cycle. *Cell 170*, 72-85 e14.

Maicher, A., **Lockhart, A**., Luke, B. (2014). Breaking new ground: digging into TERRA function. *Biochimica et Biophysica Acta 1839*, 387-394.

*: shared first-authorship

Summary

Telomeres are nucleoprotein structures that protect and maintain the ends of eukaryotic linear chromosomes. Telomeres shorten at each round of DNA replication due to the end replication problem. The enzyme telomerase, by adding telomeric repeats to chromosome ends, can counteract this process. In the absence of telomerase, telomeres progressively shorten until they reach a critical length that activates the DNA damage response, thereby halting the cell cycle in a condition referred to as replicative senescence. Telomeres are transcribed into a long, non-coding RNA dubbed TERRA, which can hybridize with its template strand, thereby forming R-loops at *S. cerevisiae* and human telomeres. Recent data implicate telomeric R-loops in the promotion of homologous recombination at telomeres, leading to telomere lengthening events which can partially compensate for telomere shortening in the absence of telomerase. Telomeric R-loops are regulated by RNase H1 and H2 enzymes, which can degrade the RNA moiety of RNA-DNA hybrids. While the accumulation of telomeric R-loops in cells lacking both enzymes delays senescence onset by promoting homologous recombination at telomeres, the depletion of telomeric R-loops by overexpressing RNase H1 leads to premature senescence onset.

This PhD thesis aims to better understand how telomeric R-loops are regulated especially during replicative senescence in *S. cerevisiae*. We found that RNase H2 localizes to long telomeres and physically interacts with the telomere-associated protein Rif2, which is required for RNase H2 recruitment to telomeres. Accordingly, in the absence of Rif2 telomeric R-loops accumulate, indicating that Rif2 and RNase H2 play a pivotal role in restricting R-loops at long telomeres. Importantly, the interaction between RNase H2 and Rif2 is strongest in late S phase, which is reflected in the degradation of telomeric R-loops in this time frame. We propose that this cell cycle regulated telomeric R-loop degradation is required to avoid collisions of the replication machinery, which replicates long telomeres in late S phase, with R-loops, an event that could have detrimental effects on telomere stability.

It was previously shown that, as telomeres shorten, Rif2 localization to telomeres is diminished. We show that decreased Rif2 association to short telomeres leads to impaired recruitment of RNase H2, which is functionally reflected in the accumulation of R-loops at

short telomeres. Moreover, while RNase H1 could not be detected at long telomeres, we observed its localization to short telomeres, thereby indicating a distinct requirement for the RNase H enzymes. By analyzing the effect of single RNase H enzymes deletion on the kinetics of senescence onset in telomerase negative cells, we revealed an opposing effect of the two enzymes, suggesting that, differently from what was proposed, RNase H enzymes do not have redundant functions at telomeres. In conclusion, we propose that, while at long telomeres R-loops are timely regulated by Rif2-RNase H2 to avoid collisions with the replication machinery, at short telomeres R-loops are allowed to accumulate, thereby promoting homologous recombination-mediated telomere extension.

Zusammenfassung

Telomere sind Nukleoprotein-Strukturen, welche die Enden linearer Chromosomen in eukaryotischen Organismen schützen und erhalten. Aufgrund des „Endreplikationsproblems“ verkürzen sich die Telomere mit jedem Replikationszyklus. Das Enzym Telomerase kann diesem Verkürzungsprozess entgegenwirken, indem es repetitive telomerische Sequenzen an Chromosomenenden ergänzt. In Abwesenheit von Telomerase verkürzen sich Telomere fortschreitend bis hin zu einer kritischen Länge, was zur Aktivierung der zellulären Antwort auf DNA Schäden führt. Daraufhin bleibt die Zelle im Zellzyklus stehen, genannt replikative Seneszenz.

Telomere werden in eine lange nicht-kodierende RNA transkribiert, die als TERRA bezeichnet wird. TERRA-RNA kann mit der telomerischen DNA einen RNA-DNA-Hybrid formen und dabei sogenannte R-Loops an den Telomeren von Human- und Hefezellen (*S. cerevisiae)* bilden. Telomerische R-Loops unterstützen die homologe Rekombination an Telomeren, was zu deren Verlängerung führen kann und so ihre Verkürzung in Abwesenheit von Telomerase teilweise ausgleicht. Die Enzyme RNase H1 und H2 regulieren telomerische R-Loops, indem sie den RNA-Anteil von RNA-DNA-Hybriden abbauen. In Zellen, denen diese beiden Enzyme fehlen, reichern sich R-Loops an Telomeren an und verzögern den Seneszenzbeginn, indem sie homologe Rekombination an Telomeren begünstigen. Im Gegensatz dazu kommt es zu verfrühtem Seneszenzbeginn, wenn RNase H1 überexprimiert wird.

Diese Doktorarbeit charakterisiert wie telomerische R-Loops reguliert werden, vor allem während der replikativen Seneszenz in *S. cerevisiae.* Wir zeigen hier, dass RNase H2 an lange Telomere lokalisiert und mit dem Telomer-assoziierten Protein Rif2 interagiert, was für die Rekrutierung von RNase H2 zu Telomeren notwendig ist. Dementsprechend reichern sich telomerische R-Loops in Abwesenheit von Rif2 an. Damit spielt RNase H2 eine entscheidende Rolle in der Begrenzung von R-Loops an langen Telomeren. Die Interaktion zwischen RNase H2 und Rif2 ist in der späten S-Phase des Zellzyklus am stärksten, was sich darin widerspiegelt, dass telomerische R-Loops in dieser Zeitspanne abgebaut werden. Wir nehmen an, dass der regulierte Abbau von telomerischen R-Loops während des Zellzyklus nötig ist, um Zusammenstöße des Replikationsapparats, der

lange Telomere in der späten S-Phase repliziert, mit R-Loops zu verhindern. Zusammenstöße dieser Art könnten sich schädlich auf die Stabilität von Telomeren auswirken.

Es wurde bereits gezeigt, dass die Lokalisierung von Rif2 an Telomere stark vermindert ist, wenn sie sich verkürzen. Wir haben herausgefunden, dass die verringerte Lokalisierung von Rif2 an kurze Telomere dazu führt, dass die Rekrutierung von RNase H2 beeinträchtigt ist. Dies verursacht die Anreicherung von R-Loops an kurzen Telomeren. Außerdem konnten wir RNase H1 nicht an langen Telomeren nachweisen, während das Enzym mit kurzen Telomeren assoziiert, was auf unterschiedliche Anforderungen an die beiden RNase H Enzyme hindeutet. Durch die Untersuchung von Gendeletionen einzelner RNase H Enzyme auf die Kinetik des Seneszenzbeginns konnten wir gegensätzliche Effekte der beiden Enzyme nachweisen. Dies deutet darauf hin, dass die RNase H Enzyme – anders als bisher angenommen – keine redundanten Funktionen an Telomeren haben. Zusammenfassend nehmen wir an, dass R-Loops an langen Telomeren von Rif2 und RNase H2 reguliert werden müssen, um Zusammenstöße mit der Replikationsmaschinerie zu vermeiden. An kurzen Telomeren hingegen können sich R-Loops anreichern, um deren Verlängerung mittels homologer Rekombination zu unterstützen.

1. Introduction

1.1 Telomeres and their function

Telomeres are indispensable nucleoprotein structures that provide a distinction between the ends of linear chromosomes and the ends of double strand breaks (DSBs), a function referred to as capping. They thereby protect the physical ends of eukaryotic chromosomes from degradation, fusions and recombination. Furthermore, telomeres are essential to solve the end replication problem, preventing sequence loss at each replication round. The work presented in this thesis was carried out in the budding yeast *Saccharomyces cerevisiae*, which therefore will be the main focus of the introduction on telomeres.

1.1.1 Telomere structure and telomeric proteins

In budding yeast, telomeres are made of 300 ± 75 base pairs (bp) of simple $C_{1-3}A/TG_{1-3}$ double stranded (ds) repeats that end in a 3' single stranded (ss) G-rich overhang (G-tail; Figure 1A). The G-tail is 12-15 nucleotides (nt) long during most of the cell cycle but 30-100 nt long in late S/G2 phases (Larrivee et al., 2004; Wellinger et al., 1993) due to telomerase-mediated addition of telomeric repeats to the G-tail but also regulated degradation of the opposite strand (C-strand)(Dionne and Wellinger, 1998; Frank et al., 2006).

S. cerevisiae telomeres are bound by highly specialized proteins, which orchestrate all telomere-related processes (Figure 1B). Telomeric double stranded repeats are bound in a sequence-specific manner by Rap1. *In vitro* data indicates that one Rap1 molecule binds every 18 bp, suggesting that a telomere of normal length would be bound by 15-20 Rap1 molecules (Gilson et al., 1993). Rap1 function is not restricted to telomeres, as it is also involved in transcription activation and repression at multiple loci in the genome (Shore and Nasmyth, 1987). The C-terminus of Rap1 is required for the recruitment of Rif1/Rif2 and Sir3/Sir4 to telomeres, which compete with each other for Rap1 binding (Moretti et al., 1994). The single stranded G-tail is bound by Cdc13, which in turn recruits Stn1 and Ten1, thereby forming the CST complex. The CST complex has been dubbed "telomeric

RPA" due to its resemblance to the trimeric single stranded DNA (ssDNA) biding complex, RPA (Gao et al., 2007). Cdc13 has been proposed to outcompete RPA for G-tail binding due to its high affinity and sequence specificity for telomeric repeats, although RPA can be detected at telomeres especially in S phase, when the G-tail is longest (Anderson et al., 2002; Schramke et al., 2004). A Cdc13 minimum binding site is made up of 11 nt of telomeric repeats (Hughes et al., 2000), suggesting that during most of the cell cycle only one CST complex molecule is bound to each telomere. Finally, Yku70 and Yku80, which form the Yku complex, also bind telomeres although in a sequence-unspecific manner (Gravel et al., 1998). Yku binds at the border between telomeric repeats and subtelomeres as well as at internal telomeric repeats (Larcher et al., 2016), and was reported to be able to bind directly to the telomeric DNA but also to localize to telomeres additionally via protein-protein interaction with Sir4 (Martin et al., 1999; Roy et al., 2004).

Centromere-proximal to telomeres are gene-poor regions referred to as subtelomeres. In *S. cerevisiae*, all subtelomeres contain the so-called X element, while about half of the subtelomeres additionally contain Y' elements that always lie between the X element and the telomeric repeats (Chan and Tye, 1983a). While X elements vary in sequence and size and are always present in single copy at each telomere, Y' elements can either be 6.7 kb (kilobases; Y' long) or 5.2 kb (Y' short) long and can be present in zero to four tandem copies (Chan and Tye, 1983a); both X and Y' elements contain potential autonomously replicating sequences (ARS; Figure 1A)(Chan and Tye, 1983b) and binding sites for the transcription factor Tbf1 (Brigati et al., 1993; Koering et al., 2000). Often, short tracts of telomeric repeats are found between X-Y' and Y'-Y' elements (Walmsley et al., 1984).

While telomeric repeats are presumably nucleosome free, *S. cerevisiae* subtelomeres are organized in nucleosomes (Wright et al., 1992) and are characterized by heterochromatin formation, causing the silencing of genes that lie near the telomeres, a phenomenon referred to as telomere position effect (TPE)(Gottschling et al., 1990). Telomeric heterochromatin formation is established by the Sir2-4 complex, which localizes to telomeres by Sir3/Sir4 interaction with Rap1 (Aparicio et al., 1991), but also by Sir4 interaction with the Yku complex (Boulton and Jackson, 1998). Sir2 is a histone deacetylase which preferentially targets H3 and H4 (Imai et al., 2000), and TPE spreads

for kilobases from telomeres thanks to the interaction of Sir3 and Sir4 with deacetylated H3 and H4 (Hecht et al., 1996; Strahl-Bolsinger et al., 1997).

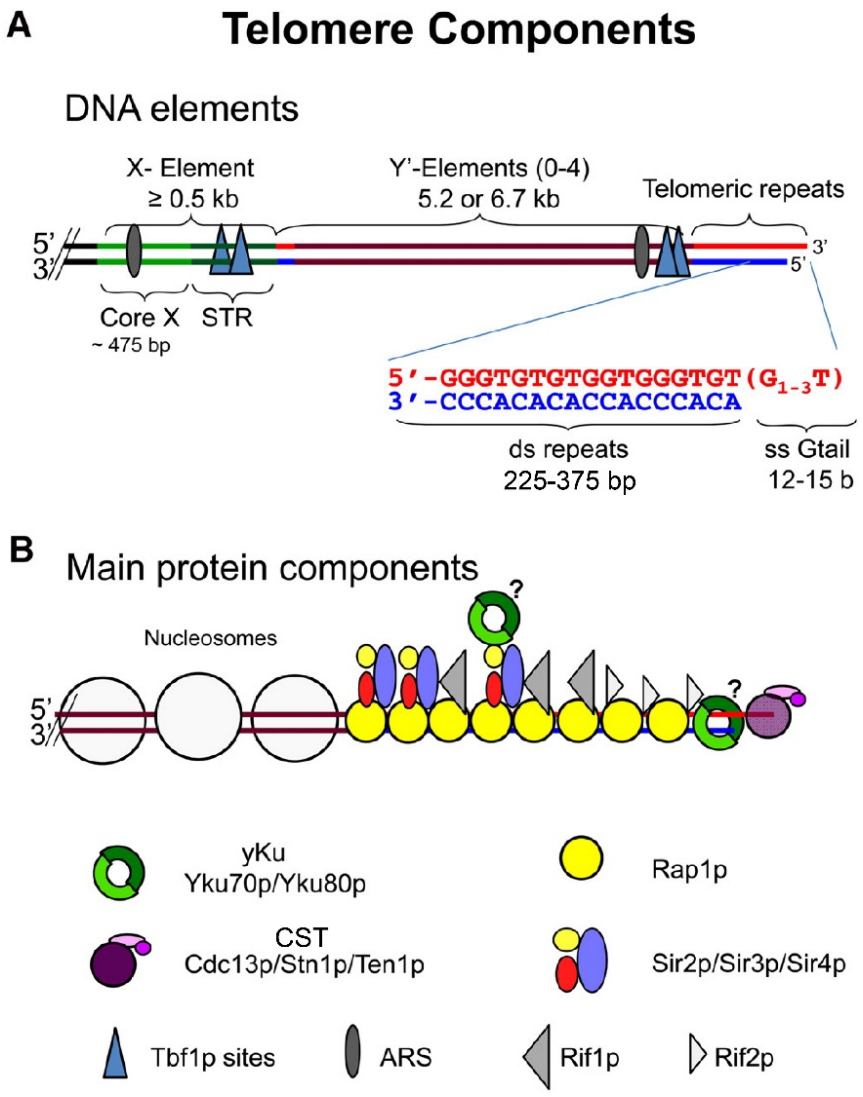

Figure 1. Telomere structure and associated proteins.

A) Telomeric DNA composition. *S. cerevisiae* telomeres are composed of 300 ± 75 ds repetitive sequences which end in a ss 3' G-tail of 12-15 bases. Subtelomeric sequences located on the centromere-oriented side of telomeres always contain an X element and 0-4 copies of Y' elements, often separated by short tracts of telomeric repeats. X elements bear a core X element and subtelomeric repeated elements (STR), and are of heterogeneous length; Y' elements can be long or short (5.2 - 6.7 kb). Both X and Y' elements contain Tbf1 binding sites and an ARS. **B**) Telomere binding proteins. The G-tail is bound by the CST complex and the ds telomeric repeats are bound by Rap1, which in turn recruits either Rif1 and Rif2 or Sir2-4. Rif2 binds more towards the distal tip of the telomere, while Rif1 more at the centromere-proximal part. The yKu complex was proposed to bind independently at the border between ss and ds telomeric repeats, but also localize to telomeres by interacting with Sir4. The subtelomere is organized in nucleosomes. Modified from (Wellinger and Zakian, 2012).

Telomeres cluster in three to eight foci at the nuclear periphery (Gotta et al., 1996; Palladino et al., 1993) and are anchored to the nuclear envelope by two redundant pathways, established by Sir4 and Yku80 (Schober et al., 2009; Taddei et al., 2004). These telomeric foci are enriched in Sir proteins and are repressive for transcription and subtelomeric recombination (Schober et al., 2009; Taddei et al., 2009).

1.1.2 End protection

The ends of linear chromosomes structurally resemble the ends of DSBs and therefore could be mistakenly recognized by the cell as such. An essential function that telomeres provide is the capping of the ends of linear chromosomes, thereby preventing unwanted repair activities. DSBs can be repaired by two pathways: non-homologous end joining (NHEJ) and homologous recombination (HR). NHEJ is prevalent in G1 and directly re-joins the two extremities of a break in a fast but error-prone manner; a critical player in this process is the Yku complex (Lieber, 2010). Alternatively, the ends of the DSB can be resected by nucleases in order to generate single stranded overhangs that can invade homologous sequences and use them as a template to repair the break. HR depends on the MRX complex (made up of Mre11, Rad50 and Xrs2) and the Rad52 epistasis group, and is active in S and G2, when a homologous sequence is present in the sister chromatid (San Filippo et al., 2008). Both pathways are inhibited at telomeres: NHEJ especially would result in catastrophic end-to-end chromosome fusions, while HR would result in recombination between telomeres. Additionally, capping of telomeres also prevents the activation of the checkpoint response, which is triggered by free DNA ends; in yeast, the major checkpoint kinases are Mec1 (homolog of human ATR) and Tel1 (homolog of human ATM). Loss of a single telomere in budding yeast, and thereby loss of capping, leads to the activation of a Rad9-dependent checkpoint (Sandell and Zakian, 1993), highlighting the active discrimination between functional telomeres and broken DNA ends by the checkpoint machinery. The capping of telomeres is accomplished by multiple players that will be described in the next paragraphs.

As a first barrier, the single-stranded telomeric G-tail is shielded by the CST complex (Grandin et al., 2001). All components of the CST complex are essential, and loss of CST

function has been primarily studied by exposing *cdc13-1* mutants to restrictive temperature, which results in resection of the C-strand for many kb and Rad9-dependent (Mec1 mediated) G2/M checkpoint activation (Garvik et al., 1995; Weinert and Hartwell, 1993). Thereby, the CST complex is essential in preventing resection and activation of the checkpoint at telomeres.

On the other hand, also the Rap1-Rif1-Rif2 complex that localizes to the double stranded telomeric DNA plays an important role in capping. Rap1, Rif2 and to a lesser extent Rif1 inhibit telomere fusions by NHEJ and end resection (Bonetti et al., 2010; Marcand et al., 2008; Vodenicharov et al., 2010). Additionally, Rif2 inhibits localization of Tel1 and MRX to telomeres, thereby preventing Tel1-mediated checkpoint activation (Bonetti et al., 2010; Hirano et al., 2009). Rif1 can promote viability when Cdc13 capping function is compromised by preventing ssDNA formation and checkpoint activation at these telomeres (Addinall et al., 2011; Anbalagan et al., 2011).

Lastly, the Yku complex provides capping function in G1 by inhibiting resection, although in this phase it would happen at such low levels that the DNA damage checkpoint would not be activated (Bonetti et al., 2010; Vodenicharov et al., 2010).

1.1.3 End replication

Telomeres are subjected to the end replication problem, as the canonical replication machinery, while capable of continuously replicating the leading strand in its entirety, causes the loss of genetic material from the lagging strand at each replication round after the removal of the last Okazaki fragment primer (Watson, 1972). The need for a special mechanism to replicate chromosome ends is thereby intrinsic to the process of semi-conservative DNA replication, as very early stated by Watson. This calls for the need of an additional mechanism to avoid loss of genetic information in most unicellular organisms and stem cells. The answer comes from the enzyme telomerase, a reverse transcriptase which is capable of adding telomeric repeats to 3’ single stranded telomeric ends, in a process that will be described in Section 1.2.1.

In a recent work, the Teixeira lab demonstrated that replication-driven telomere shortening arises from distinct processing of leading and lagging strands at each replication cycle (Figure 2; (Soudet et al., 2014)). As previously postulated, the shortening of the lagging strand telomere is indeed determined by the position of the last Okazaki fragment, which they observed to be always located at the very end of telomeric repeats, thereby leaving only a 5-10 nt gap after Okazaki primer degradation. On the other hand, replication of the leading strand creates a blunt end, which needs to be further processed to generate a 3' single stranded G-tail. This nucleolytic processing occurs after telomere replication, and is mediated by Tel1 and, likely, MRX. End-processing creates a G-tail overhang of about 40 nt, and is followed by fill-in synthesis of the C-strand, again accomplished by positioning the last Okazaki fragment at the very end and leaving a gap of 5-10 nt. This model is consistent with the measured approximate rate of telomere shortening of 2.5-5 nt per replication (Marcand et al., 1999; Singer and Gottschling, 1994).

In addition to telomerase action, the bulk of telomere replication is accomplished by the canonical replication machinery. Telomere replication is initiated at replication origins proximal to telomeres or by the ARS contained in Y' and X elements, although some X elements' ARS are inactive (Louis and Vershinin, 2005). Importantly, the timing of telomere replication, which directly correlates with origin firing, is dictated by telomere length: while telomeres of wild type length replicate in late S phase (McCarroll and Fangman, 1988; Raghuraman et al., 2001), short telomere replication is anticipated to early S phase (Bianchi and Shore, 2007). Rif1 is involved in preventing early firing of telomeric origins, as *rif1* mutants, despite having extended telomeres, replicate early (Lian et al., 2011). Tel1, which binds to short telomeres (Sabourin et al., 2007), was shown to act upstream of Rif1 in regulating telomeric origin firing, and to phosphorylate Rif1 at short telomeres, although preventing this event is not sufficient to inhibit early replication of short telomeres (Sridhar et al., 2014). Consistently, *tel1* mutants, which have short telomeres, replicate late (Sridhar et al., 2014).

Telomere replication and telomerase action are tightly regulated, as will be described in Section 1.2.1, and early replication of short telomeres might promote telomerase recruitment and action, as Cdc13 and Est1 recruitment to short telomeres occurs in early S phase (Bianchi and Shore, 2007).

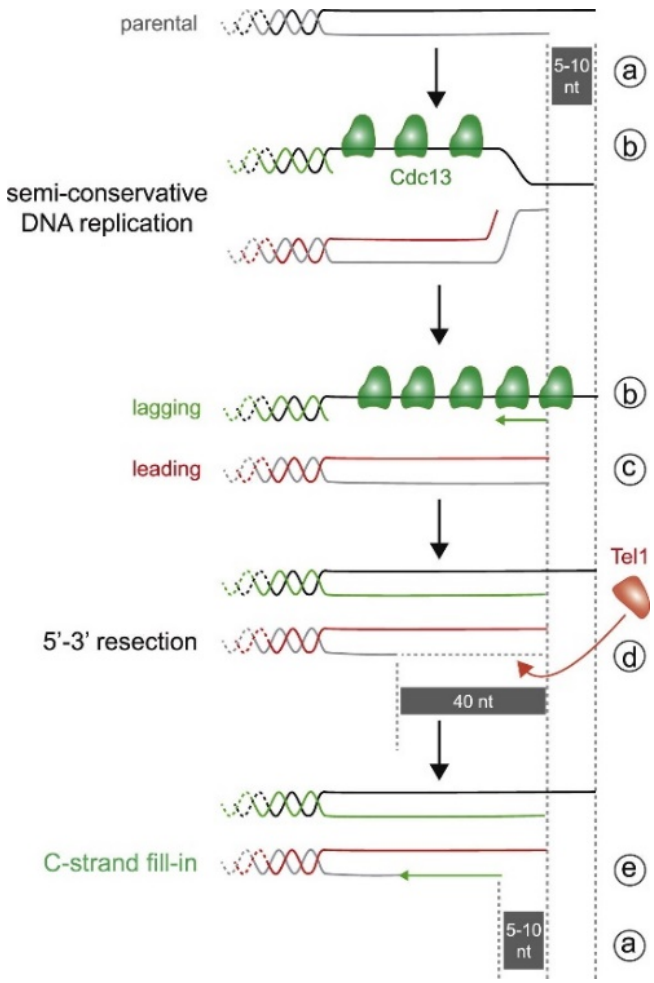

Figure 2. The end replication problem.

b) During the synthesis of the lagging strand, the last Okazaki primer is positioned near the end of the telomere, leaving a gap of 5-10 nt after primer removal. c) Synthesis of the leading strand reaches the end of the chromosome creating a blunt end and therefore the C-strand needs to be resected in 5'-3' direction, d) a process mediated by Tel1, generating a 40 nt overhang e) which is replenished by conventional replication, accomplished by positioning the last Okazaki primer near the end of the telomere, leaving a 5-10 nt gap after primer removal. a) This processing leads to the shortening of the leading strand telomere, with an average loss of 2.5-5 nt per replication round. Taken from (Soudet et al., 2014).

1.2 Telomere maintenance mechanisms

1.2.1 Telomerase

The predominant mechanisms by which yeast cells solve the end replication problem is the reverse transcriptase telomerase. Telomerase is a ribonucleoprotein complex, and in yeast it comprises the proteins Est1-2-3 and the RNA moiety TLC1. Est2 is the catalytic

subunit of the complex, and catalyzes the polymerization of telomeric DNA in 5'→3' orientation to the 3' G-tail by reverse transcribing TLC1 (Counter et al., 1997; Lendvay et al., 1996; Singer and Gottschling, 1994). Completion of telomere elongation is provided by Cdc13-mediated recruitment of Polα-primase to promote fill-in synthesis of the complementary C-strand via conventional replication (Grossi et al., 2004; Qi and Zakian, 2000). Deletion of any of the abovementioned telomerase components leads to progressive telomere shortening and replicative senescence onset, a condition in which cells stop dividing, eventually leading to cell death (Lundblad and Szostak, 1989). This suggests that telomerase is the predominant mechanism for telomere maintenance in wild type cells. The low abundance of each telomerase component (making up approximately 30 copies of telomerase per haploid cell, for 64 telomeres in late S phase)(Mozdy and Cech, 2006) suggests the need to act at a limited amount of telomeres per replication round. Telomerase access and action at telomeres is therefore tightly coordinated by multiple telomeric factors.

Telomere elongation by telomerase is cell cycle regulated: although Est2 can bind telomeres throughout the cell cycle thanks to TLC1 interaction with Yku80, this localization alone is not productive in terms of elongating telomeres (Taggart et al., 2002). Cdk1-dependent phosphorylation of Cdc13 in late S and G2 promotes Cdc13 interaction with Est1 (Liu et al., 2013), which leads to Est3 recruitment and formation of a functional complex. Telomerase cannot act on blunt ends, which are generated after the replication of the leading strand, thereby requiring the action of MRX to degrade the C-strand at leading strand telomeres (Takata et al., 2005); Cdk1 activity is also necessary to generate the single stranded overhang in late S phase (Frank et al., 2006). The transit of the replication fork in S phase promotes recruitment of MRX to the telomeres (Dionne and Wellinger, 1998; Takata et al., 2005), thereby it is plausible that telomerase acts in late S/G2 because that is when bulk replication is completed and MRX-dependent telomere overhang formation has taken place. This is also consistent with preferential action of telomerase at leading strand telomeres, where MRX processes blunt ends (Faure et al., 2010; Soudet et al., 2014).

The main regulator of telomere elongation is the checkpoint kinase Tel1. Tel1 is recruited to telomeres by the MRX complex, and its kinase activity is necessary to promote telomere

elongation, although how this is accomplished is still elusive. So far, Tel1-dependent phosphorylation of Cdc13 has been proposed to regulate Cdc13-Est1 interaction (Tseng et al., 2006). Importantly, Tel1 binding to telomeres is inhibited by Rif1 and Rif2, which are thereby two critical negative regulators of telomerase action. Rif1 and Rif2 act via two different pathways: Rif2 inhibits Tel1 and MRX localization to telomeres by competing with Tel1 for the binding of Xrn2 (Hirano et al., 2009), while Rif1 inhibition of Tel1 recruitment occurs in a still unknown manner, which is different from the Rif2 pathway (Hirano et al., 2009). The differential regulation of telomerase by the Rif proteins is demonstrated by the non epistatic effect of *RIF* genes deletions. In fact, while *rif1* and *rif2* mutants display long telomeres, the double mutant *rif1 rif2* has synergistically extended telomeres (Wotton and Shore, 1997).

Telomerase does not act on every telomere in a cell but preferentially elongates the shortest ones (Marcand et al., 1999; Teixeira et al., 2004). Additionally, telomerase is more processive at critically short telomeres, in a process promoted by Tel1 (Chang et al., 2007a). Indeed, the amount of Rap1, Rif1 and Rif2 molecules bound to telomeres was proposed to establish a ‘counting mechanism’ (Marcand et al., 1997), thereby connecting telomere length to the need for telomerase extension. By this model, loss of Rap1 binding sites at short telomeres leads to decreased Rap1-Rif1-Rif2 binding, which relieves Tel1-mediated telomerase inhibition and thereby allows telomere elongation; once the telomere is long again, the increased amount of Rap1-Rif1-Rif2 re-establishes telomerase inhibition. Loss of telomeric repeats is associated to loss of Rif2, and to a lesser extent Rif1, from short telomeres (McGee et al., 2010; Sabourin et al., 2007), suggesting a differential distribution of the Rif proteins along the telomere, with Rif2 binding more towards the distal tip and Rif1 towards the centromere-proximal telomeric tract. Diminished Rif2 binding to short telomeres relieves MRX-Tel1 inhibition, thus establishing a positive feedback loop that promotes telomere elongation.

Finally, the Pif1 helicase is also a regulator of telomerase in a telomere-length dependent manner. Pif1, which *in vitro* was shown to dissolve RNA-DNA hybrids, binds preferentially to long telomeres (Phillips et al., 2015), where it acts as a potent telomerase inhibitor, presumably by displacing telomerase from chromosome ends (Boule et al., 2005).

1.2.2 Telomere recombination

Although, as stated before, homologous recombination between telomeres is usually repressed to avoid the risk of generating harmful recombination intermediates and derived genome instability, it can be a means to maintain telomeres in telomerase deficient cells. While in telomerase positive cells the exchange of genetic material between telomeres would have virtually no beneficial effect on telomere stability, when a short telomere is generated in telomerase negative cells recombination between this telomere and another telomere would benefit cell viability by replenishing the pool of telomeric repeats and preventing checkpoint activation (Fallet et al., 2014). When telomerase deficient cells are propagated for long periods, they lose viability due to checkpoint activation stemming from short uncapped telomeres (senescence)(Lundblad and Szostak, 1989). In yeast, one critically short telomere is enough to trigger senescence, indicating that continuous shortening of bulk telomeres in a telomerase negative cell is not the leading cause for its growth arrest, but it is rather the length of the shortest telomere in a cell (Abdallah et al., 2009). Recombination at telomeres can occur when telomerase negative cells are on the way to senescence as a mean to elongate critically short telomeres, thereby delaying senescence onset (Churikov et al., 2014). Most telomerase negative cells experience a few subsequent terminal cell cycle arrests followed by cell death, consistent with telomeres reaching a critical (short) length (Xu et al., 2015). But interestingly ~40% of cells instead undergo early cell cycle arrests followed by re-gained cell growth, in a process dependent on Pol32 and HR (Xu et al., 2015), indicating that generation of short telomeres happens stochastically, probably due to replication stress, and recombination plays a protective role upon these events. Thereby, homologous recombination between short telomeres in pre-senescent cells can delay, but is not enough to avoid, senescence onset.

Strikingly, rare ‘survivor’ cells can overcome senescence and re-gain almost wild type growth kinetics. These survivors are dependent on Rad52-mediated recombination and on the Pol32-mediated break-induced replication (BIR) pathway (Lundblad and Blackburn, 1993; Lydeard et al., 2007). Two types of survivors have been described based on their arrangement of telomeric DNA and genetic requirements (Le et al., 1999). Type I survivors maintain telomeres by recombining Y’ elements, while telomeric repeats remain short (50-150 bp). This is the leading cause of the poor growth of type I survivors, which experience

frequent cell cycle arrests probably due to damage signaling stemming from these short uncapped telomeres (Cohen and Sinclair, 2001; Teng and Zakian, 1999). In type I survivors Y' repeats are expanded by recombination between telomeres, but also possibly by amplification of extrachromosomal circular Y' elements that are found in these cells (Larrivee and Wellinger, 2006). Type I survivors rely on the homologous recombination proteins Rad51, Rad54, Rad57 and Rad55 (Chen et al., 2001; Le et al., 1999). Type II survivors maintain telomeres by recombining telomeric repeats with other chromosomes, and additionally contain extrachromosomal circles of telomeric repeats, which could be used to elongate telomeres by rolling circle amplification (Larrivee and Wellinger, 2006). Telomere length in type II survivors is extremely heterogeneous, ranging from extremely long (up to 12 kb) to critically short (Teng and Zakian, 1999), but this type of survivor, differently from type I survivors, divide with kinetics very similar to wild type. Interestingly, telomeres of type II survivors shorten at every replication round, as happens in telomerase positive cells, and abruptly recombine only when a critical length is reached (Teng et al., 2000). This survivor pathway relies on the MRX complex, Rad59 and Sgs1 (Chen et al., 2001; Johnson et al., 2001; Le et al., 1999).

1.3 Telomere maintenance in other organisms

1.3.1 Human telomeres

Human telomeres are made up of double-stranded TTAGGG repeats that typically range between 10 and 15 kb, and end in a single stranded overhang of 50-500 nt. The protein complex that associates to telomeric repeats has been dubbed Shelterin and is composed of TRF1 and TRF2, which directly bind the double stranded telomeric repeats, POT1, which binds the single stranded overhang, TIN2 and TPP2, which bridge POT1 to TRF1/2, and finally RAP1, which binds to TRF2 (Palm and de Lange, 2008). In humans, the single stranded overhang loops back into the double stranded repeats, forming a lariat structure or t-loop, which protects telomere integrity by sequestering the ssDNA and thereby protecting telomeres against nucleases and checkpoint activation (Doksani et al., 2013; Griffith et al., 1999). Additionally, the Shelterin complex inhibits the activation of the DNA

damage response at telomeres, with TRF2 repressing ATM signaling and POT1 inhibiting ATR activation (Denchi and de Lange, 2007). Human telomerase is composed of TERT, the reverse transcriptase enzyme, and the RNA moiety TERC (Feng et al., 1995; Lingner et al., 1997); telomere shortening in the absence of telomerase activity leads to checkpoint activation and replicative senescence onset, eventually leading to apoptosis, analogously to yeast (d'Adda di Fagagna et al., 2003; Hayflick, 1965). Interestingly, in human cells the generation of four to five critically short telomeres is necessary to induce senescence, while in yeast one is sufficient (Kaul et al., 2012).

Human telomeres are organized in nucleosomes and are heterochromatic, being characterized by abundant H3K9me3 mark, which in mouse was shown to be imposed by the histone methyltransferase Suv39h and to recruit HP1α, and H4K20me mark, and finally are rich in deacetylated histones (Arnoult et al., 2012; Garcia-Cao et al., 2004). Indeed, SIRT6, a component of the Sir2 family, deacetylates H3K9 at human subtelomeres (Michishita et al., 2008). Additionally, human subtelomeres are highly methylated (Steinert et al., 2004).

1.3.1.1 Telomeres and cancer

In humans, most somatic cells do not express telomerase, leading to telomere shortening at each replication round (Harley et al., 1990). Cancer cells acquire the ability to divide indefinitely, and thereby require the activation of telomere lengthening mechanisms. Indeed, telomerase expression seems to correlate with lifespan, as generally short-lived organisms express telomerase (e.g. mice), while long-lived organisms do not. Repression of telomerase activity in long-lived organisms, which display increased cancer risk, is thought to be a safeguard mechanism against cancer, given to the anti-cancer role of replicative senescence. While around 85% of cancer types gain immortality by reactivating telomerase, the remaining 15% of cancers maintain their telomeres by BIR-based telomere maintenance mechanisms, which defines these cancers as alternative lengthening of telomeres (ALT) cancers (Henson and Reddel, 2010; Kim et al., 1994). ALT cancers are associated with the following hallmarks: extreme telomere length heterogeneity, accumulation of extra-chromosomal telomeric DNA, clustering of

telomeres in promyelocytic leukaemia (PML) bodies thereby forming ALT-associated PML bodies (APBs), and rampant recombination between telomeres. Additionally, ALT cells often display decreased or absent expression of the ATRX helicase, an impaired DNA damage response and finally elevated TERRA levels, which was also found to associate with APBs (see Section 1.4)(Arora et al., 2014; Azzalin et al., 2007; Episkopou et al., 2014). TERRA accumulation in ALT cells seems to be caused by increased transcription, as TERRA CpG promoters are hypomethylated and RNA Pol II is enriched at these telomeres (Arora et al., 2014; Episkopou et al., 2014; Nergadze et al., 2009).

1.3.2 *Drosophila* telomeres

Although most eukaryotic telomeres are maintained by telomerase, there are a few exceptions, of which *Drosophila* is well-studied. *Drosophila* telomeres are not maintained by telomerase but by an array of transposable elements. The capping in these organisms is sequence-independent, as it is made up of tandem copies of HeT-A, TART and TAHRE (together called HTT) non-LTR (long terminal repeat) retrotransposon elements, separated by varying extents of A repetitions (Pardue and DeBaryshe, 2008). The HeT-A retrotransposon accounts for 80-90% of the HTT arrays (George et al., 2006), and codes exclusively for a Gag nucleic acid binding protein but not for a reverse transcriptase. TART elements represent 10% of the telomeric arrays and code for a Gag protein and a Pol reverse transcriptase. TAHRE elements are very rare (1-2%) and are related to HeT-A, but contain additionally the Pol ORF. All have very long 3' non coding regions, which might be important for heterochromatin formation at telomeres (Danilevskaya et al., 1998). Also in *Drosophila*, telomeres shorten at each replication round, and chromosome length maintenance is achieved by retrotransposition of the HTT elements (Biessmann et al., 1992). The process starts by transcription of the HTT elements, after which the RNA is transported to the cytoplasm where it is translated into Gag proteins and retrotranscriptases. Gag proteins bind preferentially to their encoding RNA and efficiently return to the nucleus, where the RNA is reverse transcribed directly at the telomeric end, thereby providing a telomere elongation mechanism (Rashkova et al., 2002); the opposite strand can then be produced either by the reverse transcriptase or by the canonical

replication machinery. Interestingly, the HTT elements are inter-dependent, as HeT-A elements need TART or TAHRE reverse transcriptases to replicate, and TART and TAHRE need HeT-A Gag protein for efficient localization to telomeres (Fuller et al., 2010; Rashkova et al., 2002). Finally, although to a lesser extent, *Drosophila* telomeres were shown to be able to amplify in a recombination-mediated manner (Mikhailovsky et al., 1999), as mammalian and yeast telomeres. Interestingly, several proteins involved in maintenance of yeast and human telomeres were found to be also required at *Drosophila* telomeres, as for example MRE11, RAD50, ATM and the Ku complex (Cenci et al., 2005).

1.3.3 Telomeres in bacteria and viruses with linear chromosomes

The paradigm that eukaryotes possess linear chromosomes while prokaryotes have circular genomes was challenged by the discovery of the linear genome of the Lyme disease agent *Borrelia burgdorferi* (Ferdows and Barbour, 1989), after which more prokaryotes and viruses followed in being identified to have a similar genome organization. In general, prokaryotes and viruses that possess linear chromosomes or plasmids seem to employ a slight variation of two main genome-end organization strategies, which will be presented.

Borrelia linear chromosomes possess terminal regions made up of palindromic AT-rich sequences, which are stabilized by forming covalently closed hairpin structures (Chaconas and Kobryn, 2010). Replication of the genome from a central, bidirectional origin might lead to generation of a circular intermediate, connected by the newly replicated hairpin structures, which have to be eventually resolved. Similar terminal structures are also found in the *E. coli* prophage N15 and in various viruses, as for example poxviruses (Traktman and Boyle, 2004). These organisms express a topoisomerase-like resolvase that cleaves the terminal hairpin structures to allow genome replication.

Differently, *Streptomyces* linear chromosome and plasmids end as dsDNA comprising palindromic terminal repeats, which are covalently bound by a specialized protein during replication (Huang et al., 2007) and are probably capable of forming peculiar secondary structures (Huang et al., 1998). In *Steptomyces*, the telomere is the origin of genome

replication, and the telomere end binding protein promotes beginning of replication by recruiting DNA polymerase and priming its own replication. This end structure is conserved in adenoviruses (de Jong et al., 2003).

On the other hand, Herpesviruses possess GC-rich terminal repeats of different extension, which are essential for gene expression, replication and recombination. Some Herpesvirus family members integrate into the host telomeres thanks to the GC-rich terminal repeats that are highly similar to host telomeres (Arbuckle and Medveczky, 2011), possibly via homologous recombination, during latency (Arbuckle et al., 2010). This process might be mediated by TRF1 and TRF2 binding to viral end repeats.

In conclusion, although different mechanisms to protect linear chromosome ends have evolved in different organisms, some common features can be identified. First of all, chromosome ends are typically defined by peculiar, repeated sequences, including short repeats, palindromic sequences or unique transposable elements. Secondly, dedicated proteins recognize these repeats and orchestrate telomere maintenance, and finally a special replication process is required to maintain all chromosome-end structures.

1.4 TERRA

1.4.1 TERRA transcription

Despite being heterochromatic, telomeres are transcribed into long, non-coding RNAs dubbed TERRA (telomeric repeat containing RNA). TERRA is majorly transcribed by RNA Pol II (Azzalin et al., 2007; Luke et al., 2008), although it has been reported that RNA Pol II inhibition does not fully abolish TERRA generation, suggesting that other polymerases might contribute to TERRA transcription (Schoeftner and Blasco, 2008). TERRA is transcribed from the telomeric C-strand and comprises both telomeric and subtelomeric sequences (Azzalin et al., 2007; Luke et al., 2008). To date, TERRA has been detected in all eukaryotes tested (Luke and Lingner, 2009; Schoeftner and Blasco, 2008).

In *S. cerevisiae*, TERRA length ranges between 100 and 1200 bases, with the bulk being around 380 bases long (Luke et al., 2008), a variance that likely stems from different

transcription end points rather than multiple transcription start sites (TSS). In fact, only a few TSSs have been mapped so far in yeast, one being located at the 3' end of the X element at the 1L telomere, and six at the 3' end of Y' elements (Pfeiffer and Lingner, 2012). Recently, additional TSSs were identified in the X element of several X-only telomeres, and importantly only one TSS was identified for each telomere-derived TERRA molecule (Marco Graf PhD thesis). The majority of yeast TERRA molecules is polyadenylated by Pap1, contributing to its stability (Luke et al., 2008). TERRA levels are low in the cell, an outcome that is achieved by two means. First, TERRA transcription is limited by the Sir2-4 complex, which establishes heterochromatin at telomeres and presumably represses TERRA transcription (Iglesias et al., 2011). Second, the 5'→3' exonuclease Rat1 degrades TERRA molecules (Luke et al., 2008). Both Sir2-4 and Rat1 actions are orchestrated by telomeric proteins: regulation of TERRA levels transcribed from X-only telomeres is dictated by Rap1 both on the transcriptional (mediated by Sir2-4) and degradation level (mediated by Rat1), while at Y' telomeres Rap1 mediates TERRA transcription inhibition through Rif1 and Rif2, while it directly promotes Rat1-mediated degradation (Iglesias et al., 2011). Rat1-mediated TERRA degradation is regulated throughout the cell cycle and by telomere length. In fact, TERRA levels peak in early S phase, when it is transcribed, and decrease as cells progress through S phase, a time when Rat1 localizes to telomeres (Graf et al., 2017). On the contrary, Rat1 is lost from critically short telomeres, causing loss of TERRA cell-cycle regulation and resulting in increased TERRA levels (Graf et al., 2017), consistent with previous reports (Cusanelli et al., 2013; Iglesias et al., 2011). Importantly, the increase of TERRA levels at short telomeres in budding yeast is not caused by increased transcription (Graf et al., 2017).

In human cells, TERRA length varies between 100 bases – 9 kb (Azzalin et al., 2007) and TSSs have been mapped at CpG islands, which are present at about 25% of human telomeres. Contrary to yeast, only around 7% of mammalian TERRA is polyadenylated (Azzalin and Lingner, 2008), which in human cells contributes to its stability (Porro et al., 2010) but also to its localization: while polyadenylated TERRA is mainly found diffusely in the nucleoplasm, non-polyadenylated TERRA is majorly chromatin-associated (Porro et al., 2010). Additionally, the human TERRA 5' end is protected by a 7-methylguanosine cap (Porro et al., 2010). Human TERRA levels appear to be largely regulated on the transcriptional level. TERRA transcription is promoted by the transcriptional regulator

CTCF and the cohesin subunit Rad21. Indeed, CTCF depletion leads to decreased Rad21 and RNA Pol II binding to subtelomeres, causing decreased TERRA levels and damage signaling stemming from telomeres (Deng et al., 2012). Also the Shelterin components TRF1 and TRF2 regulate TERRA expression: they physically interact with TERRA and their depletion leads to increased TERRA levels (Arora et al., 2014; Deng et al., 2009). Additionally, TERRA transcription is highly dependent on the chromatin status of telomeres. Treatment with Trichostatin, a histone deacetylase inhibitor, causes TERRA levels increase (Azzalin and Lingner, 2008). DNMT1/3b DNA methyltransferases methylate CpG islands and thereby repress TERRA transcription; their depletion leads to increased TERRA levels and telomere shortening (Nergadze et al., 2009; Yehezkel et al., 2008). Also the H3K9 methyltransferase SUV39H1 and the H3K9me3 binding protein HP1α repress TERRA transcription; additionally, TERRA interacts with both proteins and recruits them to telomeres, thereby establishing a negative feedback loop on TERRA transcription (Arnoult et al., 2012; Deng et al., 2009; Porro et al., 2014). Finally, the expression of the ATRX helicase, which deposits the H3.3 histone variant at telomeres, is almost always repressed in ALT cancer cells, in which TERRA levels are high (Arora et al., 2014; Flynn et al., 2015; Lovejoy et al., 2012).

Also in human cells, TERRA expression is cell cycle regulated, with a peak at the transition between G1 and S phase, followed by a sharp decrease as cells progress in S phase and re-accumulation only in the next G1 phase (Porro et al., 2010). Interestingly, while in telomerase positive human cells TERRA foci that colocalize with telomeres are removed through S phase and in G2/M, in ALT cancer cells and in cells depleted for ATRX this regulation is abolished (Flynn et al., 2015).

1.4.2 TERRA localization

TERRA is present only in the nucleus (Azzalin et al., 2007), and both in yeast and human cells it was shown to localize to specific areas of the nucleus. In yeast, live-cell microscopy of TERRA molecules allowed the analysis of the dynamics of its localization (Cusanelli et al., 2013). After transcription, TERRA derived from a single short telomere was shown to move away from the telomere of origin and form a perinuclear focus. This TERRA focus

acts as a scaffold for telomerase assembly in S phase, followed by the cluster returning preferentially to the telomere of TERRA origin (Cusanelli et al., 2013). An implication of TERRA in telomerase recruitment to short telomeres has been proposed also in *S. Pombe*, where polyadenylated TERRA generated from short telomeres is mostly nucleoplasmic and interacts with telomerase; induction of TERRA expression leads to telomerase-mediated telomere elongation *in cis* (Moravec et al., 2016).

In human cells, non-polyadenylated TERRA has been reported to form foci which colocalize with a fraction of telomeres, while polyadenylated TERRA is nucleoplasmic (Azzalin et al., 2007; Porro et al., 2010). While TERRA was reported to be present exclusively in the nucleus, short forms of TERRA (~200 nt) have been recently found in human cell cultures to be part of extracellular exosomes which are potent stimulators of the inflammatory response (Wang et al., 2015). In conclusion, both in yeast and human cells two pools of TERRA can be identified: “free TERRA”, which is nucleoplasmic, and telomere-associated TERRA, the implications of which will be discussed in Section 1.5.4.

1.5 R-loops

An R-loop is a three-stranded structure that is generated when an RNA transcript anneals co- or post-transcriptionally to its template DNA strand, thereby forming an RNA-DNA hybrid and displacing the non-template ssDNA strand. R-loops occur physiologically along the genomes and can exert positive functions, but, especially when deregulated, R-loops are a potent source of genome instability. Apart from R-loops, other shorter RNA-DNA hybrids can be found physiologically in the genome. These are formed by the RNA primers that are required for replication especially of lagging strands, which form hybrids of 7-12 bp (Pellegrini, 2012), and the hybrids formed in the RNA polymerase core during transcription (~8 bp in the active site of RNA Pol II)(Westover et al., 2004).

The prevalent model that explains how an RNA molecule can gain access to its template strand, which is normally in the form of dsDNA, to form an R-loop is the “thread back model” (Roy et al., 2008). Transcribing RNA polymerases generate negative supercoils in the DNA behind them (Liu and Wang, 1987), a feature that facilitates dsDNA unwinding, and therefore allows RNA invasion and the formation of an RNA-DNA hybrid. This model

is limited to being able to explain the formation of co-transcriptional R-loops, while it cannot account for why mutants affecting RNA post-transcriptional processing also accumulate R-loops. The latter scenario could be possibly explained by the RNA being more accessible and being locally retained at the transcription locus in these mutants, increasing the chances of interaction with the template DNA. Recently, R-loop formation *in trans* has been detected in a study carried out in *S. cerevisiae*, in which RNA transcribed from one locus could form R-loops at another untranscribed locus that shared the same sequence present on a yeast artificial chromosome (YAC) when RNA biogenesis factors were mutated, in a process mediated by the recombination protein Rad51 (Wahba et al., 2013).

RNA-DNA hybrids are thermodynamically more stable than dsDNA, particularly when they have a high GC composition, and adopt a peculiar conformation that is neither the one of a molecule composed exclusively of DNA nor exclusively of RNA (Roberts and Crothers, 1992). R-loop formation is favored by particular DNA characteristics, such as high GC skew (asymmetric distribution of Gs and Cs; in this case the enrichment of Gs in the non-template strand and in the RNA is favorable)(Roy and Lieber, 2009), presence of nicks on the non-template DNA strand (Roy et al., 2010), and finally the propensity of the displaced ssDNA strand to form G-quadruplex structures (Duquette et al., 2004).

1.5.1 R-loop regulation

Cells possess a myriad of mechanisms to keep R-loop levels in check, which act at different steps and hence can be subdivided in processes that inhibit R-loop formation or remove them once formed.

Amid the inhibitors of R-loop formation, there are topoisomerases, which by releasing the torsional stress generated after the transcription machinery passage can prevent RNA invasion in the DNA duplex. In yeast, loss of Top1 and Top2 leads to R-loop accumulation in the ribosomal DNA (rDNA), causing RNA Pol I stalling and defective pre-rRNA synthesis (El Hage et al., 2010). In human cells defective for TOP1, the DNA breaks at highly transcribed genes, a phenotype which can be completely reversed by *RNH1* overexpression (Tuduri et al., 2009), an enzyme that can degrade the RNA in RNA-DNA

hybrids (see Section 1.5.3); also TOP3B, an enzyme that selectively relaxes negative supercoils, counteracts R-loop formation in human and mouse and suppresses chromosomal translocations (Yang et al., 2014). Likewise, a large amount of proteins involved in messenger ribonucleoprotein particle (mRNP) formation prevent the formation of R-loops, possibly by shielding the RNA molecule, thereby preventing invasion of the template DNA. The THO/TREX complex has been well characterized in yeast and human cells for its role in R-loop prevention, and the THO component Hrs1 was the first mutant identified that linked defective mRNP formation to R-loop accumulation as a cause of genome instability, since this mutant's hyper-recombination phenotypes could be reversed by *RNH1* overexpression (Aguilera and Klein, 1990; Huertas and Aguilera, 2003). Additionally, the TREX-2 complex, which localizes to the inner part of nuclear pore, can also prevent R-loop formation, as deletion of its components causes hyper recombination and defective transcription, phenotypes that can be rescued by *RNH1* overexpression. In addition to hiding the RNA molecule, the TREX-2 complex might suppress R-loop formation by directly coupling RNA production to nuclear export, thereby decreasing the chances of RNA-DNA hybrid formation (Gallardo et al., 2003; Gonzalez-Aguilera et al., 2008). Indeed, localization of transcribed genes to the nuclear pore complex (NPC) represses the formation of R-loops (Garcia-Benitez et al., 2017). Many more factors involved in prevention of R-loop formation have been identified, highlighting the multiplicity of pathways that cells use to inhibit this phenomenon (Li and Manley, 2005; Paulsen et al., 2009; Wahba et al., 2011).

If the mechanisms just described fail to avert R-loop formation, there are several other mechanisms in place which can remove them. Helicases like Pif1 in yeast (Boule and Zakian, 2007), but also Sen1 (Senataxin in humans)(Mischo et al., 2011; Skourti-Stathaki et al., 2011) can resolve R-loops by unwinding the RNA-DNA hybrid and releasing the RNA counterpart. Sen1 can resolve R-loops, thereby preventing transcription-associated instability (Mischo et al., 2011). Sen1 associates with the replisome, indicating a direct role in fork stability protection when it encounters R-loops (Alzu et al., 2012). Human Senataxin is involved in removing R-loops at G-rich pause sites to promote removal of the RNA by Xrn2 (Skourti-Stathaki et al., 2011). Finally, Ribonuclease H enzymes can selectively degrade the RNA counterpart of a RNA-DNA hybrid; this class of enzymes will be described in detail in Section 1.5.3.

Importantly, impairment of most of the abovementioned pathways that restrict R-loops lead to R-loop accumulation, suggesting that, although redundant, most of these factors have access and specificity (spatial/temporal) to a unique subset of R-loop substrates. Ultimately, albeit being highly regulated, hotspots for R-loop accumulation have been identified in the yeast genome, including the rDNA, telomeres, Ty transposons, tRNA genes and finally highly Pol II transcribed genes (Chan et al., 2014; El Hage et al., 2014).

1.5.2 R-loop impact on the genome

R-loops exert a number of positive physiological roles (Figure 3, bottom). The most prominent example for an R-loop-mediated process in mammals is their involvement in immunoglobulin class switch recombination (CSR) in activated B cells. Formation of an R-loop following transcription of the switch region at the IgH locus creates the ssDNA substrate that is target of activation-induced cytidine deaminase (AID) action. The deoxyuridine residues that are produced on the ssDNA are further processed and eventually generate DSBs, which start genomic rearrangements that allow for generation of different Ig isotypes (Roy et al., 2008). R-loop formation is also an essential step for mitochondrial DNA (mDNA) replication in yeast and mammals (Xu and Clayton, 1996), and primes replication in *E. coli* ColE1 plasmids, in a process that requires formation of a co-transcriptional R-loop within origin elements that must be cleaved by RNase H to serve as primer for replication (Itoh and Tomizawa, 1980). A recent study in *S. pombe* indicates that R-loop formation is required for efficient DSB repair and implicates R-loops in regulation of RPA accumulation and resection, suggesting that R-loop formation but also their timely resolution are critical to accomplish efficient repair (Ohle et al., 2016).

R-loops can also regulate gene expression. A striking example is *Arabidopsis* antisense non coding RNAs COOLAIR, generated from the flowering locus C (FLC). COOLAIR normally negatively regulate FLC expression, but stabilization of an R-loop at the COOLAIR promoter silences its expression, which in turn allows FLC expression, thereby regulating plant flowering (Sun et al., 2013). In human cells, R-loops form at active CpG islands characterized by a high GC skew, protecting them from DNMT3B1 access and thereby promoting gene expression in the unmethylated state (Ginno et al., 2012). In

addition, R-loops can also help to terminate transcription by inducing RNA Pol II pausing at G-rich pause sites, which, in turn recruits Senataxin and promotes Xrn1-mediated transcription termination (Skourti-Stathaki et al., 2011). These R-loops at pause sites can additionally induce antisense RNA transcription, which in turn recruit epigenetic modifiers that cause H3K9me2 heterochromatin formation *in cis* to further promote efficient transcription termination (Skourti-Stathaki et al., 2014). Further evidence of R-loops influence on chromatin status is suggested by the correlation of their accumulation with the presence of H3S10P heterochromatin mark in *S. cerevisiae* and human cells, a marker that is associated with chromatin condensation (Castellano-Pozo et al., 2013).

Apart from their positive roles, in the past years R-loops have been heavily studied for their propensity to generate genome instability, thereby emphasizing their negative role. R-loops are indeed hazardous structures in many circumstances, which will be shortly introduced (figure 3, top).

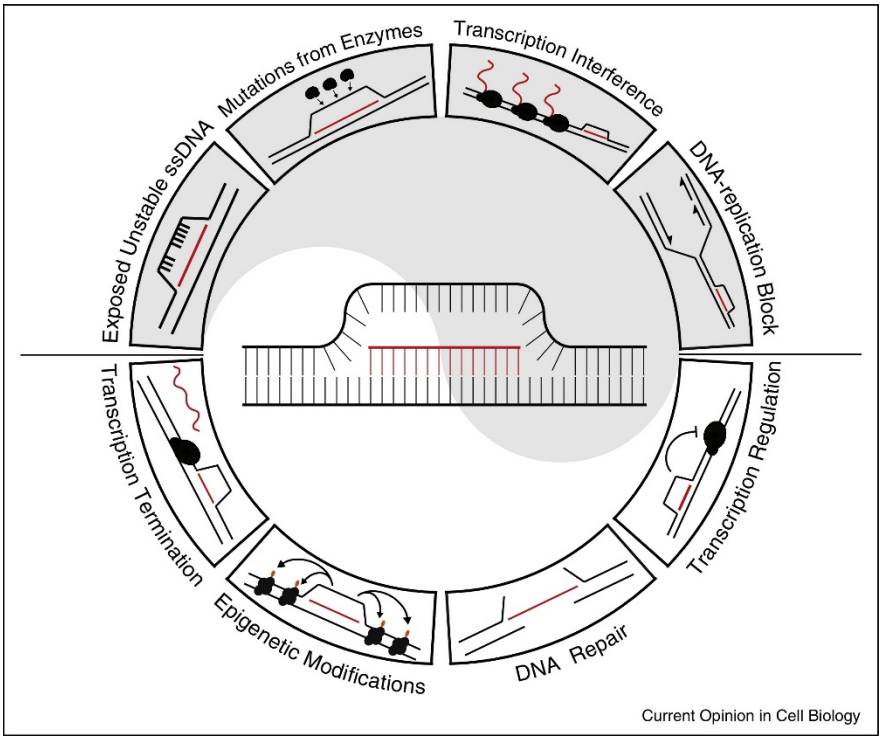

Figure 3. R-loops have both positive and negative impact on the genome.

An R-loop is a three-stranded structure, comprising an RNA-DNA hybrid and a displaced ssDNA. Top: R-loops can lead to genome instability by exposing the unstable ssDNA filament which becomes also accessible to detrimental enzymatic activities; R-loops can interfere with transcription and cause replication stress and fork collapse. Bottom: R-loops can positively contribute in promoting transcriptional regulation and efficient termination; they can lead to local changes in chromatin status and finally contribute to repair of DSBs.Taken from (Costantino and Koshland, 2015).

To begin with, the structure of an R-loop by definition contains a displaced ssDNA strand. Exposed ssDNA is chemically unstable and susceptible to damaging agents (Lindahl, 1993), and can be targeted by enzymes such as AID, which can lead to nicks and DSB formation. Moreover, R-loops were shown to be targeted by the replication-coupled nucleotide excision repair (NER) machinery in human cells and yeast, leading to DSB formation (Sollier et al., 2014). Furthermore, recent findings indicate that R-loops are capable of priming origin-independent replication within the *S. cerevisiae* rDNA locus when persistent R-loops are allowed to accumulate, a process that could potentially contribute to genome instability (Stuckey et al., 2015). Of note, an increasing number of studies link R-loop-induced genome instability to replication processes. Indeed, transcription-induced recombination in *hpr1* mutants ensues only at genes transcribed in S phase, which could cause collision between the transcription and replication machineries (Wellinger et al., 2006). The helicase Rrm3, which relieves replication stress, accumulates at highly transcribed genes in THO mutants, in an RNase H1 sensitive manner (Gomez-Gonzalez et al., 2011). Sen1 helicase localizes to replication forks and suppresses R-loop accumulation in S phase, helping progression through RNA Pol II transcribed genes (Alzu et al., 2012). Also in mammalian cells, Top1 depletion leads to transcription-dependent replication stress, in a process mediated by R-loops (Tuduri et al., 2009). Indeed, multiple reports have shown that R-loops are obstacles for replication fork progression, and collision of the replication machinery with R-loops can result in genome instability (Alzu et al., 2012; Gan et al., 2011; Gomez-Gonzalez et al., 2011; Santos-Pereira et al., 2013; Tuduri et al., 2009). A recent study in *S. cerevisiae* identified the chromatin mark H3S10P to be associated exclusively with genome instability-generating R-loops, thereby indicating that R-loop accumulation *per se* does not cause genomic instability but only when causing local chromatin modifications, the consequences of which still have to be identified (Garcia-Pichardo et al., 2017).

1.5.3 Ribonucleases H

Ribonucleases H (RNases H) are a class of enzymes capable of hydrolyzing the RNA counterpart of an RNA-DNA hybrid (Cerritelli and Crouch, 2009). In bacteria and eukaryotes two different RNase H enzymes are present that have been dubbed RNase

H1 (or HI in prokaryotes) and RNase H2 (or HII), which degrade the RNA in a sequence unspecific manner but have only partially overlapping substrate specificity.

RNase H1 is monomeric, and possesses in its N-terminus a hybrid binding domain (HBD), which binds to RNA-DNA hybrids with a 25 fold preference over dsRNA (Nowotny et al., 2008). Importantly, RNase H1 can only recognize and degrade RNA-DNA hybrids containing at least four ribonucleotides (Figure 4). In higher eukaryotes, RNase H1 is important for mitochondrial DNA replication, and indeed RNase H1 null mouse embryos arrest development because they are incapable of amplifying mitochondrial DNA (Cerritelli et al., 2003). So far no human genetic disease has been found to be associated with *RNH1* mutations, possibly due to the essentiality of this enzyme (probably leading to embryonic lethality). On the contrary, in yeast RNase H1 is not required for mitochondrial DNA replication (Arudchandran et al., 2000). A recent work in human cells identified a functional interaction between RPA and RNase H1, whereby RPA recruits RNase H1 to R-loops and promotes its activity (Nguyen et al., 2017b).

Differently from bacterial RNase HII, eukaryotic RNase H2 is a trimeric complex, composed of Rnh201/202/203 in *S. cerevisiae* and RNASEH2A/2B/2C in mammals. In addition to being able to degrade longer RNA-DNA hybrids, RNase H2 can also remove single ribonucleotides embedded in the DNA (Figure 4)(Eder et al., 1993), which can arise from misincorporation events by DNA polymerases. RNase H2 provides the most abundant RNase H activity in the cell and its function seems to be linked at least partially to replication, as RNASEH2B and Rnh202 are capable of interacting with the DNA polymerases clamp loader PCNA via their PIP-box domain located in the C-terminus (Chon et al., 2009; Nguyen et al., 2011). Importantly, human RNase H2, but not RNase H1, localizes to replication foci via RNase H2B, possibly explaining why RNase H2 provides the majority of RNase H activity in the cells (Bubeck et al., 2011). Finally, RNase H2 takes part in Okazaki primer removal, in a process in which a ribonucleotide is left attached to the newly synthetized DNA strand, requiring further processing by Rad27/FEN1 (Rydberg and Game, 2002).

In *S. cerevisiae*, Rnh201 is the catalytic subunit of the RNase H2 complex, but the enzyme is only functional when all subunits are present (Nguyen et al., 2011). Mutants in both RNase H enzymes are highly sensitive to low doses of replication stress (Lazzaro et al.,

2012) and, interestingly, mutation of *RNH201*, but not *RNH1*, increases genome instability, a phenotype related to its R-loop removal activity. However, combined mutation of both enzymes leads to synergistically increased recombination rates, suggesting a partial, although not total, redundancy in RNase H1 and H2 activities (O'Connell et al., 2015). *rnh201 sgs1* mutants are synthetic sick due to accumulation of R-loops that cannot be resolved by homologous recombination in the absence of Sgs1. Importantly, overexpression of *RNH1* in this mutant does not rescue this phenotype, suggesting that Rnh1 does not have access to, or act on, at least a fraction of the R-loops that are normally taken care of by RNase H2 (Chon et al., 2013).

In humans, RNASEH2A is the catalytic subunit of RNase H2, and importantly mutations in any of the components of human RNase H2 are cause of the severe childhood inflammatory disorder Aicardi-Goutières syndrome (AGS), which results in, amongst other symptoms, neurological dysfunction and psychomotor retardation (Rice et al., 2007). Only recently it was shown that patients' cells display global DNA hypomethylation and excessive accumulation of R-loops, possibly being the cause for the acute immune response (Lim et al., 2015).

RNase H enzymes are not essential in yeast, which could be explained by the existence of compensatory pathways for Okazaki processing, removal of single ribonucleotides insertions in the DNA and R-loop removal. Some novel data from *S. cerevisiae* indicate that RNase H activity is required for efficient repair of R-loop-induced damage, in a process that probably involves R-loop removal to allow efficient repair, and prevent repair by the mutagenic BIR pathway (Amon and Koshland, 2016).

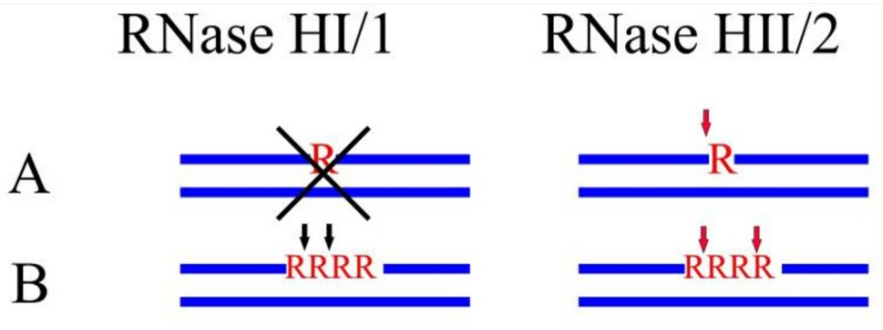

Figure 4. RNase H1 and H2 have different substrate specificity.

A) Single ribonucleotides inserted in the DNA can only be removed by RNase H2, while **B**) stretches of four or more ribonucleotides in the DNA can be removed by both RNase H1 and H2. Modified from (Cerritelli and Crouch, 2009).

1.5.4 Telomeric R-loops

TERRA has been proposed to form R-loops at telomeres as early as its discovery (Azzalin et al., 2007; Luke et al., 2008; Schoeftner and Blasco, 2008). Indeed, its G-rich composition and the ability of the displaced single strand to form G-quadruplexes are known promoters of R-loop stability (Duquette et al., 2004; Roy and Lieber, 2009). First hints that TERRA could form R-loops came from the fact that in yeast RNase H2 overexpression reduces TERRA levels in a *rat1-1* mutant (Luke et al., 2008), and from the finding that TERRA colocalizes with Rap1 in human cells, indicating that it is part of telomeric heterochromatin (Azzalin et al., 2007). R-loops can be detected using the S9.6 antibody, which specifically recognize RNA-DNA hybrids of at least 6-8 bp (Phillips et al., 2013); by this method, R-loops could indeed be identified at yeast and human telomeres in the recent years (Arora et al., 2014; Balk et al., 2013; Pfeiffer et al., 2013; Wahba et al., 2016; Yu et al., 2014).

In yeast, telomeric R-loops are restricted by the RNase H enzymes and THO-TREX components (Balk et al., 2013; Pfeiffer et al., 2013; Yu et al., 2014). Telomeric R-loops appear to be relevant in telomerase negative pre-senescent cells, where they promote telomere elongation by homologous recombination and thereby partially compensate for telomere shortening and hence, delay senescence onset (Balk et al., 2013). Indeed, *rnh1 rnh201* mutants, which accumulate R-loops at telomeres, senesce slower than otherwise wild type telomerase mutants, and RNase H1 overexpression, by decreasing telomeric R-loops, anticipates senescence onset (Balk et al., 2013). Interestingly, R-loop accumulation at telomeres influences the survivor pathway choice, as telomerase mutants that accumulate telomeric R-loops preferentially generate type II survivors in an R-loop-dependent manner (Yu et al., 2014). How exactly R-loops promote recombination at telomeres remains elusive, but it was proposed to be due to induction of replication stress at telomeres (Balk et al., 2013).

Also in human cells, TERRA has been implicated in maintenance of telomeres in telomerase negative ALT cancer cells by forming recombinogenic R-loops at telomeres. Indeed, RNase H1 accumulates specifically at ALT telomeres (Arora et al., 2014), and deregulation of RNase H1 expression is deleterious for ALT cells maintenance: while

RNH1 deletion causes increased accumulation of telomeric R-loops and telomere loss due to abrupt telomere excision, overexpression of RNase H1 leads to reduced telomeric R-loops and decreased recombinogenic potential of telomeres, and thus results in telomere shortening (Arora et al., 2014). Therefore, RNase H1 controls the recombinogenic propensity of ALT telomeres by regulating telomeric R-loops. In contrast, alteration of RNase H1 levels in telomerase positive cells has no effect on telomere maintenance (Arora et al., 2014). Finally, ATRX re-expression in ALT cells was recently shown to reduce telomeric R-loops, which could explain why most ALT cancer cell lose ATRX expression (Nguyen et al., 2017a).

1.6 Replicative senescence and senescence-associated diseases

Telomeres progressively shorten in human cells due to lack of telomerase activity in most somatic cells (Harley et al., 1990), leading to replicative senescence onset. Replicative senescence is therefore a potent barrier against cancer development, setting a limit to the amount of duplications that a cell can undergo and therefore limiting uncontrolled proliferation. The drawback of this defense mechanism is that the accumulation of senescent cells can accelerate organismal aging, which is defined as the age-dependent progressive deterioration of tissue and organ function.

1.6.1 Senescence and aging

Senescent cells are characterized by a set of common features: permanent proliferative arrest, although senescent cells are still metabolically active; expression of anti-proliferative molecules, such as $p16^{INK4a}$; persistent DNA damage response activation and expression of senescence-associated secretory phenotype (SASP) pro-inflammatory cytokines (Childs et al., 2015). Different stressors can induce cellular senescence: short or dysfunctional telomeres, oxidative stress, proteotoxic stress, and other cellular insults (Childs et al., 2015). Cellular senescence, as already introduced, also has some positive roles: apart from counteracting carcinogenesis, it can also have a tissue remodeling role

during programmed senescence in embryogenesis (Munoz-Espin et al., 2013) and in wound healing (Demaria et al., 2014).

Importantly, senescence seems to ensue when cells accumulate damage until a threshold is reached, whereby the cell permanently exits from the cell cycle. The amount of senescent cells increase as a function of age in humans (Dimri et al., 1995; Liu et al., 2009), which can be explained by both the increasing number of cells entering the senescence state but also by decreased ability of the organism to clear them, given the typical decline in immune system function with age (Munoz-Espin et al., 2013). Accumulation of senescent cells in aged tissues can disrupt tissue structure and function, and renders tissues more susceptible when hit by subsequent stresses. Aging and cancer onset share the same driver: they both ensue during ongoing genomic instability. Indeed, aging is one of the most important causes of cancer, with cancer incidence drastically raising with increased age (Siegel et al., 2015). Therefore, preserving genome stability is thought to be the main means to prevent cancer and delay/overcome aging diseases.

Selective clearance of senescent cells is currently being investigated as a mean to benefit the organism fitness and delay aging pathologies. Pioneering studies induced the selective apoptosis of $p16^{INK4a}$-expressing senescent cells in a mouse progeroid model and subsequently also in normally aging mice, which resulted in extended mouse lifespan, delayed onset of cancer and aging-related pathologies, and delayed decline of tissue aging (Baker et al., 2016; Baker et al., 2011). Additional studies that targeted senescent cells by pharmacological means demonstrated rejuvenation of stem cells within aged tissues and improvement of cardiovascular dysfunctions in aged and atherosclerotic mice (Chang et al., 2016; Roos et al., 2016). These studies propose therefore an alternative to the prevention of cellular senescence and aging onset, although their translation to human therapies has still to be approached.

1.6.2 Telomeropathies

Telomeropathies are inherited diseases whereby patients suffer from premature aging and display telomere shortening compared to age-matched controls. Poor immune system functionality and susceptibility to a subset of cancers are hallmarks of telomeropathies

(Armanios and Blackburn, 2012). They are characterized by different symptoms and age of onset, and can be caused by mutations in genes either directly or indirectly involved in telomere maintenance (Holohan et al., 2014).

Dyskeratosis congenita (DKC) and Idiopathic pulmonary fibrosis (IPF) are diseases caused by mutations in telomere maintenance mechanisms. DKC is a rare cancer-prone inherited bone marrow failure syndrome, caused in 60% of cases by mutations in genes involved in telomere maintenance (Mitchell et al., 1999). Mutations are found in the telomerase complex genes (as in TERC or TERT) or in Dyskerin (DKC1), a telomerase interactor (Parry et al., 2011). Patients suffer from organ failure, especially bone marrow failure during childhood, although pulmonary fibrosis is the most frequent cause of death in adulthood (Dokal, 2011). Importantly, patients display very short telomere length in leukocytes (Vulliamy et al., 2001). IPF is a more diffused manifestation of telomeropathy, whereby patients suffer from progressive lung failure, linked to fibrosis and inflammation (Armanios et al., 2007); 8-20% of familial cases are caused by mutations in TERT or TERC (Tsakiri et al., 2007). While telomerase disease patients do not display an overall progeroid phenotype, they suffer from progressive organ failure, with patterns of onset that reflect that of aging (Armanios and Blackburn, 2012). Furthermore, patients are predisposed to cancer, especially at highly proliferative tissues, with an eleven-fold higher risk for DKC patients compared to the non-affected population (Alter et al., 2009). In general, telomerase diseases are associated with the failure of highly proliferative tissues (e.g. the hematopoietic compartment), but also slow turnover tissues (e.g. lungs), which may have to be hit by a second insult in order to develop the disease, as modelled in mouse (Alder et al., 2011).

These diseases put forward a clear link between impaired telomere maintenance, excessive telomere shortening and accelerated organismal aging, thereby suggesting that telomere shortening must be tightly regulated in order not to induce premature cellular senescence onset and aging.

1.7 Rationale

A growing amount of studies allege the relevance of R-loops in several biological processes. R-loops were shown not only to be a cause of genome instability, but also to partake in physiological processes in the cell. Of note, recent studies have implicated R-loops in DSB repair, thereby suggesting that R-loops not only generate such lesions but are also involved in promoting their efficient repair (Ohle et al., 2016). An important step in this process was proposed to be the timely removal of the RNA-DNA hybrid itself to allow completion of repair, in a process that requires the action of RNase H enzymes (Amon and Koshland, 2016; Ohle et al., 2016). How RNase H enzyme activity is exquisitely regulated to ensure an equilibrium of these processes is still largely unknown.

A novel study implicated telomeric R-loops as an essential intermediate of telomere maintenance in ALT cancer cells, by boosting the recombinogenic potential of telomeres (Arora et al., 2014). This phenomenon seems to be highly conserved, as telomeric R-loops in telomerase negative *S. cerevisiae* also promote recombination between telomeres, thereby sustaining cellular viability (Balk et al., 2013; Yu et al., 2014). Understanding how telomeric R-loops are regulated and what is the role of RNase H enzymes in this context is of fundamental biological importance for understanding the molecular mechanisms of ALT telomere maintenance. Indeed, *S. cerevisiae* has proved to be an excellent model for the study of telomeric R-loops.

Notably, what renders telomeric R-loops relevant especially in pre-senescent yeast cells and ALT cancers is still to be understood. A differential regulation of their occurrence and/or a differential processing at normal compared to short/recombinogenic telomeres could be relevant factors in this context. Indeed, ALT telomeres are uniquely bound by RNase H1, an important factor that removes telomeric R-loops, suggesting that regulation of R-loops at ALT telomeres is an essential and distinctive process (Arora et al., 2014).

Finally, an important link that is to date still missing is the mechanism by which telomeric R-loops promote recombination, both at yeast and ALT telomeres. Indeed, collision of the replication machinery with stable R-loops results in replication stress and DSB formation, which can promote recombination (Hamperl and Cimprich, 2014; Santos-Pereira and Aguilera, 2015), but this has not been shown yet to happen at telomeres. Prompted by

novel studies, an important question to be answered is also how telomeric R-loops are taken care of during the recombination process.

This work aims to gain a deeper understanding of R-loop regulation at *S. cerevisiae* telomeres. A focus was set on the RNase H enzymes, being involved in telomeric R-loop restriction in *S. cerevisiae* (Balk et al., 2013) and at ALT telomeres (Arora et al., 2014), but also having been identified as novel important factors in damage repair processes (Amon and Koshland, 2016; Ohle et al., 2016). Furthermore, we investigated the role of the Rap1/Rif1/Rif2 complex, as its differential binding to long, compared to short, telomeres (McGee et al., 2010; Sabourin et al., 2007) could provide a molecular discrimination between long and short telomeres, which might be a critical step in the regulation of telomeric R-loops during senescence.

2. Materials and methods

2.1 Materials

2.1.1 Yeast strains used in this study

Strains derivatives of the S288C background:

Strain number	Name	Genotype	Source
yAL141	*tlc1 RNH1-TAP* het. diploid	*MATa/MATα; his3Δ1/his3Δ1; leu2Δ0/leu2Δ0; ura3Δ0/ura3Δ0; MET15/met15Δ0; TLC1/tlc1::NAT; RNH1/RNH1-TAP-HIS*	this study
yBL7	wild type	*MATa; his3Δ1; leu2Δ0; ura3Δ0; met15Δ0*	Euroscarf
yBL442	*RNH201-TAP*	*MATa; his3Δ1; leu2Δ0; ura3Δ0; met15Δ0; RNH201-TAP-HIS*	Open Biosystems
yAL12	*rif1 RNH201-TAP*	*MATa; his3Δ1; leu2Δ0; ura3Δ0; met15Δ0; RNH201-TAP-HIS; rif1::KAN*	this study
yAL14	*rif2 RNH201-TAP*	*MATa; his3Δ1; leu2Δ0; ura3Δ0; met15Δ0; RNH201-TAP-HIS; rif2::KAN*	this study
yAL24	*RNH201-TAP*	*MATα; his3Δ1; leu2Δ0; ura3Δ0; met15Δ0; RNH201-TAP-HIS*	this study
yAL13	*rif2 RNH201-TAP*	*MATα; his3Δ1; leu2Δ0; ura3Δ0; met15Δ0; RNH201-TAP-HIS; rif2::KAN*	this study
yAL11	*rif1 RNH201-TAP*	*MATα; his3Δ1; leu2Δ0; ura3Δ0; met15Δ0; RNH201-TAP-HIS; rif1::KAN*	this study
yAL213	*rnh1 RNH201-TAP* het. diploid	*MATa/MATα; his3Δ1/his3Δ1; leu2Δ0/leu2Δ0; ura3Δ0/ura3Δ0; MET15/met15Δ0; RNH1/rnh1::KAN; RNH201/RNH201-TAP-HIS*	this study
yAL212	*rnh201 RNH1-TAP* het. diploid	*MATa/MATα; his3Δ1/his3Δ1; leu2Δ0/leu2Δ0; ura3Δ0/ura3Δ0; MET15/met15Δ0; RNH201/rnh201::NAT; RNH1/RNH1-TAP-HIS*	this study
ySLG428	*rnh1 rnh201*	*MATa; his3Δ1; leu2Δ0; ura3Δ0; met15Δ0; rnh201::HYG; rnh1::KAN*	S. Luke-Glaser
yAL168	wt + *HA-RNH201*	*MATa; his3Δ1; leu2Δ0; ura3Δ0; met15Δ0;* pBL188	this study

yAL169	*RIF2-9MYC* + EV	*MATa; his3Δ1; leu2Δ0; ura3Δ0; met15Δ0; RIF2-9MYC-KAN*; pBL186	this study
yAL170	*RIF2-9MYC* + *HA-RNH201*	*MATa; his3Δ1; leu2Δ0; ura3Δ0; met15Δ0; RIF2-9MYC-KAN*; pBL188	this study
yAL224	*RIF2-9MYC* + EV	*MATa; his3Δ1; leu2Δ0; ura3Δ0; met15Δ0; RIF2-9MYC-KAN*; pBL183	this study
yAL225	*RIF2-9MYC* + *RNH201-HA*	*MATa; his3Δ1; leu2Δ0; ura3Δ0; met15Δ0; RIF2-9MYC-KAN*; pBL452	this study
yAL226	*RIF2-9MYC rnh202* + EV	*MATa; his3Δ1; leu2Δ0; ura3Δ0; met15Δ0; RIF2-9MYC-KAN; rnh202::HIS*; pBL183	this study
yAL227	*RIF2-9MYC rnh202* + *RNH201-HA*	*MATa; his3Δ1; leu2Δ0; ura3Δ0; met15Δ0; RIF2-9MYC-KAN; rnh202::HIS*; pBL452	this study
yAL228	*RIF2-9MYC rnh203* + EV	*MATa; his3Δ1; leu2Δ0; ura3Δ0; met15Δ0; RIF2-9MYC-KAN; rnh203::HIS*; pBL183	this study
yAL229	*RIF2-9MYC rnh203* + *RNH201-HA*	*MATa; his3Δ1; leu2Δ0; ura3Δ0; met15Δ0; RIF2-9MYC-KAN; rnh203::HIS*; pBL452	this study
yAL268	*RIF2-9MYC rnh202 rnh203* + EV	*MATa; his3Δ1; leu2Δ0; ura3Δ0; met15Δ0; RIF2-9MYC-KAN; rnh202::HIS; rnh203::HYG*; pBL183	this study
yAL269	*RIF2-9MYC rnh203 rnh202* + *RNH201-HA*	*MATa; his3Δ1; leu2Δ0; ura3Δ0; met15Δ0; RIF2-9MYC-KAN; rnh202::HIS; rnh203::HYG*; pBL452	this study
yAL250	*RIF1-9MYC* + EV	*MATa; his3Δ1; leu2Δ0; ura3Δ0; met15Δ0; RIF1-9MYC-NAT*; pBL186	this study
yAL251	*RIF1-9MYC* + *HA-RNH201*	*MATa; his3Δ1; leu2Δ0; ura3Δ0; met15Δ0; RIF1-9MYC-NAT*; pBL188	this study
yAL252	*RIF1-9MYC* + *RNH1-HA*	*MATa; his3Δ1; leu2Δ0; ura3Δ0; met15Δ0; RIF1-9MYC-NAT*; pBL352	this study
yAL254	*RIF2-9MYC* + *RNH1-HA*	*MATa; his3Δ1; leu2Δ0; ura3Δ0; met15Δ0; RIF2-9MYC-KAN*; pBL352	this study
yAL85	wt + EV	*MATa; his3Δ1; leu2Δ0; ura3Δ0; met15Δ0*; pBL189	this study
yAL86	wt + *RNH1-HA*	*MATa; his3Δ1; leu2Δ0; ura3Δ0; met15Δ0*; pBB39	this study
yAL89	*rif2* + EV	*MATα; his3Δ1; leu2Δ0; ura3Δ0; met15Δ0; rif2::KAN*; pBL189	this study
yAL90	*rif2* + *RNH1-HA*	*MATα; his3Δ1; leu2Δ0; ura3Δ0; met15Δ0; rif2::KAN*; pBB39	this study

yDB227	*RIF2^{AID}*	*MATa; his3Δ1; leu2Δ0; ura3Δ0; met15Δ0; leu2::AFB2::LEU2; RIF2-AID*-9MYC::HIS3; bar1::NAT*	D. Bonetti
yDB229	*RIF1^{AID}*	*MATa; his3Δ1; leu2Δ0; ura3Δ0; met15Δ0; leu2::AFB2::LEU2; RIF1-AID*-9MYC::HIS3; bar1::NAT*	D. Bonetti
yDB241	*RIF1^{AID} RIF2^{AID}*	*MATa; his3Δ1; leu2Δ0; ura3Δ0; met15Δ0; leu2::AFB2::LEU2; RIF1-AID*-9MYC::HIS3; RIF2-AID*-9MYC::HIS3*	D. Bonetti
yBL1004	*rif2 rnh1 rnh201* het. diploid	*MATa/MATα; his3Δ1/his3Δ1; leu2Δ0/leu2Δ0; ura3Δ0/ura3Δ0; MET15/met15Δ0; LYS2/lys2Δ0; RIF2/rif2::HYG; RNH1/rnh1::KAN; RNH201/rnh201::NAT*	B. Luke
yAL142	*tlc1 RIF2-9MYC RNH201-TAP* het. diploid	*MATa/MATα; his3Δ1/his3Δ1; leu2Δ0/leu2Δ0; ura3Δ0/ura3Δ0; MET15/met15Δ0; TLC1/tlc1::NAT; RIF2/RIF2-9MYC-KAN; RNH201/RNH201-TAP-HIS*	this study
yAL95	*tlc1* het. diploid	*MATa/MATα; his3Δ1/his3Δ1; leu2Δ0/leu2Δ0; ura3Δ0/ura3Δ0; MET15/met15Δ0; TLC1/tlc1::NAT*	this study
yAL204	*rif2 tlc1* het. diploid + EV	*MATa/MATα; his3Δ1/his3Δ1; leu2Δ0/leu2Δ0; ura3Δ0/ura3Δ0; MET15/met15Δ0; RIF2/rif2::HYG; TLC1/tlc1::HIS*; pBL189	this study
yAL205	*rif2 tlc1* het. diploid + *RNH1-HA*	*MATa/MATα; his3Δ1/his3Δ1; leu2Δ0/leu2Δ0; ura3Δ0/ura3Δ0; MET15/met15Δ0; RIF2/rif2::HYG; TLC1/tlc1::HIS*; pBB39	this study
yBB236	*rnh1 rnh201 est2* het. diploid	*MATa/MATα; his3Δ1/his3Δ1; leu2Δ0/leu2Δ0; ura3Δ0/ura3Δ0; MET15/met15Δ0; RNH1/rnh1::KAN; RNH201/rnh201::NAT; EST2/est2::HYG*	B. Balk
yAL196	*est2* + *EST2* + EV	*MATa; his3Δ1; leu2Δ0; ura3Δ0; met15Δ0; est2::KAN*; pBL354; pBL190	this study
yAL198	*est2* + *EST2* + *RNH1-HA*	*MATa; his3Δ1; leu2Δ0; ura3Δ0; met15Δ0; est2::KAN*; pBL354; pBL192	this study
yAL202	*est2* + *EST2* + *RNH1-HA*	*MATa; his3Δ1; leu2Δ0; ura3Δ0; met15Δ0; est2::KAN*; pBL354; pBL336	this study

yVK1290	*est2 rtt101 rnh201* het. diploid	*MATa/MATα; his3Δ1/his3Δ1; leu2Δ0/leu2Δ0; ura3Δ0/ura3Δ0; MET15/met15Δ0; EST2/est2::HIS; RTT101/rtt101::KAN; RNH201/rnh201::NAT*	V. Kellner
yAL296	*S-RNH1-TAP*	*MATa; his3Δ1; leu2Δ0; ura3Δ0; met15Δ0; NAT-S-RNH1-TAP-HIS*	this study
yAL297	*G2-RNH1-TAP*	*MATa; his3Δ1; leu2Δ0; ura3Δ0; met15Δ0; NAT-G2-RNH1-TAP-HIS*	this study
ySLG252	*RNH1-TAP*	*MATa; his3Δ1; leu2Δ0; ura3Δ0; met15Δ0; RNH1-TAP-HIS*	G. Pereira
yAL300	*rnh1*	*MATa; his3Δ1; leu2Δ0; ura3Δ0; met15Δ0; rnh1::KAN*	this study
yAL301	*rnh201 S-RNH1-TAP*	*MATα; his3Δ1; leu2Δ0; ura3Δ0; met15Δ0; rnh201::HYG; NAT-S-RNH1-TAP-HIS*	this study
yAL303	*rnh201 G2-RNH1-TAP*	*MATα; his3Δ1; leu2Δ0; ura3Δ0; met15Δ0; rnh201::HYG; NAT-G2-RNH1-TAP-HIS*	this study
yBL435	*rnh201*	*MATa; his3Δ1; leu2Δ0; ura3Δ0; met15Δ0; rnh201::KAN*	B. Luke
yAM196	*rnh1 rnh201*	*MATα; his3Δ1; leu2Δ0; ura3Δ0; met15Δ0; rnh1::KAN; rnh201::HYG*	A. Maicher
yVK1220	*rnh1 rnh201* + EV	*MATa; his3Δ1; leu2Δ0; ura3Δ0; met15Δ0; rnh1::KAN; rnh201::HYG*; pBL189	V. Kellner
yVK1221	*rnh1 rnh201* + *RNH1-HA*	*MATa; his3Δ1; leu2Δ0; ura3Δ0; met15Δ0; rnh1::KAN; rnh201::HYG*; pBB39	V. Kellner
yAL321	*rnh201 S-RNH1-TAP* + EV	*MATα; his3Δ1; leu2Δ0; ura3Δ0; met15Δ0; rnh201::HYG; NAT-S-RNH1-TAP-HIS*; pBL189	this study
yAL323	*rnh201 G2-RNH1-TAP* + EV	*MATα; his3Δ1; leu2Δ0; ura3Δ0; met15Δ0; rnh201::HYG; NAT-G2-RNH1-TAP-HIS;* pBL189	this study
yAL315	*rnh201* + EV	*MATa; his3Δ1; leu2Δ0; ura3Δ0; met15Δ0; rnh201::KAN*; pBL189	this study
yAL316	*rnh201* + *RNH1-HA*	*MATa; his3Δ1; leu2Δ0; ura3Δ0; met15Δ0; rnh201::KAN*; pBB39	this study
yAL325	*S-RNH1-TAP rnh201 rad52 est2* het. diploid	*MATa/α; his3Δ1/his3Δ1; leu2Δ0/leu2Δ0; ura3Δ0/ura3Δ0; met15Δ0/met15Δ0; RNH1/NAT-S-RNH1-TAP-HIS; RNH201/rnh201::HYG; RAD52/rad52::NAT; EST2/est2::KAN*	this study

yAL326	*rnh1 rnh201 rad52 est2* het. diploid	*MATa/α; his3Δ1/his3Δ1; leu2Δ0/leu2Δ0; ura3Δ0/ura3Δ0; met15Δ0/met15Δ0; RNH1/rnh1::HIS; RNH201/rnh201::HYG; RAD52/rad52::NAT; EST2/est2::KAN*	this study
yAL327	*G2-RNH1-TAP rnh201 rad52 est2* het. diploid	*MATa/α; his3Δ1/his3Δ1; leu2Δ0/leu2Δ0; ura3Δ0/ura3Δ0; met15Δ0/met15Δ0; RNH1/NAT-G2-RNH1-TAP-HIS; RNH201/rnh201::HYG; RAD52/rad52::NAT; EST2/est2::KAN*	this study
yAL352	*est2 rnh201 S-RNH1-TAP* het. diploid	*MATa/α; his3Δ1/his3Δ1; leu2Δ0/leu2Δ0; ura3Δ0/ura3Δ0; met15Δ0/met15Δ0; EST2/est2::KAN; RNH201/rnh201::HYG; RNH1/NAT-S-RNH1-TAP-HIS*	this study
yAL353	*est2 rnh201 G2-RNH1-TAP* het. diploid	*MATa/α; his3Δ1/his3Δ1; leu2Δ0/leu2Δ0; ura3Δ0/ura3Δ0; met15Δ0/met15Δ0; EST2/est2::KAN; RNH201/rnh201::HYG; RNH1/NAT-G2-RNH1-TAP-HIS*	this study
yAL350	*RNH202-TAP*	*MATa; his3Δ1; leu2Δ0; ura3Δ0; met15Δ0; RNH202-TAP-HIS*	Open Biosystems
yAL351	*S-RNH202-TAP*	*MATa; his3Δ1; leu2Δ0; ura3Δ0; met15Δ0; NAT-S-RNH202-TAP-HIS*	this study
yAL206	*rnh202*	*MATα; his3Δ1; leu2Δ0; ura3Δ0; met15Δ0;* Rnh202::KAN	Dharmacon
yAL365	*rnh1 rnh202*	*MATa; his3Δ1; leu2Δ0; ura3Δ0; met15Δ0; rnh1::KAN; rnh202::HIS*	this study
yAL379	*rnh1 S-RNH202-TAP*	*MATα; his3Δ1; leu2Δ0; ura3Δ0; met15Δ0; rnh1::KAN; NAT-S-RNH202-TAP-HIS*	this study
yAL373	*rnh1 RNH202-TAP*	*MATa; his3Δ1; leu2Δ0; ura3Δ0; met15Δ0; rnh1::KAN; RNH202-TAP-HIS*	this study
yAL361	*est2 S-RNH202-TAP* het. diploid	*MATa/α; his3Δ1/his3Δ1; leu2Δ0/leu2Δ0; ura3Δ0/ura3Δ0; met15Δ0/met15Δ0; EST2/est2::KAN; RNH202/NAT-S-RNH202-TAP-HIS*	this study
yAL362	*est2 rnh202* het. diploid	*MATa/α; his3Δ1/his3Δ1; leu2Δ0/leu2Δ0; ura3Δ0/ura3Δ0; met15Δ0/met15Δ0; EST2/est2::KAN; RNH202/rnh202::HIS*	this study

Strains derivatives of the FY23 background:

Strain number	Name	Genotype	Source
yAL174	wt + EV	*MATa; ura3-52; trp1-Δ63; leu2Δ1; RAP1-mCherry-KAN; 2MS2-tel6R*; pBL449; pBL211	this study
yAL175	wt + *RNH1-HA*	*MATa; ura3-52; trp1-Δ63; leu2Δ1; RAP1-mCherry-KAN; 2MS2-tel6R*; pBL449; pBL352	this study
yAL176	*rif2* + EV	*MATa; ura3-52; trp1-Δ63; leu2Δ1; RAP1-mCherry-KAN; 2MS2-tel6R; rif2::HYG*; pBL449; pBL211	this study
yAL177	*rif2* + *RNH1-HA*	*MATa; ura3-52; trp1-Δ63; leu2Δ1; RAP1-mCherry-KAN; 2MS2-tel6R; rif2::HYG*; pBL449; pBL352	this study

2.1.2 Plasmids used in this study

Code	Name	Description	Source
pBL186		pRS423 *pGAL*, 2µ, *HIS3*	M. Peter
pBL188		pRS423 *pGAL-HA-RNH201*, 2µ, *HIS3*	this study
pBL183	BG1805	BG1805 *pGAL*, 2µ, *URA3*	B. Grayhack
pBL452		BG1805 *pGAL-RNH201-HA-6HIS-Prot3C-Prot A(ZZ)*, 2µ, *URA3*	Dharmacon
pBL352		pRS425 *pGAL-RNH1-HA*, 2µ, *LEU2*	this study
pBL189		pRS426 *pGPD*, 2µ, *URA3*	(Balk et al., 2013)
pBB39		pRS426 *pGPD-RNH1-HA*, 2µ, *URA3*	(Balk et al., 2013)
pBL211		pRS425 *pGAL*, 2µ, *LEU2*	M. Peter
pBL449		*pGPD-MS2BP-GFP*, 2µ, *TRP1*	P. Chartrand
pBL190		pRS423 *pGPD*, 2µ, *HIS3*	M. Peter
pBL192		pRS423 *pGPD-RNH1-HA*, 2µ, *HIS3*	this study
pBL336	pT44	*pGPD-RNH1-HA*, CEN, *HIS3*	T. Teixeira
pBL354		pRS416, *EST2*, CEN, *URA3*	R. Knies

pBL97		pRS316, CEN, *URA3*	M. Peter
pBL399		pRS316, *RNH201-P45D-Y219A*, CEN, *URA3*	this study
pBL423		pSP100, contains probe for Southern Blot	M.P. Longhese
pBL327	pYM18	contains *9MYC-KAN* cassette	(Janke et al., 2004)
pBL334	pYM21	contains *9MYC-NAT* cassette	(Janke et al., 2004)
pBL491	pRDK1597	contains *S NAT* cassette	(Hombauer et al., 2011)
pBL492	pGIK43	contains *G2 NAT* cassette	(Karras and Jentsch, 2010)

2.1.3 Oligonucleotides used in this study

Code	Sequence 5'→3'	Use
oBL295	CGGTGGGTGAGTGGTAGTAAGTAGA	1L fw qPCR
oBL296	ACCCTGTCCCATTCAACCATAC	1L rev qPCR
oLK57	GGGTAACGAGTGGGGAGGTAA	15L fw qPCR
oLK58	CAACACTACCCTAATCTAACCCTGT	15L rev qPCR
oLK49	GGCTTGGAGGAGACGTACATG	6Y' fw qPCR
oLK50	CTCGCTGTCACTCCTTACCCG	6Y' rev qPCR
oAM47	TCCAATTGTTCCTCGTTAAG	18S rDNA fw qPCR
oAM48	ATTCAGGGAGGTAGTGACAA	18S rDNA rev qPCR
oAL22	AGAAAAACCAGCGTCTTCCACTTAAGTTAACTCGAAAAGTACATGATAGACGTACGCTGCAGGTCGAC	*RIF2-9MYC* fw
oAL23	TGCCATCTCTTTGTATTGTTCGAACTCTTTCAAAAGACCTTGGTAATTTAATCGATGAATTCGAGCTCG	*RIF2-9MYC* rev
oAL24	CTCGCTTGTCACATGCCAGT	check *RIF2-9MYC* fw
oLP1	TTGTAATTAATTTATTGCCATTTTGATCTATTCTACATACTAACAATCAATCGATGAATTCGAGCTCG	*RIF1-9MYC* fw
oLP2	ATTATTAGATTTTATGATGAGGCTCGAATATTACTCAAACAGGGATAATGATATGAATCGTACGCTGCAGGTCGAC	*RIF1-9MYC* rev
oLP3	GAACAACCCGAAGTTGCTGA	check *RIF1-9MYC* fw

oBL29	CTGCAGCGAGGAGCCGTAAT	NAT KAN rev
oAL47	GTTAAAGTGTCACTCCTTGCTTATCGAAGGAACTATCGATTCCTAATTATGCGTACGCTGCAGGTCGAC	*S*- and *G2-RNH1* fw
oAL48	GATCCCAGTTTCCCTGCCCTTTCTAACCGCGTAGAAGTTCCCTTGCCTTGCCAATTTAACAACATTTTGTGATAA	*S-RNH1* rev
oAL49	GATCCCAGTTTCCCTGCCCTTTCTAACCGCGTAGAAGTTCCCTTGCCTTGCATCAGTTTCACTTTCGGTATTTCT	*G2-RNH1* rev
oAL53	CGGTTGATCTTGGCTGTAG	check *S*- and *G2-RNH1* fw
oAL54	TCGCTTGCTCGTAGCTGT	check *S*- and *G2-RNH1* rev
oAL61	TCTGTCGCAATAGTTGACTTTCTTTTCTGGCCTCTCGAACAAAAAGCATGCGTACGCTGCAGGTCGAC	*S-RNH202* fw
oAL62	TCGTCTGGTAAAATTATTAGTCGTTCTTCCCCCCCAATGTTGGAAACGGTCAATTTAACAACATTTTGTGATAA	*S-RNH202* rev
oAL64	CAAGTTTGTCAAAAGCACG	check *S-RNH202* fw
oAL65	GCTCGATACGAGGTTTGG	check *S-RNH202* rev

2.1.4 Liquid media

YPD medium (1 l)	
Peptone	17.6 g
Bacto Yeast Extract	8.8 g
ddH_20	900 ml
Autoclave	20 min at 121˚C
20% glucose (autoclaved, 2% final)	100 ml

SC medium (1 l)	SC - aa	RAFF 2%	RAFF 1%/GAL 2%
Yeast Synthetic Complete Medium Supplemented without aminoacids	1.9 g	1.9 g	1.9 g
Yeast Nitrogen Base without aminoacids	6.7 g	6.7 g	6.7 g
Raffinose x 5 H_2O		23.6 g	11.8 g
ddH_2O	900 ml	1 l	900 ml
Autoclave	20 min at 121˚C		
20% glucose (autoclaved, 2% final)	100 ml		
20% galactose (sterile filtered)			100 ml

LB medium (1 l)	no drug	with carbenicillin
NaCl	10 g	10 g
Bacto Tryptone	10 g	10 g
Bacto Yeast Extract	5 g	5 g
NaOH to adjust pH to 7.0		
ddH_2O	to 1 l	to 1 l
Autoclave	20 min at 121˚C	
Carbenicillin 100 mg/ml (100 µg/ml final)		1 ml

Sporulation medium (1 l)	
Zinc acetate (5 mg/ml)(0.005% final)	10 ml
Potassium acetate (1% final)	10 g
ddH_2O	990 ml
Autoclave	20 min at 121˚C

2.1.5 Agar plates

YPD agar plates (1 l)	no drug	NAT	KAN	HYG
Peptone	100 g	100 g	100 g	100 g
Bacto Yeast Extract	50 g	50 g	50 g	50 g
20% glucose (2% final)	100 ml	100 ml	100 ml	100 ml
Agar	100 g	100 g	100 g	100 g
ddH_2O	to 1 l	to 1 l	to 1 l	to 1 l
Autoclave	20 min at 121˚C			
NAT 100 mg/ml (100 µg/ml final)		1 ml		
KAN (G418) 50 mg/ml (250 µg/ml final)			5 ml	
HYG 100 mg/ml (300 µg/ml final)				3 ml

More than one drug can be added to the same plates.

SC plates (1 l)	SC complete	SC - aa	SC
Yeast Synthetic Complete Medium Supplemented without aminoacids	1.9 g	1.9 g	
Yeast Nitrogen Base without aminoacids	6.7 g	6.7 g	6.7 g
Agar	24 g	24 g	24 g
ddH_2O	890 ml	900 ml	900 ml
100x amino acid	10 ml		
Autoclave	20 min at 121˚C		
20% glucose (autoclaved, 2% final)	100 ml	100 ml	100 ml

SC -HIS + 5-FOA plates (500 ml)	
Yeast Synthetic Complete Medium Supplemented without uracil, histidine, leucine and tryptophan	0.95 g
Yeast Nitrogen Base without aminoacids	3.35 g
Uracil	0.025 g
Glucose	10 g
Agar	10 g
ddH_2O	385 ml
Autoclave	20 min at 121˚C
Leucine 50X	10 ml
Tryptophan 100X	5 ml
5-FOA	0.5 g in 100 ml ddH_2O at 65˚C

LB plates (1 l)	no drug	with ampicillin
Bacto Yeast Extract	5 g	5 g
Bacto Tryptone	10 g	10 g
NaCl	10 g	10 g
NaOH to adjust pH to 7.0		
Agar	15 g	15 g
ddH_2O	to 1 l	to 1 l
Autoclave	20 min at 121˚C	
Ampicillin		100 µg/ml

Pre-sporulation plates (1l)	
Standard nutrient broth	30 g
Bacto Yeast Extract	10 g
Agar	20 g
ddH_2O	750 ml
Autoclave	20 min at 121˚C
20% glucose (autoclaved, 5% final)	250 ml

2.1.6 Buffers

LiAc-Mix (100 ml)	
1 M LiAc (sterile, 0.1 M final)	10 ml
10x TE (sterile)	10 ml
ddH_2O	80 ml

PEG-Mix (100 ml)	
Polyethylene glycol 400	40 g
Li-Ac Mix	to 100 ml
Autoclave	20 min at 121˚C

10x PBS (1 l)	
NaCl (1.37 M final)	80 g
KCl (30 mM final)	2 g
Na_2HPO_4 x 2 H_2O (80 mM final)	14.4 g
KH_2PO_4 (20 mM final)	2.4 g
HCl to adjust pH to 7.4	
ddH_2O	to 1 l
Autoclave	20 min at 121˚C

FA Lysis Buffer (1 l)	-SOD	+SOD
1 M HEPES pH 7.5 (50 mM final)	50 ml	50 ml
5 M NaCl (140 mM final)	28 ml	28 ml
0.5 M EDTA pH 8.0 (1 mM final)	2 ml	2 ml
Triton X-100 (1% final)	10 ml	10 ml
Sodium deoxycholate (0.1% final)		1 g
ddH_2O	910 ml	910 ml

FA Lysis Buffer 500 (1 l)	
1 M HEPES pH 7.5 (50 mM final)	50 ml
5 M NaCl (0.5 M final)	100 ml
0.5 M EDTA pH 8.0 (1 mM final)	2 ml
Triton X-100 (1% final)	10 ml
Sodium deoxycholate (0.1% final)	1 g
ddH_2O	838 ml

Buffer III (1 l)	
1 M Tris-HCl pH 8.0 (10 mM final)	10 ml
0.5 M EDTA pH 8.0 (1 mM final)	2 ml
1 M LiCl (250 mM final)	250 ml
NP-40 (1% final)	10 ml
Sodium deoxycholate (1% final)	10 g
ddH_2O	728 ml

10X TE (1 l)	
1 M TRIS pH 7.5 (0.1 M final)	100 ml
0.5 M EDTA pH 8 (10 mM final)	20 ml
ddH_2O	1 l
Autoclave	20 min at 121˚C

Elution Buffer B (1 l)	
1 M Tris-HCl pH 7.5 (50 mM final)	50 ml
20% SDS (1% final)	50 ml
0.5 M EDTA pH 8.0 (10 mM final)	20 ml
ddH_2O	880 ml

10X TBE (1 l)	
Tris base (0.89 M final)	108 g
Boric acid (0.89 M final)	55 g
0.5 M Na_2EDTA pH 8.0 (20 mM final)	40 ml
ddH_2O	to 1 l
Sterile filter	

Solution 1 (20 ml)	
10 M NaOH (1.85 M final)	3.7 ml
14.34 M β-mercaptoethanol (1.09 M final)	1.52 ml
ddH_2O	14.78 ml

Solution 2 (20 ml)	
100% Trichloroacetic acid (50% final)	10 ml
ddH_2O	10 ml

Solution 3 (20 ml)	
100% Acetone	20 ml

Urea Buffer (10 ml)	
1M Tris-HCl pH 6.8 (120 mM final)	1.2 ml
70% Glycerol (5% final)	714 µl
Urea (8 M final)	4.8 g
14.34 M β-mercaptoethanol (143 mM final)	100 µl
20% SDS (8% final)	4 ml
ddH_2O	to 10 ml
Bromophenol blue to color	

10x SDS running buffer (1 l)	
SDS (0.1% final)	10 g
Tris base (250 mM final)	30.3 g
Glycine (1,92 M final)	144.1 g
ddH_2O	to 1 l
Sterile filter	

Transfer buffer (100 ml)	
5x Bio-Rad transfer buffer	20 ml
Absolute ethanol (20% final)	20 ml
ddH_2O	60 ml

PBS-Tween (1 l)	
10x PBS	100 ml
Tween-20 (0.1% final)	1 ml
ddH_2O	to 1 l

Blocking buffer (50 ml)	
PBS-Tween	50 ml
Skim milk powder (5% final)	2.5 g

IP buffer (50 ml)	- NP40	+ NP40
1 M Tris pH 7.5 (50 mM final)	2.5 ml	2.5 ml
5 M Nacl (150 mM final)	1.5 ml	1.5 ml
1 M $MgCl_2$ (5 mM final)	250 µl	250 µl
NP40 (0.2% final)		100 µl
ddH_2O	44 ml	43.9 ml
Protease Inhibitor Cocktail tablets	4	4
200 mM PMSF (1 mM final)	250 µl	250 µl

20X SSC (1 l)	
NaCl (3 M final)	175.3 g
Sodium citrate tribasic dihydrate (0.3 M final)	88.2 g
HCl to adjust pH to 7.0	
ddH_2O	to 1 l

Denaturing solution (1 l)	
NaOH (0.4 M final)	16 g
NaCl (0.6 M final)	35.1 g
ddH_2O	to 1 l

Neutralizing solution (1 l)	
Trizma base (1 M final)	121.4 g
NaCl (1.5 M final)	87.75 g
HCl to adjust pH to 7.4	
ddH_2O	to 1 l

Church Buffer (500 ml)	
1 M $NaPO_4$ pH 7.4 (0.5 M final)	250 ml
0.5 M EDTA pH 8.0 (1 mM final)	1 ml
20% SDS (7% final)	175 ml
BSA (1% final)	5 g
ddH_2O	74 ml

Washing solution (100 ml)	
1 M $NaPO_4$ pH 7.2 (0.2 M final)	20 ml
20% SDS (1% final)	5 ml
ddH_2O	75 ml

2.1.7 Enzymes

Name	Source
Proteinase K	Qiagen
RNase A	Thermo Scientific
DNase I (RNase free)	Qiagen
Lyticase	Sigma-Aldrich
Zymolyase 100T	Zymo Research
XhoI	New England Biolabs
EcoRI-HF	New England Biolabs
2X Phusion HF Mastermix GC buffer	New England Biolabs
2X Taq Mastermix	New England Biolabs

2.1.8 Primary antibodies used in this study

name	Source	Application	Amount used
Mouse monoclonal anti-MYC-tag (9B11)	Cell Signaling/New England Biolabs 2276S	ChIP and western blot	3 µl for ChIP, 1:1,000 dilution for WB
Rabbit peroxidase anti-peroxidase soluble complex	Sigma-Aldrich P1291	western blot	1:1,000 dilution
Mouse monoclonal anti-phosphoglycerate kinase (22C5D8)	Invitrogen 459250	western blot	1:200,000 dilution
Mouse monoclonal anti-HA.11 (16B12)	Covance MMS-101P-1000	western blot	1:2,000 dilution
Rabbit polyclonal anti-Rap1 (y-300)	Santa Cruz sc-20167	western blot	1:1,000 dilution

Mouse monoclonal S9.6 anti-RNA-DNA hybrid	Kerafast ENH001	ChIP	2 µl
Rabbit polyclonal anti-Sic1 (FL-284)	Santa Cruz sc-50441	western blot	1:500 dilution
Rabbit polyclonal anti-Clb2 (y-180)	Santa Cruz sc-9071	western blot	1:1,000 dilution

2.1.9 Secondary antibodies used in this study

Name	Source	Application	Amount used
Goat Immun-Star anti-mouse (GAM)-HRP conjugate	Bio-Rad 170-5047	western blot	1:3,000 dilution
Goat Immun-Star anti-rabbit (GAR)-HRP conjugate	Bio-Rad 170-5046	western blot	1:3,000 dilution

2.1.10 Ladders

Name	Source	Use
1 kb DNA ladder	New England Biolabs	agarose gels
100 bp DNA ladder	New England Biolabs	agarose gels
Prestained Protein Marker, Broad range (11-190 kDa)	New England Biolabs	western blot
Prestained Protein Marker, Broad range (7-175 kDa)	New England Biolabs	western blot

2.1.11 Kits

Name	Source
DECAprime II DNA Labeling Kit	Thermo Scientific
DyNAmo Flash SYBR Green qRT-PCR Kit	Thermo Scientific
Puregene Yeast/Bact. Kit B	Qiagen
QIAprep Spin Miniprep Kit	Qiagen
QIAquick Gel Extraction Kit	Qiagen
QIAquick PCR Purification Kit	Qiagen
Trans-Blot Turbo RTA Midi Nitrocellulose Transfer Kit	Bio-Rad

2.1.12 Electronic devices

Name	Source
Analytical Balance ED224S	Sartorius
Balance Extend ED822-0CE	Sartorius
BD FACSVerse	Becton Dickinson
Benchtop Shaker Excella E24	Eppendorf
BioRuptor Pico	Diagenode
Bioruptor Water Cooler Minichiller	Diagenode
Centrifuge 5430 R	Eppendorf
Centrifuge 5810 R	Eppendorf
ChemiDoc Touch Imaging System	Bio-Rad
Chromatography Refrigerator FRCR4504V	Thermo Scientific
Dissection Microscope MSM 400	Singer Instruments
FastPrep-25	MP Biomedicals
Freezer LGex 3410 MediLine	Liebherr
Freezer LGUex 1500 MediLine	Liebherr
Refrigerator LKUexv1610-21 MediLine	Liebherr
Refrigerator /Freezer LCv 4010 MediLine	Liebherr

Heraeus Pico 17 Centrifuge	Thermo Scientific
Hybridisation Oven OV3	Biometra
IKA VORTEX genius 3	Sigma-Aldrich
Incubator Heratherm IMC18	Thermo Scientific
Incubator Heratherm IMH60	Thermo Scientific
Leica DM1000 LED	Leica
Magnetic Stirrer D-6010	NeoLab
Micro-Cubes Ice Machine	Wessamat
Microwave R941	SHARP
Mini Centrifuge CD1008	Phoenix Instrument
NanoDrop 2000	Thermo Scientific
pH Meter PB-11	Sartorius
PowerPac Basic	Bio-Rad
Real Time PCD Detection system CFX384 Touch	Bio-Rad
Shaker Duomax 1030	Heidolph
Shaker Multitron Standard	Infors HT
Sonifier 450	Branson
Spectrophotometer Ultrospec 2100 pro	Biochrom
Test-tube Rotator	Labinco
Thermal Cycler C1000 Touch	Bio-Rad
Thermal Printer DPU-414	Seiko Instruments
ThermoMixer F1.5	Eppendorf
Trans-Blot turbo Starter System	Bio-Rad
Typhoon FLA 9500	GE Healthcare
Ultra-Low Temperature Freezer MDF-U74V	Sanyo
Ultra-Low Temperature Freezer V86-8301	Ewald
Ultrapure Water System GenPure	TKA
UV Stratalinker 2400	Stratagene
Water Bath Shaker New Brunswick Innova 3100	Eppendorf

2.1.13 Software

Name	Source
Adobe Illustrator CC 21.1.0	Adobe
CFX Manager 3.1	Bio-Rad
EndNote X5	Thomson Reuters
FACSuite 1.0.5	Becton Dickinson
FileMaker Pro 13.0v1	FileMaker Inc.
Image Lab 5.2	Bio-Rad
ImageJ 1.6.0	NIH
Microsoft Office for Windows 2013	Microsoft
Prism 7	GraphPad
SnapGene 3.3.4	GSL Biotech

2.1.14 Additional Reagents

Name	Source
5-FOA	Zymo Research
3-Indoleacetic acid	Sigma-Aldrich
Acetone	Sigma-Aldrich
Agarose	Sigma-Aldrich
β-mercaptoethanol	Sigma-Aldrich
Bovine Serum Albumin, Acetylated	Promega
Bradford Solution	AppliChem
Carbecillin Disodium Salt	Sigma-Aldrich
ClonNat	WERNER BioAgents
cOmplete Mini EDTA-free Protease Inhibitor Cocktail Tablets	Roche
Concanavalin A	Sigma-Aldrich
CutSmart Buffer	New England Biolabs
dATP [α-^{32}P]	Perkin Elmer

Dimethyl sulfoxide (DMSO)	Sigma-Aldrich
Ethanol absolute	Sigma-Aldrich
Formaldehyde 37%	AppliChem
G418 Disulfate Solution	AppliChem
Glycerol	Grüssing
Glycine	AppliChem
HEPES buffer pH 7.5	AppliChem
Hydoxyurea	Sigma-Aldrich
Hygromycin B Gold Solution	InvivoGen
IgG Sepharose 6 Fast Flow	GE Healthcare
Isopropanol	Sigma-Aldrich
Methyl methanesulfonate	Sigma-Aldrich
Nonidet P40	AppliChem
nProtein A Sepharose 4 Fast Flow	GE Healthcare
Pierce Anti-HA Magnetic Beads	Thermo Scientific
Poly(ethylene glycol) (PEG 400)	Sigma-Aldrich
Ponceau S Solution	Sigma-Aldrich
Reagents for yeast media	Sigma-Aldrich
RedSafe Nucleic Acid Staining Solution	iNtRON Biotechnology
SC Medium Supplemented without amino acids	MP Biomedicals
SDS Solution 20%	AppliChem
Sodium deoxycholate (SOD)	Sigma-Aldrich
SuperSignal West Dura Extended Duration Substrate	Thermo Scientific
SuperSignal West Pico Chemiluminescent Substrate	Thermo Scientific
SYTOX Green	Thermo Scientific
Trichloroacetic acid (TCA)	Sigma-Aldrich
Triton X-100	Sigma-Aldrich
Tween-20	Sigma-Aldrich
Urea	Sigma-Aldrich
Water Molecular Biology Reagent	Sigma-Aldrich
Yeastmarker Carrier DNA	Clontech

α-factor	Zymo Research

2.1.15 Additional Materials

Name	Source
15 ml Bioruptor Pico Tubes and sonication beads	Diagenode
96-Well Plates	Corning
Amersham Hybond-NX Nylon Membrane	GE Healthcare
Amersham Protran Premium Nitrocellulose Membrane	GE Healthcare
Hard-Shell 384-Well PCR plates	Bio-Rad
Magnetic Rack DynaMag-2	Thermo Scientific
Microseal ‘B’ PCR Adhesive Seal	Bio-Rad
Mini-PROTEAN TGX Precast Gels 4-15%	Bio-Rad
Mini-PROTEAN TGX Precast Gels 7.5%	Bio-Rad
Nunc 8-Well Chambered Coverglass	Lab-Tek
Replica plater for 96-Well plate	Sigma-Aldrich
TubeSpin Bioreactor 50	TPP

2.2 Methods

2.2.1 Yeast mating and sporulation

Yeast cells were mated by patching haploid strains of opposite mating types (Mata and MATα) on YPD plates, which were incubated overnight at the appropriate temperature. Diploids were selected by streaking out the cells for single colonies on double-selection plates, which were incubated at the appropriate temperature for 2-3 days. Single clones of diploids were then patched on pre-sporulation plates and grown overnight at the appropriate temperature, after which cells were transferred into 3 ml sporulation medium and incubated at 23°C, until sporulation was efficiently induced (3-4 days). 10 µl of cultures were mixed with 10 µl of lyticase, and after incubation at room temperature for 15 min, cells were transferred onto YPD or selective plates and tetrads were dissected by micromanipulation. Plates were then grown for 3 days at the appropriate temperature.

2.2.2 Transformation of yeast

25 ml of exponentially growing liquid yeast cultures (OD_{600} 0.4-0.8) were spun down at 3,000 rpm for 3 min and cells were washed with 5 ml LiAc-mix. Cells were spun down again at 3,000 rpm for 3 min and resuspended in 250 µl of the same solution. The transformation reaction was composed of 100 µl of competent cells, 700 µl of PEG-mix, 10 µl of Yeastmarker Carrier DNA and 0.5 µg of plasmid or 7-10 µl of PCR product, and incubated 30 min rotating at room temperature. After a 15 min heat shock at 42˚C, cells were spun down at 3,000 rpm for 1 min and resuspended in 300 µl of YPD, and subsequently incubated for 30 min at 30˚C (for plasmid transformation) or up to 6 hours (for integration). Cells were then plated on appropriate selective plates and grown at 30˚C for 2-3 days.

2.2.3 Transformation of bacteria

0.5 µg of plasmid were added to 50 µl of competent DH5α *E. coli*, mixed gently and incubated for 30 min on ice. After a 1 min heat shock at 42°C, the reactions were incubated for 1 min on ice and subsequently 300 µl of LB media were added. The reactions were then incubated for 30 min at 37°C and finally 100 µl of the reactions were plated on LB plates containing ampicillin and incubated overnight at 37°C.

2.2.4 Construction of strains

2.2.4.1 Generation of 9myc C-terminally tagged Rif2

The *RIF2-9MYC* strain was created by amplifying the *9MYC-KAN* cassette by PCR from the plasmid pBL327 by using the oligonucleotides oAL22 and oAL23, which were designed in accordance to (Janke et al., 2004). The PCR reaction was composed of 100 ng pBL327, 25 µl Phusion HF 2x Mastermix, 0.64 µl of each 5 µM oligonucleotide and water to 50 µl. The PCR was performed as follows: 98°C 30 sec, 98°C 10 sec, 72°C 30 sec, 72°C 1 min (to step 2 x 34 times), 72°C 10 min. Correct PCR product length was verified by agarose gel, and subsequently 10 µl of cassette were transformed in yBL7 and plated on YPD + KAN plates, which were grown at 30°C for 3 days. Colonies that grew were restreaked on YPD + KAN to exclude false positives, and those which could re-grow were verified for correct integration by PCR on genomic DNA, which was extracted with Puregene Yeast/Bact. Kit B. The PCR to verify correct construct integration and for subsequent sequencing was performed with the oligonucleotides oAL24 and oBL29, and the reaction was composed of 200 ng genomic DNA, 5 µl of each 5 µM oligonucleotide, 12.5 µl Phusion HF 2X Mastermix and water to 25 µl. The PCR was performed as follows: 98°C 30 sec, 98°C 10 sec, 64°C 30 sec, 72°C 1 min 30 sec (to step 2 x 34 times), 72°C 10 min. Correct product length was verified by agarose gel and sequencing was performed on the PCR product purified with QIAquick PCR Purification Kit, using oAL24 and oBL29. Expression of the tagged protein was confirmed by western blot.

2.2.4.2 Generation of 9myc C-terminally tagged Rif1

The *RIF1-9MYC* strain was created by amplifying by PCR the *9MYC-NAT* cassette from the plasmid pBL334 by using the oligonucleotides oLP1 and oLP2, which were designed in accordance to (Janke et al., 2004). The PCR reaction was composed of 100 ng pBL334, 25 µl Phusion HF 2x Mastermix, 0.64 µl of each 5 µM oligonucleotide, 3% DMSO and water to 50 µl. The PCR was performed as follows: 98°C 30 sec, 98°C 10 sec, 62°C 30 sec, 72°C 1 min 10 sec (to step 2 x 34 times), 72°C 10 min. Correct PCR product length was verified by agarose gel and subsequently 10 µl of cassette were transformed in yBL7 and plated on YPD + NAT plates, which were grown at 30°C for 3 days. Grown colonies were restreaked on YPD + NAT to exclude false positives, and those which could re-grow were verified for correct integration by PCR on genomic DNA, which was extracted with Puregene Yeast/Bact. Kit B. The PCR to verify correct construct integration and for subsequent sequencing was performed with the oligonucleotides oLP3 and oBL29, and was composed of 200 ng genomic DNA, 5 µl of each 2.5 µM oligonucleotide, 12.5 µl Phusion HF 2X Mastermix and water to 25 µl. The PCR was performed as follows: 98°C 30 sec, 98°C 10 sec, 65°C 30 sec, 72°C 1 min (to step 2 x 34 times), 72°C 5 min. Correct PCR product length was verified by agarose gel and sequencing was performed on the PCR product purified with QIAquick PCR Purification Kit, using oLP3 and oBL29. Expression of the tagged protein was confirmed by western blot.

2.2.4.3 Generation of S- and G2-RNH1-TAP alleles

The *S*- and *G2-RNH1-TAP* alleles were created by amplifying the *S* cassette (containing the *CLB6* promoter, the first 585 bp of *CLB6* and the *NAT* resistance cassette) from the plasmid pBL491 with the oligonucleotides oAL47 and oAL48, or the *G2* cassette (containing the *CLB2* promoter, the first 540 bp of *CLB2* and the *NAT* resistance cassette) from the plasmid pBL492 with the oligonucleotides oAL47 and oAL49. The PCR reactions were composed of 100 ng plasmid DNA, 0.64 µl of each 5 µM oligonucleotide, 25 µl Phusion HF 2x Mastermix and water to 50 µl. The PCRs were performed as in (Janke et al., 2004): 97°C 3 min, 97°C 1 min, 54°C 30 sec, 72°C 2 min 40 sec (to step 2 x 10 times), 97°C 1 min, 54°C 30 sec, 72°C 2 min 40 sec (to step 5 x 20 times, extending the elongation time of 20 sec per cycle). Correct cassette lengths were verified by agarose gel, and

ySLG252 was transformed independently with 7.5 µl of each cassette, and plated on YPD + NAT plates, which were grown at 30°C for 3 days. Grown colonies were restreaked on YPD + NAT to exclude false positives, and those which could re-grow were verified for correct integration by PCR on genomic DNA, with the oligonucleotide pairs oAL53 + oAL54 and oAL53 + oBL29. The PCR reactions were composed of: 2 µl of cells (boiled 10 min in 0.02 N NaOH), 2 µl of each 5 µM oligonucleotide, 10 µl Taq 2x Mastermix and water to 20 µl. The PCRs were performed as follows: 98°C 3 min, 98°C 10 sec, 52°C 30 sec, 68°C 4 min (to step 2 x 34 times), 68°C 5 min. Correct product lengths were verified on an agarose gel, and correct expression of *RNH1* in the desired cell cycle phases was assayed by western blot (Figure 15).

2.2.4.4 Generation of the S-RNH202-TAP allele

The *S-RNH202-TAP* allele was created by amplifying the *S* cassette (containing the *CLB6* promoter, the first 585 bp of *CLB6* and the *NAT* resistance cassette) from the plasmid pBL491 with the oligonucleotides oAL61 and oAL62. The PCR reaction was composed of 100 ng pBL491, 0.64 µl of each 5 µM oligonucleotide, 25 µl Phusion HF 2x Mastermix and water to 50 µl. The PCR program was as in (Janke et al., 2004): 97°C 3 min, 97°C 1 min, 54°C 30 sec, 72°C 2 min 40 sec (to step 2 x 10 times), 97°C 1 min, 54°C 30 sec, 72°C 2 min 40 sec (to step 5 x 20 times, extending the elongation time of 20 sec per cycle). Correct cassette length was verified by agarose gel, and yAL350 was transformed with 10 µl cassette and plated on YPD + NAT plates, which were grown at 30°C for 3 days. Grown colonies were restreaked on YPD + NAT to exclude false positives, and those which could re-grow were verified for correct integration by PCR on genomic DNA with the oligonucleotide pairs yAL64 + yAL65 and yAL64 + oBL29. The PCR reactions were composed of: 2 µl cells (boiled 10 min in 0.02 N NaOH), 2 µl of each oligonucleotide, 10 µl Taq 2x Mastermix and water to 20 µl. The PCRs were performed as follows: 98°C 3 min, 98°C 10 sec, 52°C 30 sec, 68°C 4min (to step 2 x 34 times), 68°C 5 min. Correct product length was verified on an agarose gel, and correct expression of *RNH1* in the desired cell cycle phase was assayed by western blot (Figure 19).

2.2.5 Chromatin Immunoprecipitation (ChIP) and DNA-RNA Immunoprecipitation (DRIP)

Exponentially growing liquid yeast cultures (OD_{600} 0.7-0.9) were diluted to the same OD_{600} value and crosslinked for 10 min with formaldehyde (1.2% final concentration). Quenching was performed for 5 min with glycine (360 mM final concentration), after which cells were incubated for at least 5 min on ice. Cell were pelleted at 3,000 rpm for 3 min at 4˚C and pellets were then washed twice with 20 ml of ice-cold PBS and resuspended in 200 µl of ice-cold FA lysis buffer - SOD + protease inhibitor. Cells were lysed in Lysing Matrix C tubes via FastPrep (2 times 30 sec at 6.5M/S with 1 min on ice between runs) at 4˚C. Cell extracts were recovered by adding 800 µl of ice-cold FA lysis buffer + SOD + protease inhibitor, and after centrifugation at 13,000 rpm for 7 min at 4˚C, the pellet was resuspended in 1.5 ml of FA lysis buffer + SOD + protease inhibitor tablets and SDS (0.263% final concentration). Chromatin fragments of <500 bp length were obtained by 19 cycles of sonication 30 s on/off at 4˚C via Biorupter Pico. After centrifugation at 13,000 rpm for 15 min at 4˚C, the supernatant (ChIP Extract) concentration was measured by Bradford and was diluted to 1 mg/ml protein concentration in FA lysis buffer + SOD + protease inhibitor and used for immunoprecipitation. In addition, an input volume representing 5% of the IP volume was used as normalization control in the qPCR reaction. Sonication efficiency was verified by incubating 100 µl of ChIP extract overnight at 65˚C, followed by treatment with 7.5 µl of Proteinase K (20 mg/ml stock) for 2 hours at 37˚C, purification of the DNA via QIAquick PCR Purification Kit and additional treatment with 1 µl RNase A (10 mg/ml stock) for 30 min at 37˚C. DNA fragment length was then analyzed by loading the samples on a 1.5% agarose gel and analyzed by ChemiDoc.

To perform the immunoprecipitation reaction, the appropriate sepharose beads were washed once with ice-cold PBS, incubated for 1 hour at 4˚C in the same media supplemented with 5% BSA, rinsed in ice-cold PBS and finally washed with ice-cold FA lysis buffer + SOD.

For TAP ChIPs, 50 µl IgG sepharose beads were used per sample. For the MYC ChIP, Protein A sepharose beads were used; samples were precleared for 1 hour at 4˚C with 30 µl beads alone and then 3 µl of anti-myc antibody were added to each sample with 50 µl fresh beads. For DRIP, Protein A sepharose beads were used; samples were

precleared for 1 hour at 4 ˚C with 30 µl beads alone and then 2 µl of S9.6 antibody were added to each sample with 50 µl fresh beads.

Immunoprecipitation was performed overnight at 4˚C and was followed with washes at 4˚C for 5 min each with 1 ml of the following ice-cold solutions: FA lysis buffer + SOD, FA lysis buffer 500, buffer III and 1X TE; centrifugation happened at 3,000 rpm for 2 min at 4˚C. DNA bound to the beads was eluted twice in 100 µl of Elution Buffer B for 8 min at 65˚C, following centrifugation at 13,000 rpm for 2 min. Immunoprecipitated samples and inputs were reverse-crosslinked with 7.5 µl of Proteinase K (10 mg/ml stock) overnight at 65˚C. Finally, DNA was purified with QIAquick PCR Purification Kit and eluted in 50 µl ultrapure water.

qPCR were performed using CFX384 Real Time PCR with SYBR-Green, and the annealing was set at 60˚C. All primers used are listed in Section 2.1.2. The measured Cq values were corrected to input values.

For ChIPs and DRIPs performed on telomerase negative strains, PD60 was obtained by streaking out for single colonies telomerase negative spores taken directly from the dissection plates (grown 3 days at 30 ˚C), further incubated 3 days at 30˚C, and subsequently inoculated overnight for the experiment.

2.2.6 Protein extraction and western blot

2.2.6.1 Protein extraction and SDS-PAGE

Liquid culture volumes corresponding to 2 OD_{600} units were spun down at 13,000 rpm for 2 min, and cell pellets were resuspended in 150 µl of ice-cold Solution 1 and incubated for 10 min on ice. 150 µl of ice-cold Solution 2 were then added and, after a brief vortexing, samples were incubated for 10 min on ice. Samples were then centrifuged at 13,000 rpm for 2 min at 4˚C and the pellets were washed with 1 ml of ice-cold Solution 3. Samples were spun down again at 13,000 rpm for 2 min at 4˚C and pellets were resuspended in 100 µl of urea buffer and incubated for 5 min at 75˚C. After a brief spin down at 8,000 rpm for 30 sec, typically 8-10 µl of protein samples were loaded onto pre-casted polyacrylamide gels, and run at 150 V with 1X SDS running buffer.

2.2.6.2 Western Blot

Gels were blotted onto nitrocellulose membranes using the TurboBlot system selecting the “High Molecular Weight” program after being wetted in 1X Transfer buffer. After having assessed the efficiency of transfer by Ponceau staining, the membranes were blocked with Blocking buffer shaking for 1 h at room temperature. The membranes were then incubated overnight at 4˚C with the primary antibody at the appropriate dilution in Blocking buffer (see Section 2.1.8). After washing three times the membranes with PBS-Tween, blots were incubated for 1 h with the secondary antibody in Blocking buffer at room temperature (see Section 2.1.9). Membranes were then washed four times in PBS-Tween and treated with ECL, and the signal was detected using the ChemiDoc.

2.2.7 Spotting assay

Cells from overnight cultures in the appropriate media were diluted to 0.5 OD_{600} and spotted on appropriate agar plates in ten-fold dilutions. The plates were then incubated at 30˚C for the indicated times, and subsequently imaged with the ChemiDoc.

2.2.8 Co-immunoprecipitation (Co-IP)

Liquid cultures were grown overnight in selective media containing raffinose at 30°C, and diluted in the morning in 100 ml selective media containing galactose to induce overexpression of the plasmids. Liquid cultures were then grown to OD_{600} 0.8-1 at 30°C in untreated conditions, arrested in α-factor or treated with the indicated concentrations of HU (see Section 2.2.8.1) when cells were pelleted at 13,000 rpm for 3 min. Pellets were then resuspended in 200 µl of ice-cold IP buffer and cells were lysed using Lysing Matrix C tubes via FastPrep (2 times 30 sec at 6.5M/S with 1 min on ice between runs) at 4°C. Samples were recovered by adding 800 µl of ice-cold IP buffer + NP40, and were then centrifuged twice at 13,000 rpm for 5 min at 4°C, always recovering the supernatant. After protein concentration measurement by Bradford assay, 2 mg of proteins in 1 ml final volume of ice-cold IP buffer + NP40 were added to 25 µl prewashed Pierce anti-HA

magnetic beads (two washes with 1 ml IP buffer + NP40). 4 µl of DNase I were added to each sample and the IP occurred for 2 h at room temperature; the sample Rif2-9myc Rnh201-HA in Figure 6B was additionally treated with 2 µl of RNase A (10 mg/ml stock) for 30 min at room temperature prior to the IP. In addition, 2.5% of the IP volume was resuspended in urea buffer in 15 µl final volume and served as input. IPs were washed 4 times for 5 min each with ice-cold IP buffer + NP40. After removal of the buffer, beads were resuspended in 50 µl urea buffer and vortexed gently. Finally, input and IPs were incubated for 7 min 30 sec at 95°C, and 15 µl of each sample were loaded onto a pre-casted polyacrylamide gels, following western blot as in Section 2.2.6.2. All Co-IPs were performed with IP buffer and IP buffer + NP40 containing 150 mM NaCl, excluding the one shown in Figure 7B in which IP buffer and IP buffer + NP40 contained 300 mM NaCl.

2.2.8.1 Cell cycle arrest in G1 and S phases for Co-IP

For the experiment shown in Figure 7, liquid cultures of the indicated genotypes of mating type a were grown overnight in SC -HIS medium containing raffinose at 30°C, and diluted in the morning in SC -HIS medium containing galactose to induce overexpression of the plasmids at 30°C. A faction of the exponential liquid cultures was incubated until OD_{600} 0.8-1 was reached, following collection of exponential samples for Co-IP and FACS, while the rest was treated with 3 µg/ml of α-factor when it reached OD_{600} 0.2-0.4, and incubated further for 2 h 30 min at 30˚C. After checking efficient G1 arrest at the light microscope, part of the culture was collected for Co-IP and FACS analysis (α-factor sample), while the rest was spun down and washed three times with pre-warmed water (30˚C), and then finally resuspended in fresh pre-warmed SC -HIS medium containing galactose (30˚C) and either 250 mM or 75 mM hydroxyurea (HU), and cultures were further grown for 2 h 30 min at 30˚C. S phase arrest efficiency was verified at the light microscope by presence of large-budded cells, and samples were spun down for FACS and Co-IP (HU samples).

2.2.9 FACS for DNA content

0.18 OD_{600} units of cells were spun down at 13,000 rpm for 2 min and washed with 1 ml of ultrapure water, and subsequently resuspended in 70% ethanol and fixed overnight at 4˚C. After spinning out the ethanol at 13,000 rpm for 5 min, cells were washed with ultrapure water and resuspended in 500 µl of 50 mM Tris-Cl pH 7.5. 10 µl of RNase A (10 mg/ml stock) were added to each sample, and samples were incubated for 3 h at 37˚C. Subsequently, 25 µl of Proteinase K (20 mg/ml stock) were added to each sample and they were further incubated for 1 h at 50˚C. After spinning down the cells at 13,000 rpm for 5 min, they were resuspended in 500 µl of 50 mM Tris-Cl pH 7.5 and sonicated manually for 10 sec at 4˚C. Samples were then transferred to FACS tubes and 500 µl of 1x Sytox Green (1 µM final) in 50 mM Tris-Cl pH 7.5 were added. Each sample was vortexed immediately before analysis with BD FACSVerse.

2.2.10 Microscopy detection of TERRA and Rap1 foci

Liquid cultures of the interested genotypes were grown overnight at 30˚C in SC -LEU -TRP medium containing raffinose and diluted in the morning to OD_{600} 0.1 into SC -LEU -TRP medium containing galactose to induce *RNH1* overexpression. 0.06 OD_{600} units of exponentially growing yeast cells at 30˚C were spun down at 13,000 rpm for 2 min, resuspended in 200 µl of fresh SC -LEU -TRP medium containing galactose and transferred to microscopy chambers coated with concanavalin A (200 µl of concanavalin A (stock 2 mg/ml) were incubated in each chamber for 15 min, and then removed). Detection of TERRA and Rap1 foci was performed at 30˚C with Leica AF7000 widefield fluorescence microscope using a 63x NA/1.4 oil immersion objective, and images were taken with Hamamatsu CCD Camera ORCA-R2 and analyzed with Image J. Only TERRA foci overlapping or adjacent to Rap1 signal were counted and matched with the total of cells analyzed.

2.2.11 Southern blot for telomere length measurement

2.2.11.1 Yeast genomic DNA extraction

50 ml of exponentially growing cultures (OD_{600} 0.7-0.9) were spun down at 3,000 rpm for 3 min and resuspended in 1 ml of a 0.9 M sorbitol + 0.1 M EDTA pH 8 solution. Cells were then pelleted by centrifugation at 13,000 rpm for 1 min and resuspended in 0.4 ml of the same solution supplemented with 14.3 mM β-mercaptoethanol, and the cell wall was digested by incubation for 45 min at 37˚C after addition of 20 µl of 100T zymolyase (2.5 mg/ml stock) to the samples. Spheroplasts were recovered by centrifugation at 14,000 rpm for 30 sec and were resuspended in 400 µl of 1X TE. 90 µl of a solution containing 0.5 ml 0.5 M EDTA pH 8, 0.2 ml 1M Tris-base and 0.2 ml 10% SDS were added and samples were incubated for 30 min at 65˚C, after which 80 µl of 5 M potassium acetate were added and samples were kept on ice for at least 1 hour. Cell residues were eliminated by centrifugation at 14,000 rpm for 15 min at 4˚C and the DNA was precipitated by mixing the supernatant with 600 µl ice-cold ethanol. DNA was pelleted at 14,000 rpm at 4˚C and, after air drying, was resuspended in 500 µl of 1X TE. Samples were further incubated for 30 min at 37˚C with 1.5 µl RNase A (10 mg/ml stock) and DNA was precipitated by adding 500 µl of isopropanol. After pelleting the DNA at 14,000 rpm for 30 min, it was washed with 70% ethanol and finally resuspended in 50 µl of 1X TE.

2.2.11.2 Southern blot

5 µg of DNA were digested for 5 hours at 37˚C with XhoI (1 µl XhoI and 2.5 µl CutSmart buffer, in 25 µl total volume of reaction), and subsequently loaded on a 0.8% agarose gel which was run overnight at 50 V. The DNA in the gel was then denatured for 1 hour in 1 l denaturing solution and then neutralized for 1 hour with 1 l neutralizing solution. The DNA was subsequently transferred to a neutral nylon membrane (GE HybondNX) via capillary transfer in 10X SSC overnight. After rinsing the membrane in water and letting it dry, the DNA was crosslinked to the membrane with UV light, selecting the “auto X-link” program on the Stratalinker. The membrane was then pre-hybridized with 25 ml Church buffer for 5 hours at 55˚C. Hybridization took place overnight at 55˚C with a telomere-specific probe, which was generated by random primed radioactive labelling with dATP [α-^{32}P] of a DNA

fragment obtained by EcoRI digestion of pBL423 followed by gel extraction. The membrane was washed in pre-warmed (55°C) washing solution for 1 hour and again for 30 min and then was air dried. A radio-sensitive film (Fujifilm) was then exposed to the membrane for 3 days and the signal was detected via Typhoon FLA 9500.

2.2.12 Senescence curve

Freshly dissected telomerase negative spores, which had grown for 3 days at 30˚C after dissection, were inoculated to 0.01 (in YPD medium) or 0.02 OD_{600} (in SC medium) in 5 ml of appropriate media and incubated for 24 h at 30˚C. The OD_{600} of the cultures was then measured and each of the cultures was re-diluted to the starting OD_{600} in 5 ml of new media. This process was repeated every 24 h until cultures re-gained the initial viability. Viability was measured by setting the starting culture OD_{600} to 100% and comparing each daily measurement to the initial one, for each sample. 4-6 biological replicates were performed for each genotype. Population doublings for each genotype were calculated as $\log_2(OD_{600}/0.01)$ or $\log_2(OD_{600}/0.02)$ were OD_{600} is the average value measured every 24 h for each genotype.

For the senescence curve shown in Figure 14, the strain yVK1290 was transformed with either pBL97 or pBL399, following dissection on selective plates, after which the senescence curve was started. Differently, for the senescence curve shown in Figure 13B, haploid *est2* strains covered with a wild type copy of the *EST2* gene on a URA plasmid (pBL354) were streaked out for single colonies on SD -HIS + 5-FOA plates to counter select for the pBL354 plasmid. Plates were incubated for 3 days at 30˚C and then single clones which lost pBL354 plasmid were inoculated for the senescence curve.

2.2.13 Cell cycle arrest in G1 and release

Exponentially growing liquid yeast cultures (OD_{600} 0.2-0.4) of mating type a in YPD medium at 30˚C were treated with 4 µg/ml of α-factor and incubated further for 2 h 15 min at 30˚C. After checking efficient G1 arrest at the light microscope, cells were spun down

at 3,000 rpm for 3 min and washed three times with pre-warmed water (25˚C), and finally resuspended in new pre-warmed YPD medium (25˚C) and further grown at 25˚C in a water bath. Protein and FACS samples were collected every 15 min.

3. Results

3.1 RNase H2 localizes to telomeres in a Rif2-dependent manner

Both RNase H1 and H2 enzymes regulate R-loops at yeast telomeres (Balk et al., 2013; Pfeiffer et al., 2013). So far, only studies on the deletion or overexpression of these proteins have been performed to study their role in telomere biology. To investigate how the endogenous proteins are regulated relative to their telomeric role, we decided to approach the question by testing whether these proteins localize to telomeres. We performed a Chromatin Immunoprecipitation (ChIP) assay followed by quantitative PCR (qPCR) pulling down endogenously TAP-tagged Rnh1 (Rnh1-TAP) or TAP-tagged Rnh201 (Rnh201-TAP), the catalytic subunit of the RNase H2 complex. While telomeric sequences were not enriched by qPCR following Rnh1-TAP immunoprecipitation compared to untagged wild type cells (Figure 5A), we found that they were significantly enriched over background after Rnh201-TAP immunoprecipitation (Figure 5B), suggesting that RNase H2 localizes to telomeres.

The telomeric protein Rif2 interacts with Rnh201, as it was reported by a large-scale two-hybrid screen (Jeong et al., 2004). Besides its unique roles, Rif2 also shares some redundant functions with Rif1, as described in Section 1. Based on these data, we asked whether RNase H2 localization to telomeres is dependent on the presence of either of the two Rif proteins. While *RIF1* deletion had no effect on Rnh201-TAP localization to telomeres as seen by ChIP-qPCR, deletion of *RIF2* completely abrogated Rnh201-TAP binding to telomeres (Figure 5B). As a control, we excluded, by western blot analysis, that deletion of either *RIF1* or *RIF2* affects Rnh201-TAP protein levels (Figure 5C). We also confirmed by spotting assay that endogenously expressed TAP-tagged Rnh1 and Rnh201 were functional. As a readout, we took advantage of the sensitivity of the double mutant *rnh1 rnh201* to the genotoxic agent methyl methanesulfonate (MMS)(Lazzaro et al., 2012). As expected, we observed high sensitivity of the *rnh1 rnh201* mutant to the drug, while mutants bearing the combinations of *RNH1-TAP rnh201* or *rnh1 RNH201-TAP* grew at wild type levels (Figure 5D), indicating that the tagged alleles are functional. Taken

together, these results show that RNase H2, but not RNase H1, localizes to telomeres in a Rif2-dependent manner.

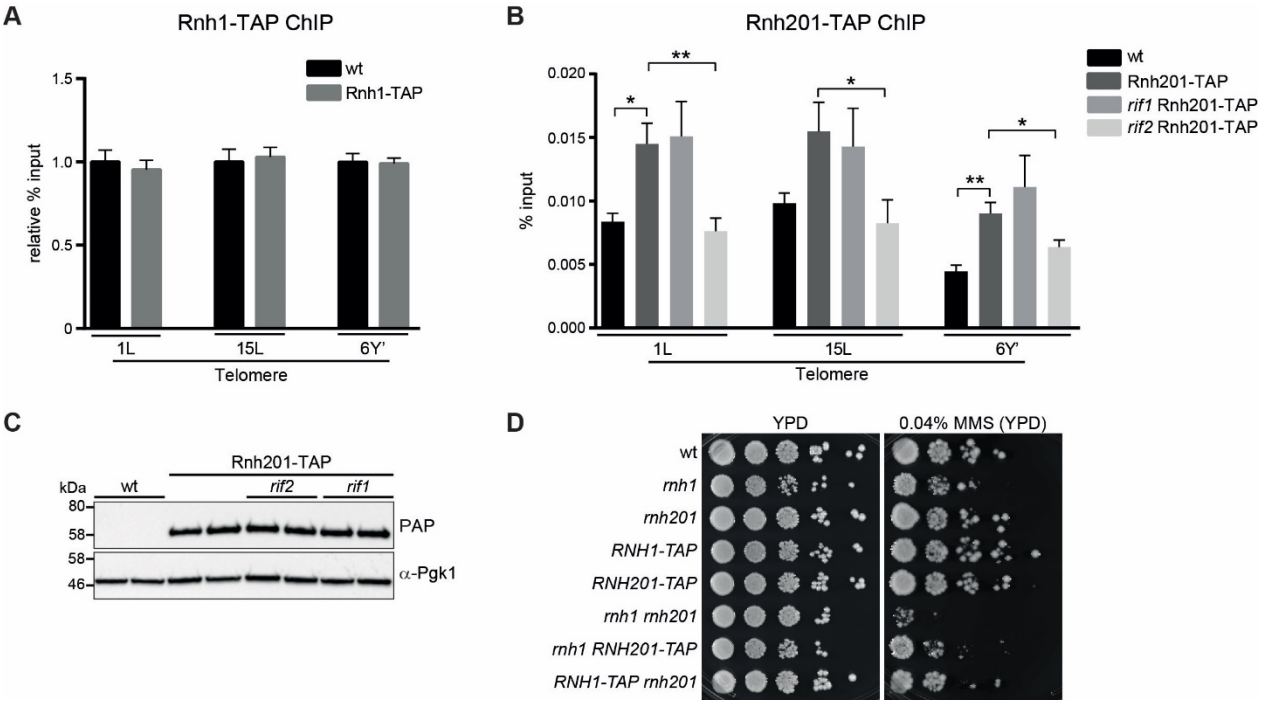

Figure 5. Rif2 recruits RNase H2 to telomeres.

(**A**) RNase H1 does not localize to telomeres in wild type cells. Exponentially growing cultures of the indicated genotypes were crosslinked and subjected to ChIP using IgG coupled beads. Chromatin associated to Rnh1-TAP was analyzed by qRT-PCR. Values are presented as % input of DNA recovered relative to wild type, which is set to 1 for each primer set. Data are shown as mean + SEM; n=3. (**B**) Rnh201 is recruited to telomeres by Rif2. Exponentially growing cultures of the indicated genotypes were crosslinked and subjected to ChIP using IgG coupled beads. Chromatin associated to Rnh201-TAP was analyzed by qRT-PCR. Data is presented as mean % input + SEM; n=3 (wt), 6 (Rnh201-TAP; Rnh201-TAP *rif1*) and 4 (Rnh201-TAP *rif2*). *: p<0.05; **: p<0.01 (Student's t-test). (**C**) Rnh201-TAP protein levels are not affected by *RIF1* and *RIF2* deletion. Protein extracts from cells of the indicated genotypes were analyzed by western blot. Rnh201-TAP was detected with PAP antibody, and Pgk1 serves as a loading control. (**D**) Rnh1-TAP and Rnh201-TAP are functional. Cells of the indicated genotypes were spotted in serial dilutions onto YPD and MMS-containing YPD plates. Plates were imaged after 36 h of incubation at 30˚C.

3.2 RNase H2 and Rif2 interact

We then set out to confirm in a more direct and targeted way the physical interaction between Rnh201 and Rif2. We performed a Co-Immunoprecipitation (Co-IP) assay with endogenously expressed 9myc-tagged Rif2 and HA-tagged Rnh201, which was transiently overexpressed from a plasmid under the control of a galactose-inducible promoter. When HA-Rnh201 was immunoprecipitated with anti-HA antibodies, we were

able to recover Rif2-9myc in the eluate as seen by western blot (Figure 6A). When the HA-immunoprecipitation was performed in cells containing *RIF2-9MYC* and an empty vector (EV), or when cells expressed HA-Rnh201 but untagged Rif2, we could not detect Rif2-9myc in the eluate (Figure 6A). Thus, we could confirm that Rif2 and Rnh201 can physically interact with each other in the conditions described.

Rnh201 is the catalytic component of the RNase H2 trimeric complex, which additionally contains the proteins Rnh202 and Rnh203. We therefore asked whether the interaction between Rif2 and Rnh201 is mediated by the other components of the RNase H2 complex. To test this, we performed an immunoprecipitation against transiently overexpressed HA-tagged Rnh201 in cells lacking either *RNH202*, *RNH203* (Figure 6B) or both (Figure 6C) and bearing the *RIF2-9MYC* allele. In the tested settings we were always able to recover Rif2-9myc in the eluate, suggesting that the interaction between Rif2 and Rnh201 is independent of the presence of the other two components of the RNase H2 complex. As a control, HA-immunoprecipitations performed in cells containing an empty vector (EV) did not lead to Rif2-9myc recovery in the eluate (Figures 6B and C). Moreover, each immunoprecipitation reaction presented in this work (Figures 6, 7 and 8) was treated with DNase I to exclude DNA-mediated interactions, and the Co-IP of Rif2-9myc and Rnh201-HA in Figure 6B was additionally treated with RNase A to exclude RNA-mediated interactions.

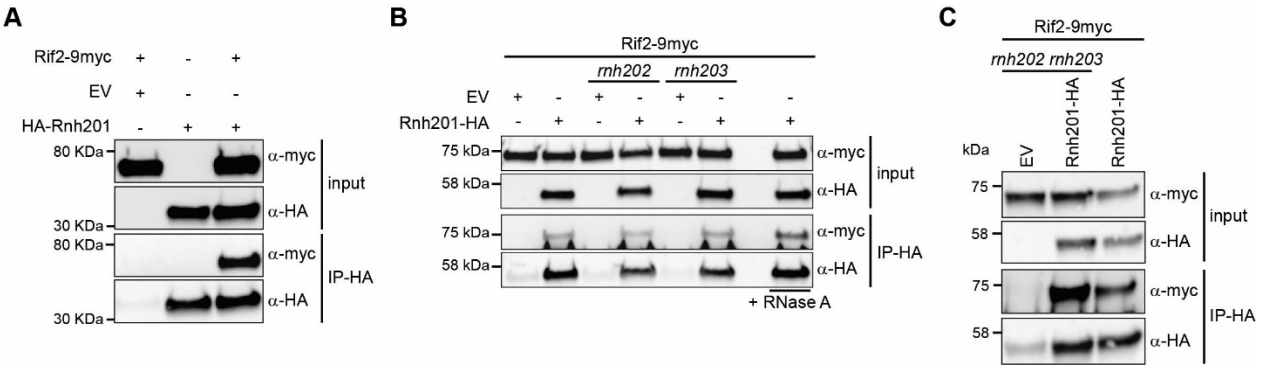

Figure 6. Rif2 interacts with RNase H2.

(**A**-**C**) Rif2-9myc co-immunoprecipitates with RNase H2. Cell extracts derived from exponentially growing cells of the indicated genotypes containing either an empty vector (EV) or transiently overexpressed HA-Rnh201 (**A**) or Rnh201-HA (**B**-**C**) were immunoprecipitated with anti-HA antibody coupled magnetic beads. Samples were then analyzed by western blot and probed with anti-HA and anti-myc antibodies. 2.5% of input protein was loaded as control. (**A**-**C**) All samples were treated with DNase I during immunoprecipitation and sample Rif2-9myc Rnh201-HA (**B**) was treated additionally with RNase A.

We were also able to co-immunoprecipitate Rif2-9myc with overexpressed HA-tagged Rnh202 and Rnh203 (data not shown), indicating that the entire RNase H2 complex is able to interact with Rif2.

We next wondered whether the interaction between Rif2 and Rnh201 is regulated throughout the cell cycle. To assess this, we arrested Rif2-9myc tagged cells overexpressing *HA-RNH201* in G1 with α-factor, and subsequently released them into media containing either 250 mM or 75 mM hydroxyurea (HU), thereby halting the cultures in early and late S phase, respectively (Figure 7A)(Graf et al., 2017). Interestingly, even though HA-Rnh201 was expressed from a GAL-inducible promoter, we observed a drop of its levels in G1 and an increase towards the end of S phase (Figure 7B); nonetheless, we were able to immunoprecipitate similar amounts of the protein in all cell cycle phases using antibodies against HA. We observed interaction between Rif2 and Rnh201 through all the tested phases, but while interaction was clearly lowest in G1 and early S, the highest amount of Rif2-9myc was recovered when the Co-IP was performed in late S phase-arrested cells (Figure 7B).

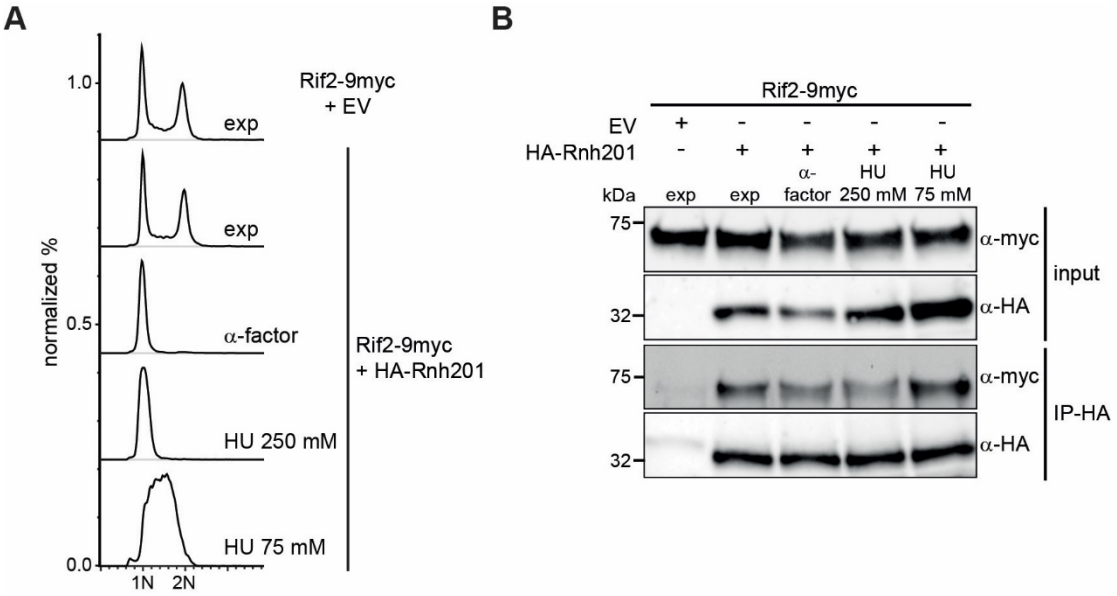

Figure 7. Rif2-Rnh201 interaction is strongest in late S phase.

(**A**) Efficient synchronization of cultures in G1 and early/late S phase. Exponentially growing cultures of the indicated strains were arrested in G1 with α-factor and subsequently released at 30˚C in media containing either 250 mM or 75 mM HU for 2 h 30 min, when samples for FACS and Co-IP were collected. (**B**) Rif2-Rnh201 interaction varies in the cell cycle. Cell extracts deriving from cells of the indicated genotypes in different cell cycle stages (**A**) and containing either an empty vector (EV) or transiently overexpressing HA-Rnh201 were immunoprecipitated with anti-HA antibody coupled magnetic beads. Samples were then analyzed by western blot and probed with anti-HA and anti-myc antibodies. 2.5% of input protein was loaded as control. (**A**-**B**) All samples were treated with DNase I during immunoprecipitation.

This result is consistent with the finding that Rnh201 binding to telomeres is highest in late S phase (Graf et al., 2017), and suggests that the increased interaction between Rif2 and Rnh201 in late S phase is reflected in increased recruitment of RNase H2 to telomeres.

We then decided to test whether Rif2 also interacts with RNase H1, and furthermore if Rif1 is capable of interacting with RNase H enzymes as well. To do this, we transiently overexpressed either *RNH1-HA* or *HA-RNH201* from plasmids in cells in which Rif1 or Rif2 were 9myc-tagged (Figure 8A). We observed that in all tested conditions, HA-immunoprecipitation led to recovery of Rif1 and Rif2 in the eluate, indicating that both Rif2 and Rif1 are able to interact with RNase H1 and RNase H2. As a control, we tested for presence of Rap1, an interactor of both Rif1 and Rif2 in the immunoprecipitate. We were not able to detect Rap1 in the eluate following Rnh1-HA and HA-Rnh201 immunoprecipitations (Figure 8B), indicating specificity of the interactions of RNases H with Rif1 and Rif2. Although both RNase H enzymes can interact physically with both Rif1 and Rif2 (Figure 8A), it seems that only RNase H2 can be found at telomeres by ChIP (Figures 5A and B). Perhaps there is a competition between the two enzymes that we were unable to detect in these conditions (see below for more on this).

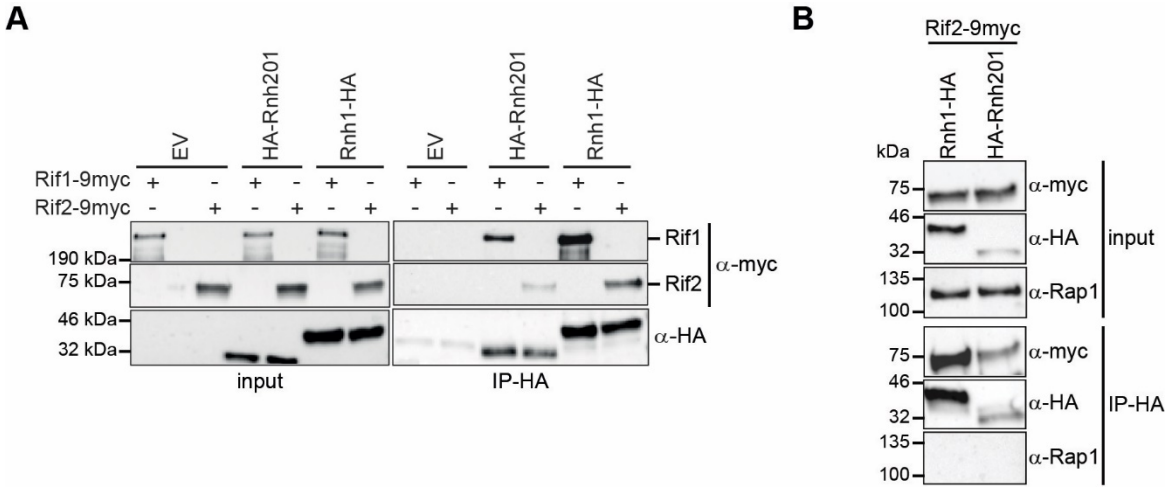

Figure 8. Rif1 and Rif2 interact with RNase H1 and H2.

(**A**-**B**) Rif1 and Rif2 co-immunoprecipitate with Rnh1 and Rnh201. Cell extracts deriving from exponentially growing cells of the indicated genotypes containing either an empty vector (EV) or transiently overexpressing *HA-RNH201* or *RNH1-HA* were immunoprecipitated with anti-HA antibody coupled magnetic beads. Samples were then analyzed by western blot and probed with anti-HA and anti-myc antibodies. In addition, samples in (**B**) were also probed with anti-Rap1 antibodies. 2.5% of input protein was loaded as control. (**A**-**B**) All samples were treated with DNase I during immunoprecipitation.

3.3 Rif2 regulates telomeric R-loops

RNase H enzymes can catalyze the nucleolytic degradation of RNA molecules that are hybridized to DNA (RNA-DNA hybrids or R-loops; reviewed in (Cerritelli and Crouch, 2009)). Several studies in recent years have identified the presence of R-loops at telomeres in diverse organisms, including budding yeast (Arora et al., 2014; Balk et al., 2013; Pfeiffer et al., 2013; Wahba et al., 2016; Yu et al., 2014). Given the interaction between Rif2 and RNase H2, as well as the Rif2-mediated association of RNase H2 to telomeres, we speculated that the Rif2-RNase H2 axis might impact R-loop levels at telomeres.

To assess this, we utilized the S9.6 antibody, which selectively binds RNA-DNA hybrids of at least 6-8 bp (Phillips et al., 2013), to perform a DNA-RNA Immunoprecipitation (DRIP) experiment followed by qPCR. When we performed the DRIP in wild type and Rif2 depleted cells, we could observe that *rif2* mutants displayed an approximate 1.5-2 fold increase of R-loops at telomeres compared to wild type cells (Figure 9A), consistent with the loss of Rnh201 from telomeres in this mutant (Figure 5B). Furthermore, constitutive *in vivo* overexpression of *RNH1* from a plasmid reduced the telomeric R-loop signal in *rif2* mutants to wild type levels, while not significantly affecting the wild type telomeric R-loop levels. As a positive control, we measured R-loops at the 18S rDNA locus, which is highly prone to forming R-loops (El Hage et al., 2010). *RIF2* deletion had no effect on R-loops at rDNA, suggesting that Rif2 regulates RNA-DNA hybrids specifically at telomeres. Altogether, these results suggest that the Rif2-mediated Rnh201 localization to telomeres is functional in restricting R-loops, and that the R-loops that accumulate at telomeres in *rif2* mutants are sensitive to *RNH1* overexpression. The latter result also further confirms that the telomeric DRIP signal that accumulates in *rif2* mutants stems from RNA-DNA hybrids, and furthermore indicates that Rnh1 can act at telomeres even though we could not detect it by ChIP (Figure 5A).

rif2 mutants, as well as *rif1* mutants, display elongated telomeres (Wotton and Shore, 1997). To control for possible effects of telomere length on the DRIP results, we made use of auxin-inducible degron (AID) alleles of these proteins. This system allows rapid degradation of the targeted proteins upon addition of auxin (indole-3-acetic acid, IAA) to

the growth media (Morawska and Ulrich, 2013)(Figure 9B). We performed DRIP experiments in *RIF1*^{AID}, *RIF2*^{AID} and *RIF2*^{AID} *RIF1*^{AID} in presence or absence of IAA treatment, in order to analyze the effect of the depletion of these proteins on R-loops without affecting telomere length. We could confirm that, also in these conditions, depletion of Rif2 leads to the accumulation of R-loops at telomeres, but not at the rDNA locus (Figure 9C); furthermore, depletion of Rif1 had no effect on telomeric R-loop levels and did not contribute to the R-loop accumulation in *RIF2*^{AID} *RIF1*^{AID} cells. This result confirms previous findings and suggests that Rif1 is not a regulator of R-loops at wild type telomeres.

RNase H2 has a genome-wide role in promoting genome stability (Lazzaro et al., 2012; O'Connell et al., 2015), so we decided to investigate whether the Rif2 interaction with Rnh201 has implications on the genome-wide role of RNase H2. To test this, we again took advantage of the high sensitivity of the *rnh1 rnh201* mutant to MMS, as a readout. We performed a spotting assay to test sensitivity to MMS of several mutants. As seen previously (Figure 5D), *rnh1 rnh201* mutants are highly sensitive to MMS, while the double mutant *rif2 rnh1* grew at wild type levels (Figure 9D), indicating that Rif2 is not required for RNase H2 function in response to genome-wide MMS-induced genotoxic stress.

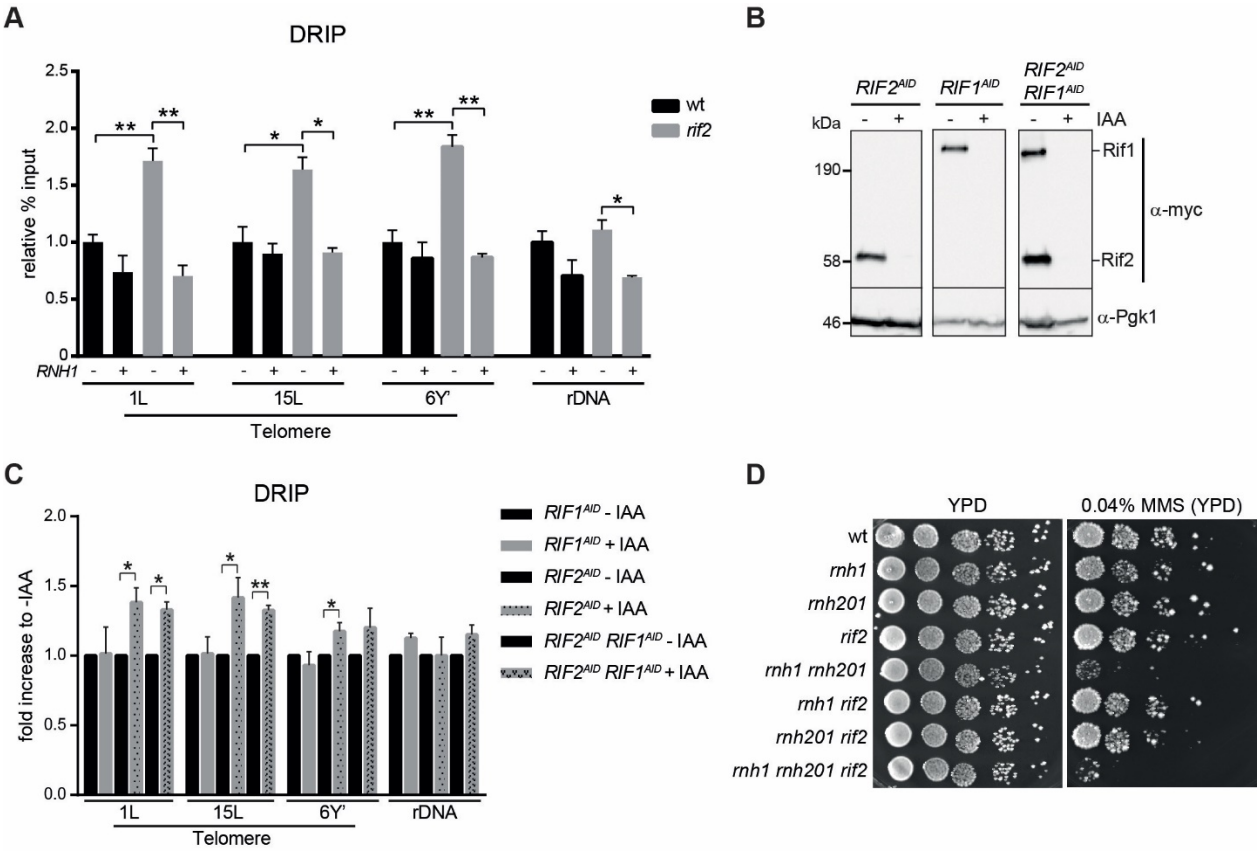

Figure 9. Rif2 restricts telomeric R-loops.

(**A**) *rif2* mutants accumulate telomeric R-loops. Exponentially growing cultures of the indicated genotypes containing either an empty vector (-) or overexpressed *RNH1* (+) were crosslinked and subjected to DRIP using the S9.6 antibody. R-loop associated chromatin was further analyzed by qRT-PCR. Values are presented as % input of DNA recovered relative to wild type, which is set to 1 for each primer set. Data are shown as mean + SEM; n=3. *: p<0.05; **: p<0.01 (Student's t-test). (**B**) IAA-inducible degradation of Rif1 and Rif2. Cells of the indicated genotypes were collected before and after 1 h treatment with 500 μM IAA. Protein extracts were analyzed by western blot. Rif1 and Rif2 were detected with anti-myc antibodies, and Pgk1 serves as a loading control. (**C**) *RIF2^{AID}* mutants accumulate R-loops in the presence of IAA. Cultures of the indicated genotypes were grown to exponential phase and half of each culture was treated with 500 μM IAA for 3 h, after which cultures were crosslinked and subjected to DRIP using the S9.6 antibody. R-loop associated chromatin was analyzed by qRT-PCR. Values are plotted as % input of DNA recovered relative to the correspondent uninduced control, which is set to 1 for each primer set. Data are shown as mean + SEM; n=4. *: p<0.05; **: p<0.01 (Student's t-test). (**D**) Rif2 does not contribute to Rnh201 genome-wide function. Cells of the indicated genotypes were spotted in serial dilutions onto YPD and MMS-containing YPD plates. The YPD plate was imaged after 48 h of incubation at 30˚C and the MMS plate was further incubated 48 h at room temperature before being imaged. Experiments presented in (**B**-**C**) were performed by Diego Bonetti.

3.4 Rif2 regulates TERRA-telomere R-loops

The long non-coding RNA TERRA has been proposed to form R-loops at telomeres because of its G-rich composition and because of it was found to colocalize with telomeres in microscopy experiments (Arora et al., 2014; Azzalin et al., 2007; Balk et al., 2013; Luke et al., 2008; Pfeiffer et al., 2013). However, so far there has not been a direct observation of this phenomenon in budding yeast. Having identified a mutant that accumulates R-loops specifically at telomeres (*rif2*) coupled to the availability of a system that allows the visualization of TERRA molecules by microscopy (Cusanelli et al., 2013), we could approach the question of whether TERRA is the RNA counterpart of R-loops at telomeres and whether TERRA-telomere R-loops are restricted by Rif2.

In this microscopy approach, telomere 6R (on the right arm of chromosome 6) is modified to harbor two MS2 cassettes 80 bp upstream of the telomeric repeats that, when transcribed, form hairpin structures in the product RNA (Figure 10A). These RNA structures are recognized by the MS2 phage protein, which is expressed as a GFP-fusion protein from a plasmid to allow its visualization by fluorescent microscopy. In addition, the transcription regulator and telomeric factor Rap1 was endogenously tagged with mCherry. This set of constructs allows the simultaneous visualization of TERRA molecules as MS2-GFP foci, and of the nuclear space and telomeres by Rap1-mCherry. We analyzed the amount of cells containing one or more TERRA-MS2-GFP foci colocalizing with Rap1-mCherry in a wild type background and in *rif2* mutants. As previously observed (Cusanelli et al., 2013), *rif2* mutants display a two-fold increased amount of TERRA foci-positive cells compared to wild type (Figures 10B and C). To investigate the nature of these TERRA foci, we overexpressed *RNH1 in vivo* from a plasmid in the same backgrounds. Strikingly, we observed a significant reduction in the number of cells with TERRA foci following *RNH1* overexpression in *rif2* cells to almost wild type levels. *RNH1* overexpression had a minimal, although significant, effect on wild type TERRA foci. This result hints at TERRA forming R-loops at telomeres, as its signal can be reduced by *RNH1* overexpression; furthermore, it confirms that Rif2 regulates TERRA-telomere R-loop levels.

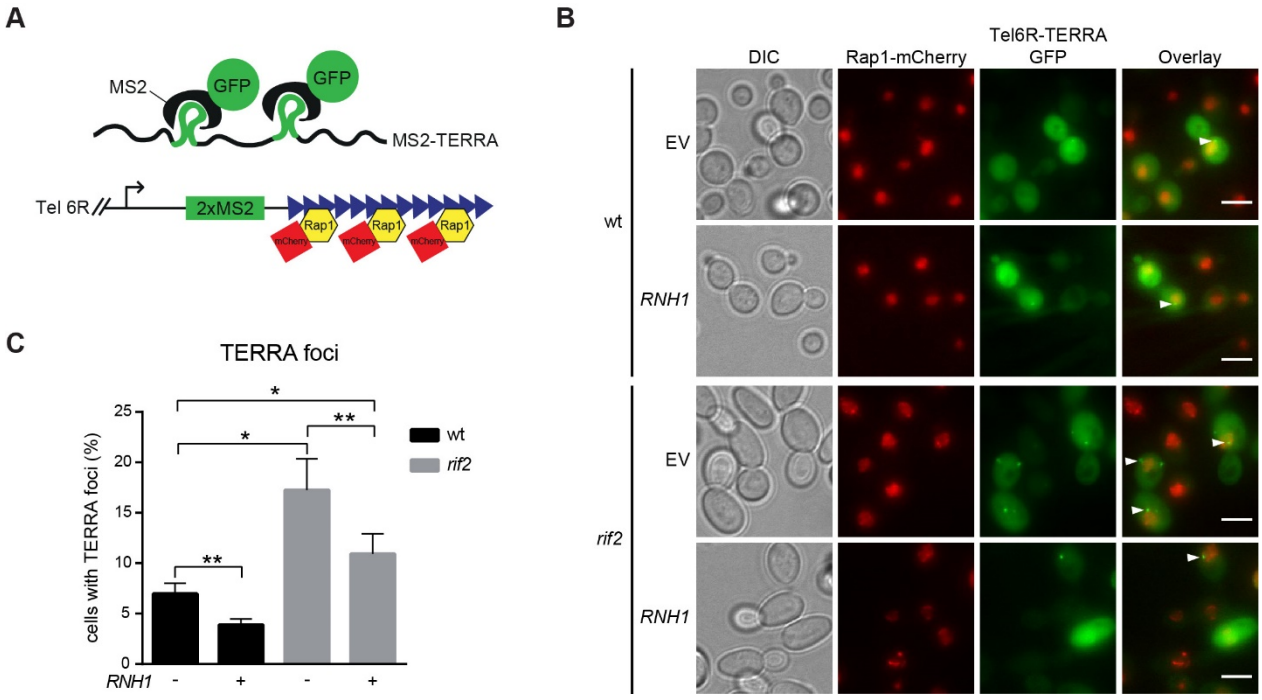

Figure 10. RIF2 restricts TERRA-telomere R-loops.

(**A**) Scheme of the microscopy approach used to detect TERRA nuclear foci. Telomere 6R is modified to contain two MS2 sequences, which form hairpin structures in 6R-transcribed TERRA molecules. MS2 expressed from a plasmid is fused to GFP, and endogenous Rap1 is fused to mCherry. Blue arrowheads indicate telomeric repeats and the black arrow indicates approximate TERRA transcription start site. (**B**-**C**) *rif2* mutants display increased amounts of nuclear 6R-TERRA foci. (**B**) Live-cell analysis of Tel6R-TERRA-MS2-GFP foci and Rap1-mCherry. Representative images are shown of cells of the indicated genotypes containing either an empty vector (EV) or overexpressing *RNH1*. Scale bar: 5 µm. (**C**) Quantification of the percent of cells containing a Tel6R-TERRA-MS2-GFP focus adjacent or overlapping with Rap1-mCherry signal. Data are shown as mean + SEM of two independent experiments in which more than 300 cells were counted. *: p<0.05; **: p<0.01 (ratio-paired Student's t-test).

3.5 Rif2 and RNase H2 are lost from short telomeres

It has been previously observed that Rif2 binds to telomeres in a length-dependent manner, i.e. as telomeres shorten, less Rif2 can be found associated with them (McGee et al., 2010; Sabourin et al., 2007), while Rif1 binding is not affected. The model that was put forward is that Rif2 binds more towards the distal tip of the telomere, while Rif1 associates with the centromere-oriented part of the telomere, providing a basis for the polar loss of Rif2 from short telomeres.

When considering our above described results, we hypothesized that this Rif2 behavior might be mirrored by Rnh201. To test this, we freshly dissected a diploid strain in which

one copy of the telomerase RNA moiety, *TLC1*, was deleted, and harbored tagged versions of Rif2 and Rnh201, with 9myc-tag and TAP-tag respectively. This allowed us to generate telomerase negative spores of nearly wild type telomere length, as telomerase was expressed in the diploid strain. At the same time this strategy allows continued and controlled telomere shortening by subsequent streak outs of the spores, as verified by Southern blotting (Figure 11A). Importantly, Southern blot analysis of telomere length also confirmed that protein tags did not affect Rif2 and Rnh201 protein functions in respect to telomere length maintenance, as cells containing Rif2-9myc and Rnh201-TAP had telomeres of wild type length, while both *rif2* and *rnh201* mutants are known to display lengthened telomeres (Luke et al., 2008; Wotton and Shore, 1997).

As previously reported, we observed by ChIP-qPCR a decrease in Rif2-9myc binding to telomeres when cells were propagated for 60 population doublings (PD60) after telomerase loss, corresponding to short telomeres (Figure 11A and B); we also observed decreased Rnh201-TAP binding to telomeres at PD60 (Figure 11C). This suggests that decreased Rif2 binding to shortened telomeres might be responsible for impaired RNase H2 localization at the same loci. As a control, we measured by western blot analysis Rif2-9myc and Rnh201-TAP protein levels at PD30 and PD60 after telomerase loss, and observed a slight decrease in the levels of both proteins at PD60 (Figure 11D and E), which might partially explain their reduced recruitment to telomeres at this stage (Figure 11B and C). The implications of this phenomenon are consistent with the results obtained when examining R-loop levels at shortened telomeres. We performed a DRIP experiment in wild type and telomerase negative cells which had been propagated for 60 PDs: shortened telomeres showed an almost doubled amount of R-loops compared to telomeres of wild type length (Figure 11F). Taken together, these findings suggest a model in which Rif2 has a pivotal role in regulating telomeric R-loops in a telomere length-dependent manner. When telomeres are of wild type length, Rif2 binding is permitted and in turn recruits RNase H2, thereby keeping R-loop levels to a minimum. When a telomere becomes critically short, Rif2 binding to that telomere is diminished, causing impaired RNase H2 localization, and as a consequence R-loops are not degraded and are allowed to accumulate.

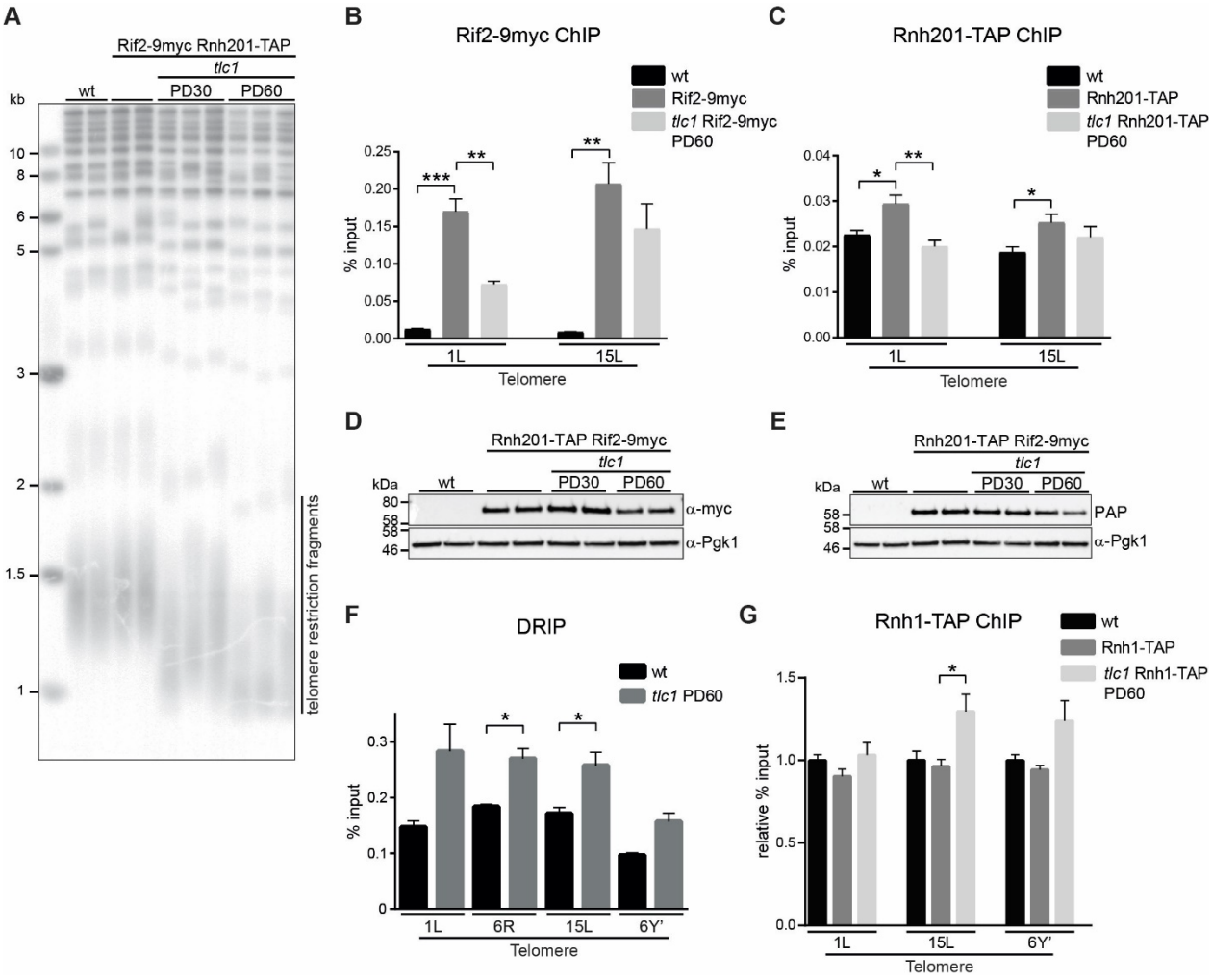

Figure 11. RNase H2 binding is decreased at short telomeres.

(**A**) Rif2-9myc and Rnh201-TAP are functional and progressive telomere shortening can be observed in telomerase negative cells. Southern blot analysis of bulk telomere length of cells of the indicated genotypes. Genomic DNA was digested with XhoI and hybridized with a radioactive telomeric probe. PD30 and PD60 samples were generated by subsequent streakouts of the indicated telomerase negative strains. (**B**-**C**) Rif2-9myc and Rnh201-TAP binding are decreased at short telomeres. Exponentially growing cultures of the indicated genotypes were crosslinked and assessed by ChIP using anti-myc antibodies (**B**) or IgG coupled beads (**C**). Chromatin associated to Rif2-9myc (**B**) or Rnh201-TAP (**C**) was analyzed by qRT-PCR. Data is presented as mean % input + SEM; n=5. *: p<0.05; **: p<0.01; ***: p<0.001 (Student's t-test). (**D**-**E**) Rif2 and Rnh201 protein levels slightly decrease in pre-senescent cells. Protein extracts from cells of the indicated genotypes were analyzed by western blot. Rif2-9myc was detected with anti-myc antibodies and Rnh201-TAP was detected with PAP antibody, and Pgk1 serves as a loading control (**F**) R-loops accumulate at short telomeres. Exponentially growing cultures of the indicated genotypes were crosslinked and subjected to DRIP using the S9.6 antibody. R-loop associated chromatin was analyzed by qRT-PCR. Values are presented as mean % input + SEM; n=3. *: p<0.05 (Student's t-test). (**G**) Rnh1-TAP is recruited to short telomeres. Exponentially growing cultures of the indicated genotypes were crosslinked and subjected to ChIP using IgG coupled beads. Chromatin associated to Rnh1-TAP was analyzed by qRT-PCR. Values are presented as % input of DNA recovered relative to wild type, which is set to 1 for each primer set. Data are shown as mean + SEM; n=3. This panel was partially presented in figure 5A. *: p<0.05 (Student's t-test). The experiment presented in panel (**A**) was performed in collaboration with Diego Bonetti and the experiment presented in panel (**F**) was performed by Marco Graf.

Rnh1 contains a hybrid binding domain (HBD; reviewed in (Cerritelli and Crouch, 2009)) which we reasoned could lead to Rnh1 recruitment to the R-loop accumulating short telomeres. We therefore performed a ChIP for TAP-tagged Rnh1 in *tlc1* cells propagated for 60 PDs. We could observe a small but consistent enrichment of telomeric sequences compared to untagged wild type cells (Figure 11G), indicating that Rnh1 might specifically localize to critically shortened telomeres.

Telomeric R-loops can delay senescence onset by promoting homologous recombination (HR) events between telomeres, thereby partially compensating for telomere shortening (Balk et al., 2013). In line with this, mutants that accumulate telomeric R-loops (as RNase H mutants) display a delayed senescence onset, while cells that have decreased R-loop levels (overexpression of *RNH1*) senesce fast (Balk et al., 2013). On the other hand, telomerase mutants lacking Rif2 senesce fast perhaps due to the capping defect of this mutant, which causes an increased access of the DSB repair complex MRX to the telomeres (Bonetti et al., 2010; Chang et al., 2011). Based on these observations, we asked what would be the effect of overexpressing *RNH1* in telomerase deficient *rif2* mutants, thereby degrading the telomeric R-loops that accumulate in this mutant (Figure 9A).

We performed a senescence curve in *tlc1* and *tlc1 rif2* mutants containing either an empty vector or overexpressing *RNH1*. As seen before (Balk et al., 2013), *RNH1* overexpression led to faster senescence of *tlc1* cells compared to *tlc1* cells containing the empty vector (Figure 12). We also observed that *tlc1 rif2* mutants bearing the empty vector senesced fast, as expected, but interestingly *RNH1* overexpression in these already impaired cells led to further exacerbation of their accelerated senescence rate. This result suggests that although telomerase negative *rif2* mutants display a fast senescence phenotype, the R-loops that accumulate at the telomeres of this mutant still have a protective role in avoiding premature senescence onset, in a similar manner to loss of RNase H function.

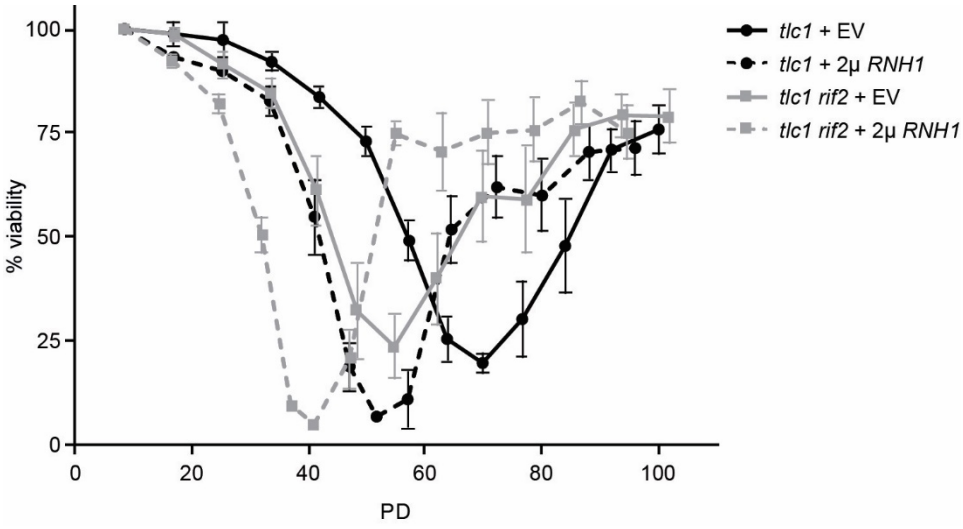

Figure 12. R-loops delay senescence in *rif2* mutants.

Senescence assay performed in selective media (SC -URA) on freshly dissected spores of the indicated genotypes, containing an empty vector (EV) or overexpressing *RNH1* constitutively from a plasmid. Cell viability was estimated daily by measuring cell culture density. Data are shown as mean ± SEM; n=5 for all genotypes but *tlc1 rif2* + *RNH1* n=4.

3.6 RNase H1 and RNase H2 play different roles at telomeres

The initial observation that, while deletion of *RNH1* or *RNH201* has no effect on telomeric R-loop levels, deletion of both enzymes leads to a two-fold increase in R-loops, led to the conclusion that RNase H enzymes may play redundant roles at yeast telomeres (Balk et al., 2013). Nonetheless, in the work presented here we have shown that RNase H2 plays a critical role in controlling R-loops at telomeres in a telomere-length dependent manner, suggesting that the two enzymes might play non-overlapping roles at telomeres. Based on these new findings, we asked whether the single deletions of *RNH1* or *RNH201* would have an effect on senescence rates.

We performed a senescence curve to compare senescence rates of *est2* (telomerase negative), *est2 rnh1*, *est2 rnh201* and *est2 rnh1 rnh201* mutants (Figure 13A). Interestingly, *est2 rnh201* cells senesce extremely slow compared to *est2* mutants, indicating that *RNH201* deletion can delay senescence onset dramatically, even when a wild type copy of *RNH1* is present. This phenotype is consistent with accumulation of HR-promoting R-loops at the telomeres of this mutant. On the other hand, *est2 rnh1* cells showed a fast senescence phenotype compared to *est2* cells, an unexpected result, and

opposite to that of *rnh201*. Additionally, we also observed that deletion of *RNH1* anticipated the senescence onset in *est2 rnh201* mutants, again supporting a negative effect of *RNH1* deletion on senescence kinetics.

These observations are even more peculiar when considering the effect of *RNH1* overexpression on senescence. As observed before (Figure 12)(Balk et al., 2013), *RNH1* overexpression leads to early senescence onset, and this effect is dosage dependent (Figure 13B): when *RNH1* is expressed from a multicopy plasmid (2μ *RNH1*, 50-100 copies per genome) the increase in senescence rate of a *tlc1* mutant is stronger than when *RNH1* is overexpressed from a single-copy centromeric plasmid (CEN *RNH1*). In conclusion, both *RNH1* deletion and overexpression accelerate senescence rates, and importantly RNase H1 and RNase H2 seem to play unique, and not redundant, roles at telomeres.

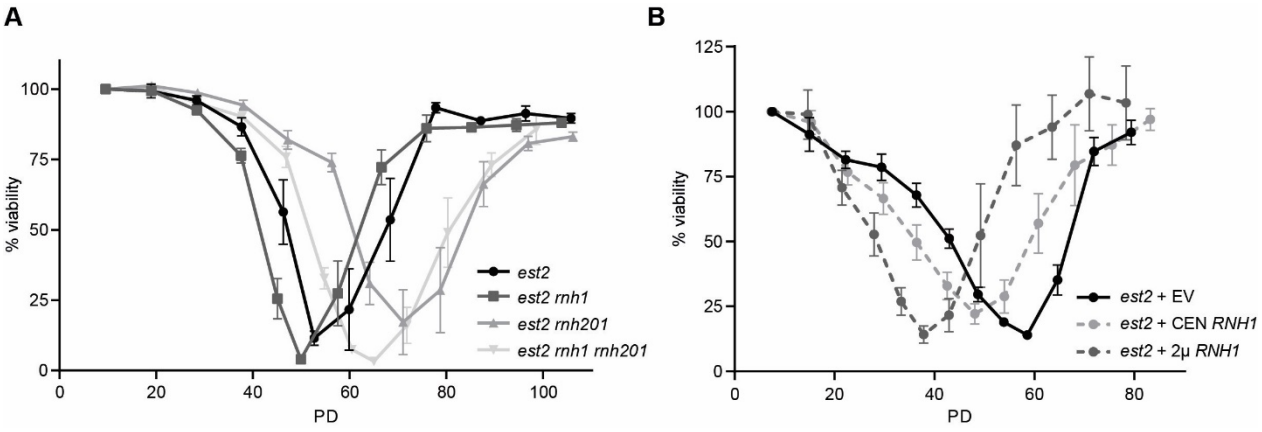

Figure 13. RNase H1 and RNase H2 affect differently senescence onset.

(**A**) Deletion of *RNH1* and *RNH201* have opposite effects on senescence rates. Senescence assay performed on freshly dissected spores of the indicated genotypes. Cell viability was estimated daily by measuring cell culture density. Data are shown as mean ± SEM; n=6 for all genotypes. (**B**) *RNH1* overexpression has a dosage-dependent effect on senescence rates. Senescence assay performed in selective media (SC –HIS) on *est2* cells containing either an empty vector (2μ EV), *RNH1* overexpressed from a single copy plasmid (CEN *RNH1*) or from a multicopy plasmid (2μ *RNH1*). Telomerase negative cells covered with a URA plasmid expressing telomerase were selected for plasmid loss on 5-FOA –HIS plates and then inoculated and assayed for senescence kinetics. n=6 for each genotype.

3.7 RNase H2 does not require its ribonucleotide excision activity at telomeres

RNase H2 has two discernable activities: it can degrade longer RNA-DNA hybrids containing at least 4 ribonucleotides, such as R-loops, an activity that is shared with RNase H1, and it can remove single ribonucleotides (rNTPs) from the DNA (reviewed in (Cerritelli and Crouch, 2009)). This led us to question whether the unique role of RNase H2 at telomeres requires its single ribonuclease excision activity. An allele of *RNH201* has been identified that is unable to remove rNTPs from the genome but fully maintains the ability to degrade longer RNA-DNA hybrids (Chon et al., 2013; Cornelio et al., 2017; Epshtein et al., 2016; Huang et al., 2017). This allele, which was named *Rnh201-RED* (ribonucleotide excision defective), is characterized by the two point mutations: P45D and Y219A. We therefore tested the effect of the *Rnh201-RED* allele on senescence onset. We generated telomerase negative strains bearing *RNH201* deletion (*est2 rnh201*) that expressed the *Rnh201-RED* allele from a vector, and were tested for their senescence kinetics compared to *est2* cells containing an empty vector. Interestingly, *est2 rnh201* cells bearing the *Rnh201-RED* allele were fully complemented as they exhibited a senescence kinetic similar to *est2* cells (Figure 14), while *est2 rnh201* cells display delayed senescence onset (Figure 13A). This result indicates that the loss of ribonucleotide excision activity of RNase H2 does not account for the delay in senescence observed in telomerase negative mutants lacking Rnh201.

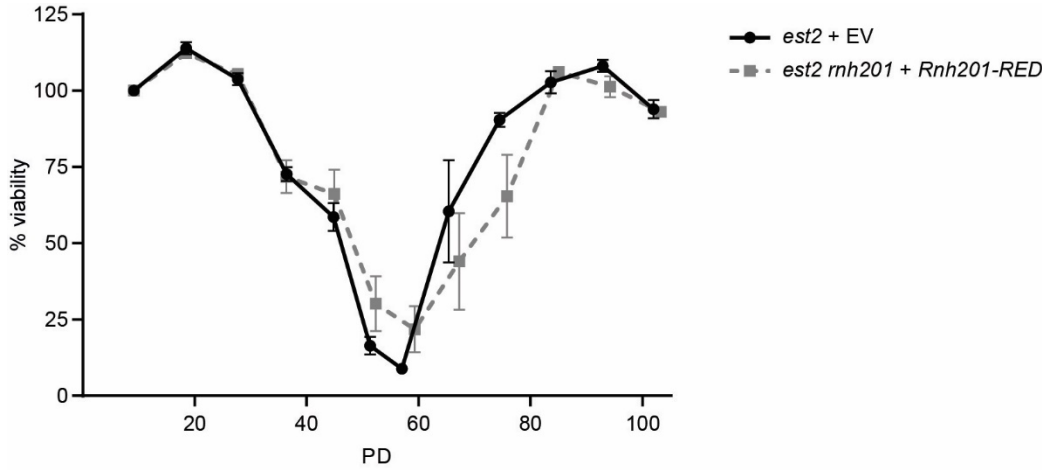

Figure 14. The ribonucleotide excision function of Rnh201 doesn't affect senescence rate.

Senescence assay performed in selective media (SC -URA) on freshly dissected spores of the indicated genotypes, containing an empty vector (EV) or expressing the Rnh201 ribonucleotide excision defective allele from a single copy plasmid under its endogenous promoter (*Rnh201-RED)*. Cell viability was estimated daily by measuring cell culture density. Data are shown as mean ± SEM; n=5 for each genotype. This experiment was performed by Vanessa Kellner.

3.8 Generation of S and G2/M phase restricted *RNH1* alleles

In order to better understand the unique roles that RNase H1 and RNase H2 perform at telomeres, and possibly also genome-wide, we addressed the question of when in the cell cycle their function is necessary. As a first approach, we restricted the expression of Rnh1 either in the S phase or in the G2/M phases of the cell cycle. We made use of two previously published constructs that allow the tight expression of desired proteins in selected cell cycle phases (Hombauer et al., 2011; Karras and Jentsch, 2010).

To construct an *RNH1* allele that is only expressed in S phase (*S-RNH1-TAP*), a PCR-generated construct was integrated in the genome that substituted the natural *RNH1* promoter with the cell-cycle regulated cyclin 6 (*CLB6*) promoter. Moreover, the N-terminus of Rnh1 was fused in frame to the first 195 amino acids of Clb6, which contain the putative Cdc4 degron motifs that promote degradation of the protein before G2 (Figure 15A). This construct allows transcription of *S-RNH1-TAP* in late G1/S phase and the degradation of the protein before G2. A complementary construct generated the *G2-RNH1-TAP* allele. The approach is based on the same strategy, but in this case the mitotic cyclin *CLB2* promoter was integrated in front of the *RNH1* ORF and the first 180 amino acids of Clb2 were fused to the N-terminus of Rnh1 (Figure 15A). In this construct, the *CLB2* fragment contains the D- and KEN-box degrons that promote protein degradation at the end of M and in G1 phases; additionally the L26A mutation is present to prevent nuclear export of the protein. This allele is therefore expressed in late S phase and the protein is degraded after M. We confirmed the cell cycle specific expression of these two alleles by western blotting. Cells were arrested in G1 with α-factor and subsequently released at 25°C to allow cycling in a synchronous manner, and at 15 minutes timepoints samples for FACS and western blot were collected. FACS analysis confirmed successful arrest in G1 by α-factor treatment, and subsequent synchronous and comparable release into the cell cycle (Figure 15B). By western blot we could observe that while in G1-arrested cells there was no detectable signal of both S- and G2-Rnh1-TAP, at the 15 minutes timepoint, when the G1 cyclin Sic1 starts to be degraded, S-Rnh1-TAP accumulated at high levels, and was well-expressed in the 30 and 45 minutes timepoints, corresponding to S phase, after which it quickly faded away as the G2/M cyclin Clb2 started to accumulate (Figure 15C). We also observed a re-accumulation of S-Rnh1-TAP at the 90-105 minutes timepoints, when

the population enters the next cell cycle (Figure 15B). On the other hand, G2-Rnh1-TAP expression completely mirrored the expression of the G2/M cyclin Clb2, with a peak at 60-75 minutes, corresponding to G2/M phases, which then fades as the population enters the next cell cycle (Figure 15B and C).

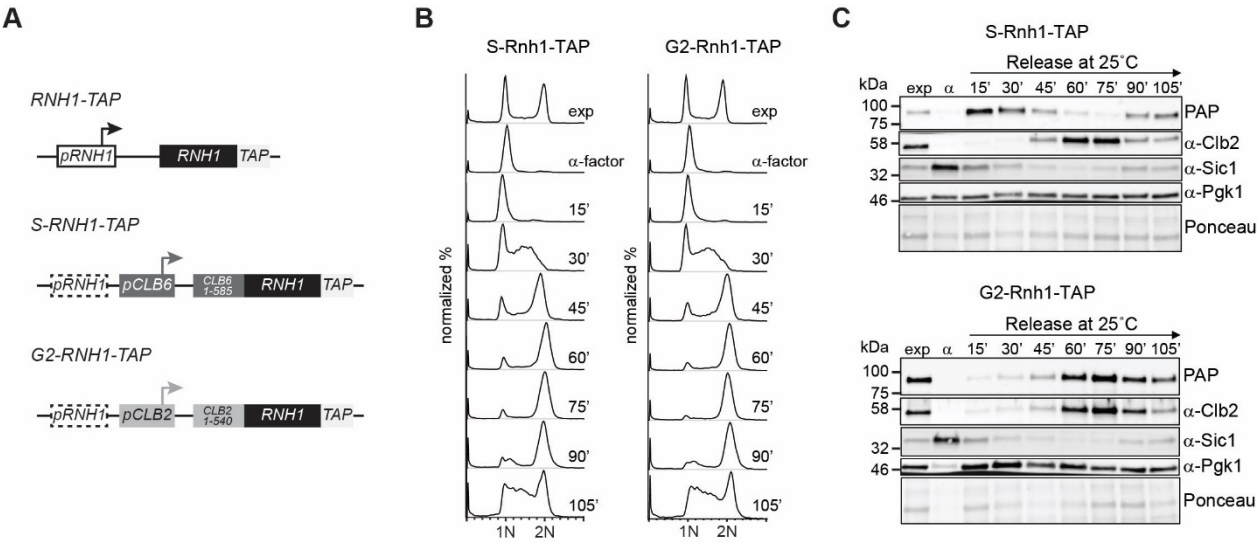

Figure 15. Generation of S and G2/M phase restricted *RNH1-TAP* alleles.

(**A**) Schematics of the *S*- and *G2-RNH1-TAP* alleles. The promoter of *CLB6* (*pCLB6*) or *CLB2* (*pCLB2*) were cloned upstream of *RNH1-TAP* ORF, thereby rendering *RNH1* endogenous promoter dysfunctional (*pRNH1*; dashed lines). In addition, the first 585 nucleotides of *CLB6* (S) or the first 540 nucleotides of *CLB2* (G2; additionally containing the mutation L26A) were cloned upstream of *RNH1* ORF. Arrows indicate approximate transcription start site. (**B**) Synchronous release of S and G2-Rnh1-TAP cultures. Exponentially growing cultures of the indicated strains were arrested in G1 with α-factor and subsequently released at 25˚C. Samples for FACS and proteins were collected every 15 minutes. (**C**) S- and G2-Rnh1-TAP are cell cycle regulated. Protein extracts collected at the indicated timepoints were analyzed by western blot. S- and G2-Rnh1-TAP were detected with PAP antibody; Clb2 is a cyclin specific for G2/M and Sic1 for G1. Pgk1 and the Ponceau staining serve as loading control.

To better characterize these two novel *RNH1* alleles, we compared their protein expression levels in the different cell cycle phases to the levels of endogenously expressed Rnh1-TAP, which we arrested in α-factor and released in the same manner as we did with *S*- and *G2-RNH1-TAP* alleles. The FACS profile of this α-factor arrest and release (Figure 16A) is fully comparable to the ones performed in figure 15B, allowing direct comparison of protein levels at the different time points. We thus loaded side-by-side on a western blot protein extract from the different strains at the most relevant time points (Figure 16B). We could observe that wild type Rnh1-TAP is expressed at constant

levels throughout the cell cycle; in addition, we also acknowledged that both of the cell cycle-restricted *RNH1-TAP* alleles, when expressed, are present in higher levels compared to the wild type protein. Of note, we could detect an additional band in the G2-Rnh1-TAP samples which resembled wild type length Rnh1-TAP (Figure 16B), suggesting that there might be another initiation site in the *G2-RNH1-TAP* allele or that the degron might be cleaved from G2-Rnh1-TAP. Altogether, we have obtained two novel alleles of *RNH1* whose expression is restricted in S or G2/M phases, at levels moderately higher than wild type Rnh1.

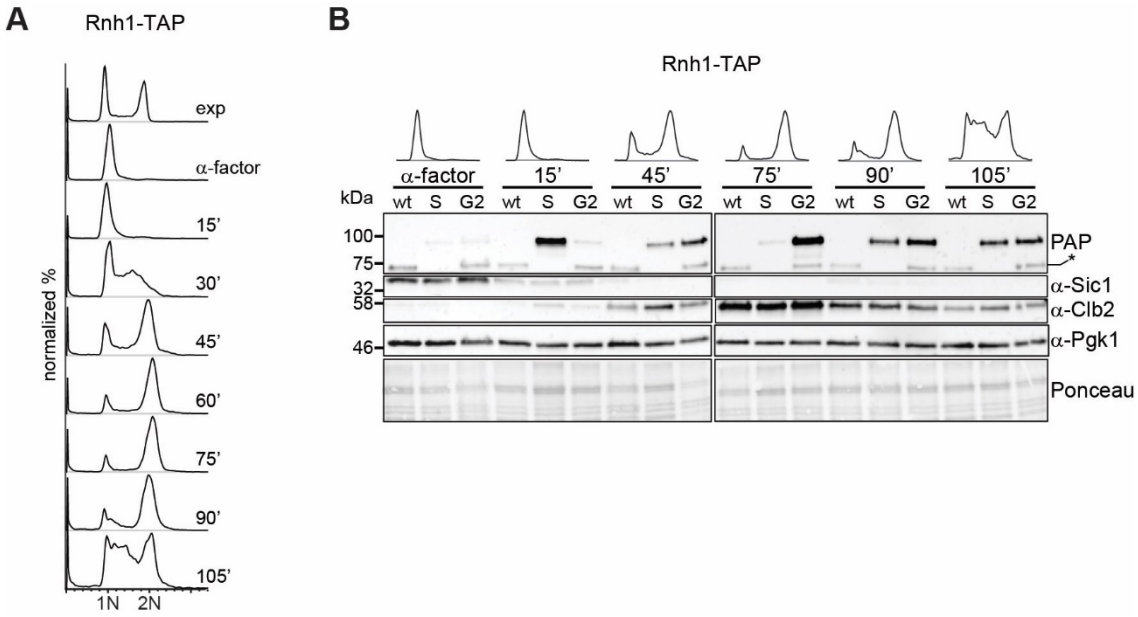

Figure 16. S- and G2-Rnh1-TAP are overexpressed compared to endogenous Rnh1-TAP.

(**A**) Release of a culture expressing Rnh1-TAP from its endogenous promoter. An exponentially growing culture of the indicated strain was arrested in G1 with α-factor and subsequently released at 25˚C. Samples for FACS and proteins were taken every 15 minutes. (**B**) S- and G2-Rnh1-TAP are overexpressed. Protein extracts collected at the indicated timepoints were analyzed by western blot. Endogenous, S- and G2-Rnh1-TAP were detected with PAP antibody; Clb2 is a cyclin specific for G2/M and Sic1 for G1. Pgk1 and the Ponceau staining serve as loading controls. FACS profiles of Rnh1-TAP are chosen as representative for FACS of all cultures, which are comparable (compare (**A**) and Figure 15B). In G2-Rnh1-TAP samples an unspecific band (*) is detected.

3.9 Rnh1 is needed outside of G2/M phases to promote genome stability

Together with RNase H2, RNase H1 has a role in maintaining genome stability (Lazzaro et al., 2012; O'Connell et al., 2015). We used the high sensitivity of *rnh1 rnh201* cells to the genotoxic agent MMS as a readout to investigate when in the cell cycle Rnh1 is needed in absence of RNase H2 to support viability on MMS-containing plates. We therefore performed a spotting assay to test different combinations of the *RNH1* alleles and *RNH201* deletion (Figure 17A). As expected, cells containing the *S-* and *G2-RNH1-TAP* alleles alone are not sensitive to MMS, consistent with *rnh1* mutants not being sensitive. Interestingly, while expression of Rnh1 in S phase was able to sustain viability on MMS in an *rnh201* background, its expression exclusively in G2/M led to high sensitivity in *rnh201* cells, even greater than in the double mutant *rnh1 rnh201*.

To exclude that the observed effect in *G2-RNH1-TAP rnh201* cells was caused by the moderate overexpression of Rnh1 in G2/M phases (Figure 16B), we tested the effect of *RNH1* overexpression in *rnh1 rnh201* by a spotting assay on MMS-containing plates. We observed that overexpression of *RNH1* in an *rnh1 rnh201* background resulted in wild type growth capacity (Figure 17B), demonstrating that *RNH1* overexpression *per se* is not detrimental in this context. Taken together, these results suggest that, in the absence of RNase H2 activity, Rnh1 expression is required outside of G2/M phases of the cell cycle to confer resistance to MMS. Furthermore, the increased sensitivity of the *G2-RNH1-TAP rnh201* mutant compared to *rnh1 rnh201* suggests that the presence of Rnh1 exclusively in the G2/M phases is more detrimental than complete absence of Rnh1. Lastly, this effect cannot be explained by the fact that the *G2-RNH1-TAP* allele is moderately overexpressed.

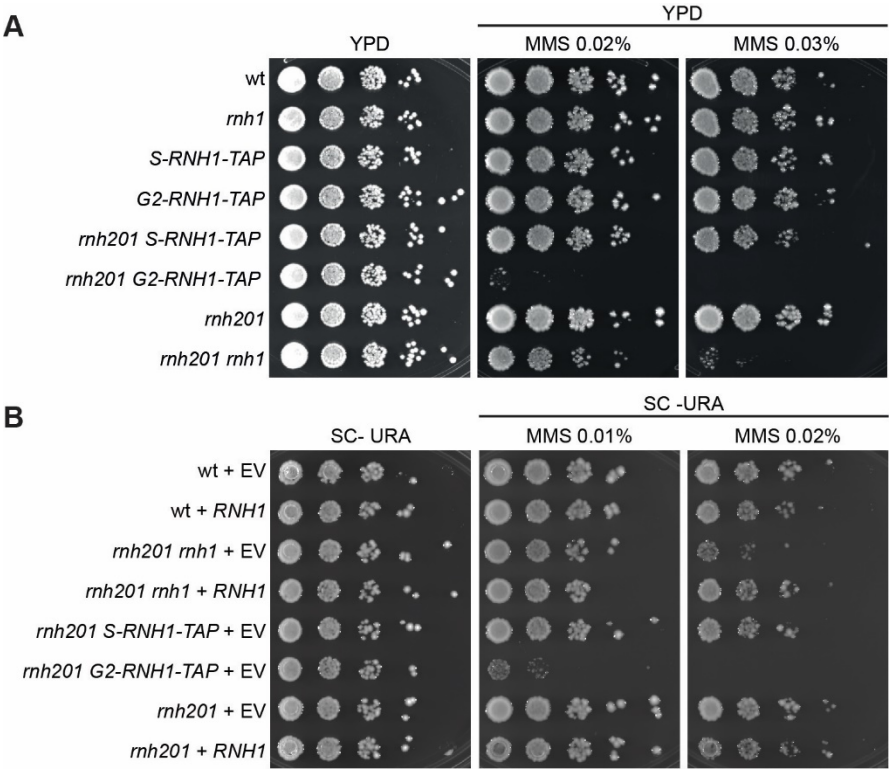

Figure 17. RNase H1 is required outside G2 phase to sustain viability on MMS.

(**A**) *rnh201 G2-RNH1-TAP* mutants are hypersensitive to MMS. Cells of the indicated genotypes were spotted in serial dilutions onto YPD and MMS-containing YPD plates. Plates were imaged after 48 h (YPD) or 72 h (MMS plates) of incubation at 30˚C. (**B**) *RNH1* overexpression doesn't induce sensitivity to MMS. Cells of the indicated genotypes containing either and empty vector (EV) or overexpressing *RNH1* from a plasmid were spotted in serial dilutions onto SC -URA and MMS-containing SC -URA plates. Plates were imaged after 48 h (SC –URA) or 72 h (MMS plates) of incubation at 30˚C.

3.10 RNase H1 is required at telomeres in S phase during senescence

Next, we addressed the cell cycle timing of RNase H1 function at telomeres. Loss of RNase H1 and H2 function causes accelerated senescence in the absence of both telomerase and the recombination machinery (*rad52* background)(Balk et al., 2013). This phenotype has been explained by the accumulation of R-loops at telomeres of this mutant that cause instability (e.g. causing replication stress) which cannot be rescued by the HR pathway. We therefore tested the effect of the *S-* or *G2-RNH1-TAP* alleles in this background (Figure 18A). Unexpectedly, limited expression of Rnh1 in G2/M phases in this background (*est2 rad52 rnh201 G2-RNH1-TAP*) leads to senescence rates comparable to that of *est2 rad52 rnh201* mutants, suggesting that restricted expression of

Rnh1 in G2/M phases has a phenotype similar to that of wild type Rnh1 expression. On the other hand, expression of Rnh1 in S phase alone in this background (*est2 rad52 rnh201 S-RNH1-TAP*) led to the same accelerated senescence kinetics as the complete absence of *rnh1* (*est2 rad52 rnh201 rnh1*). This result suggests that, in senescent cells lacking the recombination machinery, expression of Rnh1 in G2/M phases is enough to fully accomplish Rnh1 functions.

We then tested the effect of the differential expression of Rnh1 in HR-proficient cells. In this experiment, we compared senescence rates of *est2*, *est2 rnh1*, *est2 S-RNH1-TAP* and *est2 G2-RNH1-TAP* mutants (Figure 18B). Again, restricting Rnh1 expression in S phase resulted in a fast senescence phenotype comparable to that of *RNH1* deletion. Expression of Rnh1 in G2/M phases, while initially phenocopying *est2* cells, eventually accelerated senescence rates as *est2 rnh1* mutants. Taken together, these results suggest that Rnh1 is needed at telomeres in the G2/M phase of the cell cycle, especially when the recombination machinery is not functional.

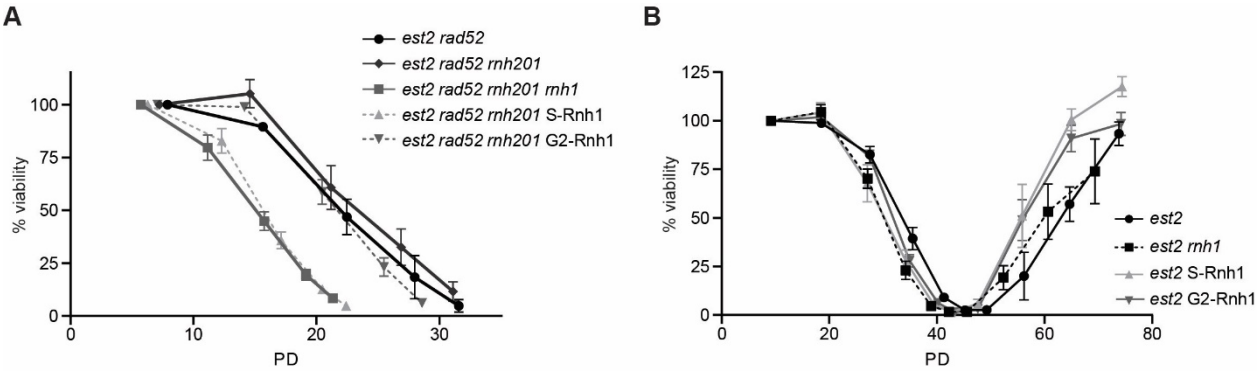

Figure 18. RNase H1 is required outside S phase during senescence.

(**A**-**B**) S phase restricted expression of *RNH1* accelerates senescence onset. Senescence assay performed on freshly dissected spores of the indicated genotypes. Cell viability was estimated daily by measuring cell culture density. Data are shown as mean ± SEM; n=6 for all genotypes but (**A**) *est2 rad52 rnh1 rnh201* n=5.

3.11 Generation of an S phase restricted *RNH202* allele

Lastly, we turned to the cell cycle requirements for RNase H2 function at telomeres. We generated an S phase restricted allele of the RNase H2 subunit Rnh202 (*S-RNH202-TAP*), adopting the same cloning strategy as for the creation of *S-RNH1-TAP* (Figure 19A)(Hombauer et al., 2011). We reasoned that restricting *RNH202* expression would limit RNase H2 complex activity, as the complex is active only in its trimeric form and deletion of any of the components leads to identical phenotypes (Lazzaro et al., 2012; Nguyen et al., 2011).

We confirmed cell-cycle regulation of S-Rnh202-TAP expression by α-factor arrest and release, collecting samples for FACS and western blot. In parallel we also analyzed wild type Rnh202-TAP levels by the same means. We could observe that while expression of Rnh202-TAP is constant throughout the cell cycle (Figure 19B and C), S-Rnh202-TAP was not expressed in G1 but its levels increased at 15 minutes and peaked at 30 and 45 minutes, corresponding to S phase, after which protein levels quickly fade as the G2/M cyclin Clb2 starts to accumulate again. A new peak emerges at 105 minutes, when cells enter the next cell cycle (Figure 19B). This assay confirms that S-Rnh202-TAP is expressed in S phase and, by comparing protein levels to Rnh202-TAP, reveals that its expression in S phase is at wild type levels.

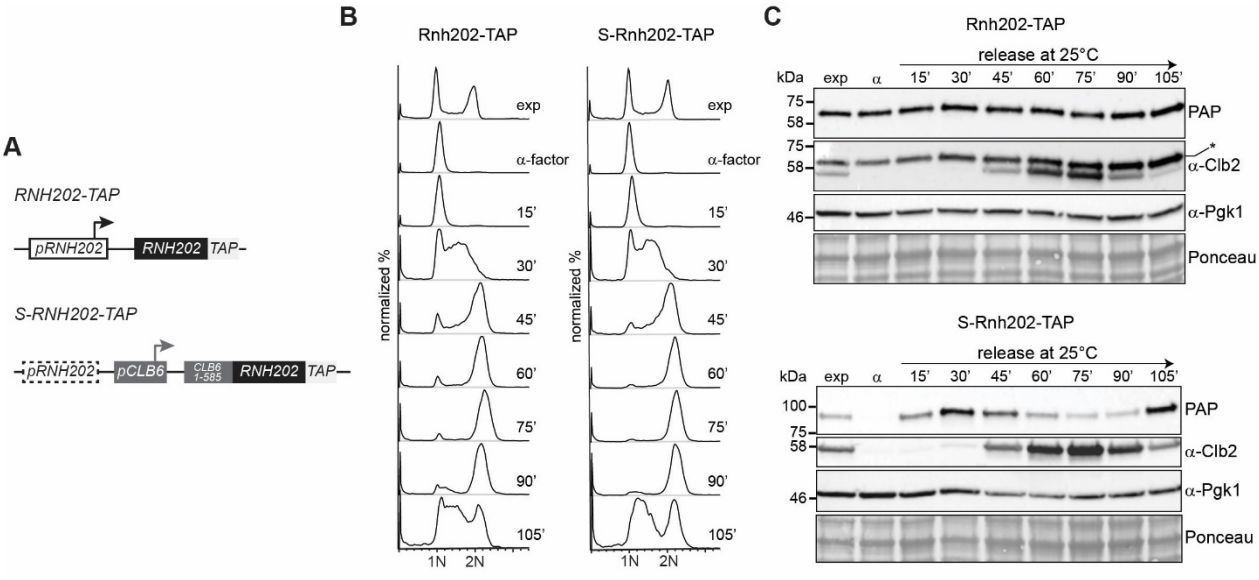

Figure 19. Generation of an S phase restricted Rnh202-TAP allele.

(**A**) Schematics of the *S-RNH202-TAP* allele. The promoter of *CLB6* (*pCLB6*) was cloned upstream of *RNH202-TAP* ORF, thereby rendering *RNH202* endogenous promoter dysfunctional (*pRNH202*; dashed lines). In addition, the first 585 nucleotides of *CLB6* were cloned upstream of *RNH202* ORF. Arrows indicate approximate transcription start site. (**B**) Synchronous release of Rnh202-TAP and S-Rnh202-TAP cultures. Exponentially growing cultures of the indicated strains were arrested in G1 with α-factor and subsequently released at 25˚C. Samples for FACS and proteins were taken every 15 minutes. (**C**) S-Rnh202-TAP is cell cycle regulated. Protein extracts collected at the indicated timepoints were analyzed by western blot. Rnh202-TAP and S-Rnh202-TAP were detected with PAP antibody; Clb2 is a cyclin specific for G2/M. Pgk1 and the Ponceau staining serve as loading control. Band intensities of the PAP blots can be compared, as the two blots were exposed simultaneously. (*) indicates the Rnh202-TAP residual signal on the Clb2 blot.

3.12 RNase H2 is required outside of S phase in response to genotoxic stress and during senescence

We now investigated the effect of restricting RNase H2 function in S phase on its role in genome maintenance. We performed a spotting assay on MMS-containing plates of different mutants containing the *S-RNH202-TAP* allele (Figure 20A). As expected, *rnh1 rnh202* mutants are highly sensitive to MMS. Surprisingly, expression of Rnh202 exclusively in S phase in combination with *RNH1* deletion lead to high MMS sensitivity, comparably to *rnh1 rnh202* mutants. This suggests that RNase H2 is needed outside of S phase to support resistance to MMS in an *rnh1* background, an observation that is in contrast to the need of RNase H1 in S phase (Figure 17A).

Finally, we tested the requirement for RNase H2 cell cycle specific role during senescence. To do this, we performed a senescence curve to compare *est2 S-RNH202-TAP* senescence kinetics to that of *est2* and *est2 rnh202* mutants (Figure 20B). Strikingly, expression of Rnh202 in S phase phenocopied *RNH202* deletion, displaying delayed senescence onset compared to *est2* cells. Taken together, these results suggest that, as RNase H1, also RNase H2 is acting at telomeres of pre-senescent cells outside of S phase. On the other hand, while Rnh1 supports genome stability by acting in S phase, RNase H2 is needed outside of S phase.

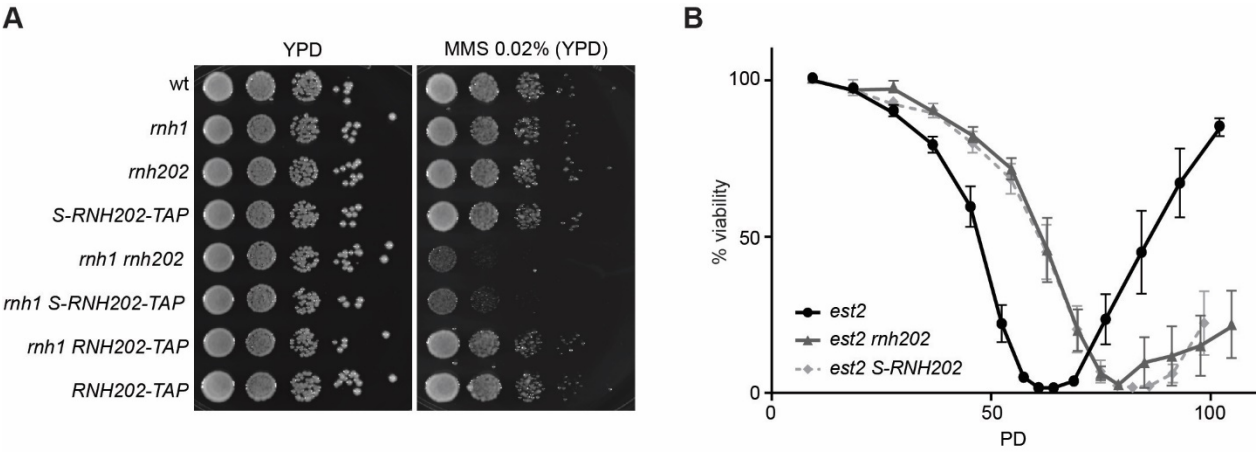

Figure 20. RNase H2 is required outside S phase to promote resistance to MMS and during senescence.

(**A**) *rnh1 S-RNH202-TAP* mutants are hypersensitive to MMS. Cells of the indicated genotypes were spotted in serial dilutions onto YPD and MMS-containing YPD plates. Plates were imaged after 48 h of incubation at 30˚C. (**B**) S phase restricted expression of *RNH202* delays senescence onset. Senescence assay performed on freshly dissected spores of the indicated genotypes. Cell viability was estimated daily by measuring cell culture density. Data are shown as mean ± SEM; n=6 for all genotypes.

4. Discussion

We have uncovered a mechanism that tightly regulates R-loop accumulation at *S. cerevisiae* telomeres. An interaction between the telomeric protein Rif2 and RNase H2 directs RNase H activity to wild type length telomeres, thereby maintaining R-loop levels to a minimum. We found that the previously reported diminished Rif2 binding to short telomeres (McGee et al., 2010; Sabourin et al., 2007) is accompanied by reduced recruitment of RNase H2, which is functionally reflected in increased R-loop levels at short telomeres. The Rif2/RNase H2 axis thus provides a distinction between long and short telomeres: while long telomeres display a minimum amount of R-loops, short telomeres accumulate R-loops, which in telomerase negative cells promote compensatory HR events that can elongate short telomeres and hence buffer against premature senescence onset (Balk et al., 2013; Fallet et al., 2014).

4.1 Avoidance of R-loops at long telomeres

Telomeric R-loops form in early S phase, after TERRA transcription takes place (Graf et al., 2017). At long telomeres, both TERRA and R-loops are degraded towards the end of S phase by Rat1 and RNase H2 activities, respectively. Indeed, the localization of both enzymes to telomeres peaks in mid-to-late S phase (Graf et al., 2017). Long telomeres are replicated in late S phase (McCarroll and Fangman, 1988; Raghuraman et al., 2001), a time in which telomeric R-loops have already been degraded (Graf et al., 2017), thereby indicating that at long telomeres R-loops are degraded approximately at the same time of the replication fork arrival at telomeres. In this scenario, the replication machinery would neither collide with TERRA R-loops nor with RNA Pol II transcribing TERRA, two events that could be potentially deleterious for telomere stability (Hamperl and Cimprich, 2014; Santos-Pereira and Aguilera, 2015). Therefore, timely RNase H2 mediated removal of R-loops at long telomeres might promote unperturbed telomere replication by providing a strict coordination between R-loop degradation and arrival of the replication fork at telomeres (Figure 21). In contrast, RNase H1 seems to play only a minor role in R-loop

removal at long telomeres, although it might play an auxiliary role when RNase H2 activity is impaired. Indeed, while *rnh201* and *rnh1* mutants do not display increased R-loop levels at telomeres, the double mutant *rnh1 rnh201* does (observation by A. Maicher; (Balk et al., 2013)).

Long telomeres are stable due to sufficient recruitment of telomere binding proteins that provide their capping. Moreover, long telomeres do not require elongation, suggesting that at long telomeres R-loops might be generated by default, while not having any physiological function. Consistently, degradation of telomeric R-loops by RNase H1 overexpression has no effect on telomere length in wild type *S. cerevisiae* (D. Bonetti, personal communication and data not shown) nor on telomere stability in telomerase positive human cells (Arora et al., 2014).

Whereas reduced telomeric R-loop levels do not seem to influence telomere maintenance in wild type cells, their untimely or impaired degradation might have a negative impact, leading to detrimental encounters of the replication fork with R-loops (Hamperl and Cimprich, 2014; Santos-Pereira and Aguilera, 2015). Interestingly, *rnh201* mutants display elongated telomeres (Luke et al., 2008), a phenotype typically associated with mutants that experience replication stress at telomeres (Miller et al., 2006), which might be due to untimely resolution of telomeric R-loops. Similarly, RNase H1 silencing in human telomerase positive cancer cells leads to an increased frequency of telomere-free ends, which could be explained by DNA replication defects at telomeres (Parajuli et al., 2017). Moreover, accumulation of telomere-bound TERRA molecules in human cells depleted for UPF1 (Azzalin et al., 2007), an RNA helicase implicated in nonsense mediated decay (NMD; (Chang et al., 2007b)), might be the cause for the impaired telomeric leading strand replication in these mutants (Chawla et al., 2011), as TERRA R-loops form at the telomeric leading strand. Interestingly, UPF1 binds to telomeres in S and G2/M phases, when TERRA and possibly TERRA R-loops levels decrease (Chawla et al., 2011; Flynn et al., 2011; Flynn et al., 2015; Porro et al., 2010), suggesting that UPF1 might protect telomere stability especially during replication of the leading strand by removing TERRA R-loops. Taken together, these observations suggest that at long telomeres, deregulated degradation of telomeric R-loops could lead to detrimental consequences.

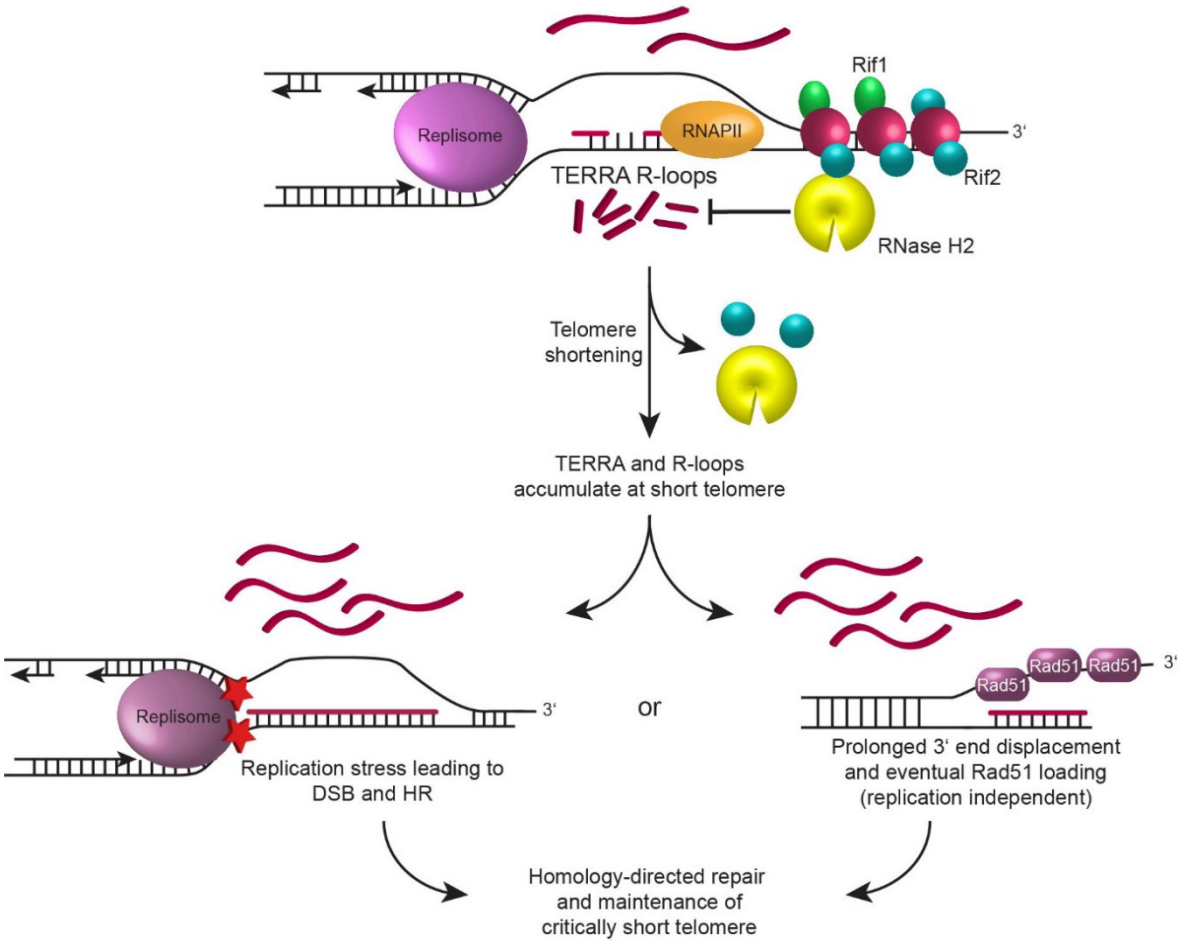

Figure 21. A Rif2/RNase H2 axis provides a distinction between long and short telomeres.

At long telomeres, efficient Rif2 binding allows RNase H2 localization to telomeres, and consequent degradation of telomeric R-loops (top). As telomeres shorten, loss of telomeric repeats leads to Rif2 loss from telomeres and reduced recruitment of RNase H2. Local depletion of RNase H2 is reflected in the accumulation of R-loops at telomeres, which promote HR-mediated re-elongation of the short telomere, thereby preventing premature senescence onset (bottom). HR induction by telomeric R-loops might be caused by the induction of replication stress or by prolonged displacement of the opposite 3' single stranded end. Modified from (Graf et al., 2017).

In conclusion, the formation of telomeric R-loops appears to be a ubiquitous phenomenon which is readily taken care of at long telomeres, while their stabilization at short telomeres seems to be an 'emergency' signal which targets them for elongation *in cis*. On the contrary, encounters of the replication machinery with R-loops at long telomeres would have no beneficial effect but rather cause telomere instability (Hamperl and Cimprich, 2014; Santos-Pereira and Aguilera, 2015), potentially explaining why at long telomeres TERRA R-loops are timely degraded. Importantly, the increase of TERRA and telomeric R-loop levels at critically short telomeres does not influence TERRA and R-loop levels at

other telomeres in the same cells, and does not promote the elongation of all telomeres (Cusanelli et al., 2013; Graf et al., 2017). This suggests that increased TERRA and telomeric R-loop levels do not activate a cell-wide response, but strictly affect telomeres *in cis*.

4.2 Functional accumulation of R-loops at short telomeres

In telomerase negative cells, the accumulation of R-loops at critically short telomeres activates the DNA damage response, leads to the recruitment of recombination factors *in cis* (Graf et al., 2017), and promotes their recombination with sister chromatids to partially compensate for telomere loss, in a process that buffers against premature replicative senescence onset (Balk et al., 2013; Fallet et al., 2014). In the absence of telomerase, telomere shortening leads to R-loop accumulation *in cis* and local enrichment of the recombination protein Rad51 in an R-loop dependent manner (Graf et al., 2017), thereby suggesting that R-loops are required for efficient HR to ensue at short telomeres. Consistently, telomerase negative cells bearing an artificially induced critically short telomere senesce faster than the control cells in which telomere shortening was not induced, and are exquisitely sensitive to RNase H1 overexpression, which causes fast senescence kinetics at early timepoints after telomerase loss (Graf et al., 2017), thereby highlighting the protective role of R-loops at critically short telomeres.

Short telomeres, as opposed to long telomeres, are replicated in early S phase, given Rif1's weakened repression of origin firing (Bianchi and Shore, 2007; Lian et al., 2011). This different replication timing leads to the increased chance of the concomitant presence of two phenomena at telomeres: the passage of the replication fork and the presence of R-loops, which are stabilized by the diminished recruitment of RNase H2 to short telomeres. R-loops across the genome have been widely implicated in causing replication stress and DSB generation, processes that can initiate homologous recombination (Hamperl and Cimprich, 2014; Santos-Pereira and Aguilera, 2015), especially when the mechanisms that usually are in place to avoid their formation or remove them are impaired. Likewise, this might be true also for critically short telomeres; indeed, the novel findings of the impaired Rif2/RNase H2 mediated coordination between telomere

replication and R-loop resolution at short telomeres support the idea that telomeric R-loops might promote HR at telomeres by causing replication stress (Balk et al., 2013)(Figure 21, bottom left). Telomeric regions are by nature structures difficult to replicate, as suggested by the requirement for the action of the 5' to 3' DNA helicase Rrm3, which is found to localize to telomeres (Ivessa et al., 2002). Of note, a series of observation suggest that the replication stress normally present at telomeres is exacerbated during senescence. Pre-senescent cultures display checkpoint activation, which stems from critically short and uncapped telomeres (Ijpma and Greider, 2003; Sandell and Zakian, 1993). Interestingly, pre-senescent cells display increased Rnr3 protein levels (Ijpma and Greider, 2003), a readout for DNA damage checkpoint activation and replication stress (Elledge and Davis, 1990). Importantly, Rnr3 levels can be reduced by RNase H1 overexpression in pre-senescent cells, indicating that telomeric R-loops that accumulate at short telomeres contribute to the activation of the DNA damage checkpoint (Graf et al., 2017); whether this outcome is directly caused by replication stress is still to be determined. Remarkably, Mrc1, a well described sensor of replication stress, is phosphorylated in pre-senescent cells and contributes together with Rad9 to activate the checkpoint (Grandin et al., 2005). Furthermore, Mms1, a subunit of the E3 ligase complex involved in maintenance of replication fork stability during replication stress by preventing fork collapse and promoting fork restart (Buser et al., 2016; Zaidi et al., 2008), supports cell viability in pre-senescent cells (Abdallah et al., 2009). These observations suggest that the replication of short telomeres is challenging, and that HR could be necessary for its completion to avoid premature entry in senescence induced by critically short telomeres. Furthermore, they suggest that the activation of DNA damage signaling pathways and the protection against replication stress promote viability in telomerase negative cells. Importantly, R-loops seem to play an important role in these processes. Interestingly, depletion of the telomeric proteins Taz1 and TRF1, in *S. pombe* and human cells respectively, causes replication stress at telomeres, which result in elongated telomeres (Miller et al., 2006; Sfeir et al., 2009). Interestingly, both mutants display increased TERRA levels, again suggesting a link between TERRA accumulation and replication stress at telomeres (Greenwood and Cooper, 2012; Porro et al., 2014).

Alternatively, R-loop accumulation might promote recombination at short telomeres by causing prolonged displacement of the opposite 3' single-stranded overhang, which might

become covered by the single-strand binding protein RPA, and successively Rad51, leading to strand invasion and HR ensue (Figure 21, bottom right). This second hypothesis would not be mutually exclusive with R-loops promoting HR by causing replication stress, and importantly could take place also in the absence of the replication machinery passage through telomeres.

4.3 Telomeric R-loops are increased in ICF syndrome cells

The increase of R-loop levels at short telomeres and the consequent activation of the DNA damage response could be conserved from yeast to human cells. Interestingly, recently it has been reported that stable R-loops accumulate at short telomeres in ICF (Immunodeficiency, centromeric instability and facial anomalies) syndrome cells (Sagie et al., 2017). Furthermore, these R-loops activate the DNA damage signaling at telomeric ends and cause telomere dysfunction, as RNase H1 overexpression could highly reduce the damage signaling stemming from telomeres in ICF syndrome cells (Sagie et al., 2017). ICF syndrome is caused by hypomorphic mutations in the DNA methyltransferase DNMT3B, which *de novo* methylates repetitive sequences during development (Okano et al., 1999; Xu et al., 1999). Indeed, the subtelomeres in ICF syndrome patients' cells are hypomethylated, resulting in increased TERRA levels throughout the cell cycle and telomeric R-loop accumulation (Sagie et al., 2017; Yehezkel et al., 2008). Telomeres in ICF cells are short, undergo accelerated shortening and enter replicative senescence prematurely (Yehezkel et al., 2008; Yehezkel et al., 2013). Increased TERRA expression in ICF syndrome cells appears not to be a mere consequence of telomere shortening, as telomere elongation in ICF syndrome cells by ectopic overexpression of telomerase does not downregulate TERRA levels in these cells (Yehezkel et al., 2008). These observations suggest that TERRA and telomeric R-loop levels need to be kept in check in order to preserve telomere maintenance homeostasis also in human cells. While telomeric R-loops might promote telomere maintenance by HR mechanisms, rampant R-loop accumulation might have a contrary effect, inducing excessive replicative stress at telomeres and abrupt telomere loss, as seen in human ALT cancer cells accumulating excessive R-loops (Arora et al., 2014). In conclusion, while telomeric R-loops do not seem to be needed at long

telomeres, they should not accumulate in an uncontrolled manner also in human cells (Arora et al., 2014; Parajuli et al., 2017; Sagie et al., 2017), and regulated removal of R-loops before arrival of the replication fork might be a conserved mean to avoid R-loop induced instability at human long telomeres.

4.4 Telomeric R-loops promote HR-mediated telomere maintenance mechanisms

S. cerevisiae type II survivors and ALT cancer cells are thought to be functionally equivalent. Indeed, both cell types maintain their telomeres in a telomerase-independent fashion, and elongate them by a BIR-dependent recombination mechanism (Dilley et al., 2016; Lydeard et al., 2007). In both cell types, in fact, terminal telomeric repeats are elongated by replicating through other telomeres in the cell, which serve as a template. In recent years, additional features have been identified that are shared between these two cell types: both display increased TERRA levels (Misino et al., manuscript submitted; Tina Balk PhD thesis; (Arora et al., 2014; Lovejoy et al., 2012; Pfeiffer and Lingner, 2012)), and more importantly, both ALT cancer cells and yeast type II survivors appear to rely on telomeric R-loops for efficient telomere maintenance by prompting recombination at telomeres (Misino et al., manuscript submitted; (Arora et al., 2014)). Although the accumulation of telomeric R-loops seems to be required for this process in ALT cells, telomeric R-loops must nonetheless be regulated to a certain extent, and must not accumulate in an uncontrolled manner. Indeed, in ALT cancer cells RNase H1 is specifically recruited to telomeres and both its downregulation and upregulation destabilize cellular integrity (Arora et al., 2014). RNase H1 depletion leads to increased telomeric R-loop levels, increased formation of ssDNA at telomeres and abrupt telomere excisions especially at leading strand telomeres (where the R-loops form). On the other hand, RNase H1 overexpression, by decreasing telomeric R-loop levels, reduces the recombinogenic potential of telomeres, and leads to telomere shortening thereby impairing ALT cell growth (Arora et al., 2014). Interestingly, we observed the same outcome in *S. cerevisiae* telomerase negative cells: both RNase H1 deletion and overexpression (in a level dependent manner) lead to premature senescence onset, again suggesting that R-loops are required but their levels must also be regulated.

Furthermore, novel data indicate that telomeric R-loops sustain type II survivor growth, as RNase H1 overexpression in unchallenged established type II survivors decreases their viability, while it has no effect on wild type cells (Misino et al., manuscript submitted). Importantly, telomeric R-loops have been shown to promote the generation of type II survivors (Yu et al., 2014). While telomerase negative cells that accumulate excessive telomeric R-loops form type II survivors efficiently, RNase H1 and H2 overexpression inhibits type II survivor formation (Yu et al., 2014). Interestingly, while *rnh1* mutants seem to efficiently form type II survivors, *rnh201* mutants, while still forming them, seem to generate type II survivors in a less efficient manner; this could be caused simply by the delay in senescence (and survivor formation) of *rnh201* mutants, but also by a defect in the establishment of type II survivors in this mutant. This observation might point to different roles of RNase H1 and 2 also in established type II yeast survivors and suggest that impaired R-loop processing reduces their recombinogenic potential (Yu et al., 2014). Moreover *rif2*, but not *rif1*, mutants preferentially form type II survivors (Teng et al., 2000), which could be linked to the accumulation of R-loops in this mutant. Interestingly, telomeres in *S. cerevisiae* type II survivors undergo shortening at each replication round, comparable to pre-senescent cells, and only when they become critically short they undergo abrupt and dramatic HR-dependent lengthening events (Fu et al., 2014; Teng et al., 2000). It is tempting to speculate that R-loops accumulate exclusively at these critically short telomeres, as we propose for pre-senescent cells, and thereby allow HR-mediated lengthening. However, neither the preservation of the Rif2/RNase H2 pivotal role in regulating R-loops nor the accumulation of R-loops exclusively at short telomeres in type II survivors has been shown yet.

Replication stress has been identified at telomeres in ALT cancer cells, and has been hypothesized to be a promoter of telomere recombination (Flynn et al., 2015; O'Sullivan et al., 2014). Chronic replication stress is reflected in SMARCAL1 localization to ALT telomeres (Cox et al., 2016), a DNA annealing helicase which promotes fork restart and is highly enriched at stalled replication forks (Bansbach et al., 2009; Dungrawala et al., 2015). SMARCAL1 is required to resolve replication stress at ALT telomeres and maintain their stability (Cox et al., 2016). Importantly, the removal of TERRA foci at ALT telomeres, which might represent R-loops, is impaired: while in normal cells TERRA foci colocalizing with telomeres are removed throughout S phase into G2/M, in ALT cells this regulation is

impaired, and telomere-associated TERRA foci are stabilized in S phase and G2/M (Flynn et al., 2015). This deregulation of telomeric TERRA foci removal at ALT telomeres has been proposed to be caused by the common lack of the ATRX helicase expression in ALT cells (Flynn et al., 2015). Whether TERRA deregulated accumulation at ALT telomeres is the cause for the replication stress present at these telomeres has not been directly tested, although several indications suggest that this might be the case (Arora et al., 2014; Flynn et al., 2015). Finally, TERRA has been identified as novel component of APBs, the telomere recombination factories characteristic of ALT cells (Arora et al., 2014), again pointing to a direct involvement of TERRA in the promotion of the ALT mechanism.

Therefore, the dependence on telomeric R-loops seems to be a feature shared between type II survivors and ALT cancer cells. While in ALT cells the role of RNase H2 has not yet been investigated at telomeres, previous data and our new observations in yeast show a clear important role for this enzyme. Indeed, it will be of great interest to study if RNase H2 has a role also at normal human and ALT telomeres, thereby allowing the understanding of the fine regulation of telomeric R-loops. Interestingly, we could detect a minor but consistent enrichment of RNase H1 at *S. cerevisiae* short telomeres in pre-senescent cells, an observation reminiscent of the exclusive recruitment of RNase H1 at R-loop accumulating telomeres in ALT cancer cells (Arora et al., 2014). Furthermore, it will be interesting to test whether also in type II survivors the Rif2/RNase H2 axis regulates telomeric R-loop accumulation in a telomere length dependent manner.

4.5 Telomeric R-loops might promote efficient telomerase-mediated elongation of short telomeres.

There are indications that the role of TERRA and telomeric R-loops in promoting short telomere elongation in telomerase negative cells might be a pathway conserved in telomerase positive cells. Paradoxically, initially TERRA had been thought to be an inhibitor of telomerase, as it can basepair with the template sequence for telomeric repeats on the telomerase RNA moiety. Indeed, *in vitro* TERRA-mimicking oligonucleotides are potent inhibitors of telomerase enzymatic activity (Redon et al., 2010; Schoeftner and

Blasco, 2008). Importantly, additional studies revealed that TERRA can interact with telomerase *in vivo* in a variety of organisms (Cusanelli et al., 2013; Moravec et al., 2016; Redon et al., 2010). But in contrast to the initial hypothesis, the latest results propose instead a positive outcome deriving from this interaction, namely the recruitment of telomerase to critically short telomeres in order to promote their elongation (Cusanelli et al., 2013; Moravec et al., 2016).

The gradual or abrupt generation of critically short telomeres in telomerase positive cells renders them targets of the enzyme telomerase, which will subsequently elongate them. Indeed, telomerase preferentially acts on short telomeres compared to long (Marcand et al., 1999; Teixeira et al., 2004). Also in telomerase positive cells, Rif2 and RNase H2 loss from the short telomere would lead to telomeric R-loops stabilization *in cis*; additionally, short telomeres would be unique due to the increased amounts of free (not chromatin associated) TERRA molecules transcribed from them (Cusanelli et al., 2013; Graf et al., 2017; Moravec et al., 2016). An appealing idea would be that these newly identified features of short telomeres would have a role in the elongation of critically short telomeres by telomerase. Recent work carried out in *S. cerevisiae* investigated TERRA localization by live cell microscopy, and led to the observation that, after transcription, TERRA molecules originating from a short telomere formed a focus in the nucleoplasm. Subsequently, telomerase molecules clustered over this focus (forming a telomerase recruitment cluster or T-Rec) and together they re-localized with high preference to the same telomere from which TERRA had been transcribed. Whether this interaction of TERRA with telomerase is functional, was not further investigated in this study, but it put forward the idea that increased TERRA levels deriving from short telomeres could direct telomerase to its substrate. The induction of a critically short telomere containing a terminator sequence downstream of TERRA TSS, causing reduced TERRA expression, led to impaired elongation of the short telomere by telomerase *in cis* (Marco Graf PhD thesis). This observation suggests that TERRA might promote the efficient elongation of critically short telomeres in *S. cerevisiae*. Indeed, one could speculate that free TERRA could help to direct telomerase in a specific manner to the parental telomere by base pairing with it, i.e. forming an R-loop, which would be stabilized at short telomeres due to the absence of RNase H2 (Figure 22). A preliminary experiment, in which telomerase-mediated elongation of an induced critically short telomere was measured in RNase H1

overexpressing cells or control cells resulted in slightly reduced telomere elongation kinetics in the presence of RNase H1 overexpression (data not shown), suggesting that telomeric R-loops accumulating at short telomeres might promote telomerase recruitment *in cis*. Of note, we can exclude that this mechanism is required for telomerase action at telomeres, as overexpression of RNase H1 has no effect on bulk telomere length in telomerase positive cells (D. Bonetti, personal communication and data not shown). However, this leaves open the possibility that R-loops might affect the kinetics of telomerase recognition of the short telomeres while not affecting the final outcome, bulk telomere length. Interestingly, *rif2* and *rnh201* mutants display increased telomere length, and in light of the novel results on RNase H2 pivotal role in regulating telomeric R-loops, it would be tempting to speculate that increased stability of R-loops in these mutants could stabilize T-Recs recruitment/binding even to long telomeres, and therefore lead to increased bulk telomere length.

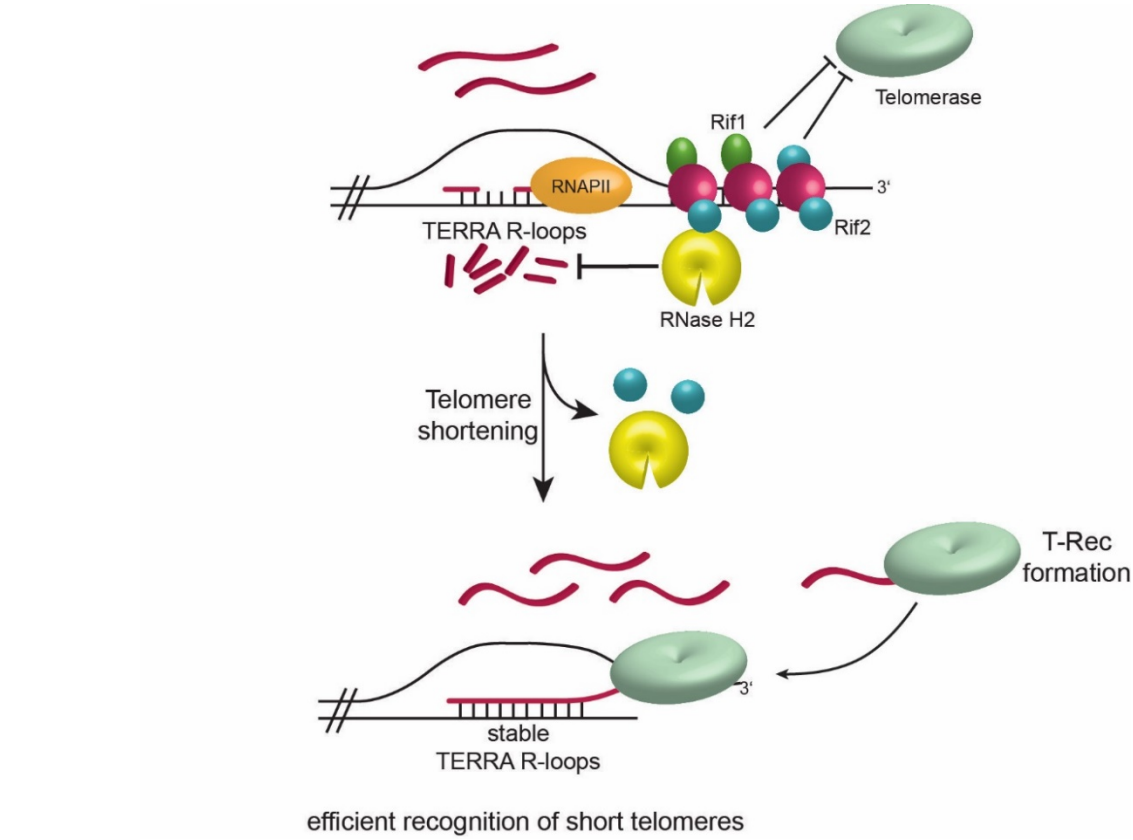

Figure 22. TERRA and telomeric R-loops might promote telomerase recruitment to short telomeres.

At long telomeres, telomerase action is inhibited by the telomeric proteins Rif1 and Rif2 (Wotton and Shore, 1997). As telomeres shorten, telomerase inhibition is released, and R-loops accumulate due to RNase H2 loss; furthermore, TERRA levels are upregulated (Graf et al., 2017). TERRA interacts with telomerase in the nucleoplasm, forming T-Recs (telomerase recruitment clusters) that re-localize to the telomere from which TERRA was transcribed to elongate it (Cusanelli et al., 2013). The formation of an R-loop might be involved in this process, conferring specificity of the TERRA-telomere interaction and improving the efficiency of short telomere recognition by telomerase.

Importantly, a role for TERRA in promoting telomerase activity has been identified in a novel study in *S. pombe*, in which a functional interaction between polyadenylated TERRA and telomerase was observed (Moravec et al., 2016). The generation of a short telomere leads to increased TERRA transcription *in cis*, and especially leads to the accumulation of the polyadenylated TERRA form; moreover, this TERRA pool was found to physically interact with telomerase. Importantly, artificial induction of TERRA expression from one telomere led to telomere elongation *in cis*, thereby demonstrating that increased TERRA expression at short telomeres is functional in promoting and directing telomerase activity to that same telomere (Moravec et al., 2016). Conversely, artificially highly induced transcription of a single *S. cerevisiae* telomere leads to telomere shortening *in cis*, in a telomerase-independent manner (Maicher et al., 2012; Pfeiffer and Lingner, 2012). The observed shortening requires the passage of the replication fork, and is mediated by Exo1 resection, which is active in S and G2/M phases (Maicher et al., 2012; Pfeiffer and Lingner, 2012). It can be speculated that the increased chance of encounters between the replication machinery and RNA Pol II transcribing TERRA might be the cause of this effect, and not TERRA inhibition of telomerase. Furthermore, such forced transcription of telomeric ends is fundamentally different from what happens at natural short telomeres, where increased TERRA levels are not caused by increased transcription but rather increased TERRA stabilization, due to loss of the exonuclease Rat1 from short telomeres (Graf et al., 2017).

In conclusion, a functional interaction between TERRA and telomerase has not been formally proven yet in *S. cerevisiae*, but it would definitely explain the increased pool of “free TERRA” molecules that derives from short telomeres, both in telomerase positive and negative cells (Cusanelli et al., 2013; Graf et al., 2017). Whether free TERRA has a role in telomerase negative cells remains unclear, especially because TERRA regulation seems to be independent of R-loop regulation, as RNase H1 overexpression, while decreasing R-loop levels in pre-senescent cells, has no effect on TERRA levels (Graf et al., 2017).

4.6 RNase H1 and H2 play different roles genome-wide in the removal of R-loops

We have identified a differential requirement for RNase H1 and H2 in response to genome-wide replication stress: interestingly, the two enzymes are required in different cell cycle phases (Figures 17A and 20A). Previous data showed that, in the presence of low doses of replication stress, expression of one of the two RNase H enzymes is sufficient to support cell growth, while lack of both enzymes leads to high sensitivity to replication stress, suggesting that RNase H1 and H2 act redundantly (Lazzaro et al., 2012). By making use of cell-cycle regulated RNase H1 and H2 enzymes, we could identify that the timing of RNases H action must be tightly regulated, and that the two enzymes act in different cell cycle phases in response to MMS-induced replication stress, thereby suggesting non-overlapping functions of RNase H enzymes in this context.

4.6.1 RNases H1 and H2 may act in different cell cycle phases.

In this work, we have found that, when replication stress is induced by MMS treatment, the exclusive expression of RNase H2 in S phase leads to a phenotype equal to that of the depletion of RNase H enzymes (Figure 20A). This suggests that, in the presence of genome-wide replication stress, RNase H2 cannot remove all R-loops present during S phase, which might persist until G2 and cause cell lethality. Differently, the exclusive expression of RNase H1 in S phase in presence of replication stress can fully support cell viability (Figure 17A). On the contrary, alone RNase H1 expression exclusively in G2/M phases leads to high sensitivity to replication stress, more acute than when both RNase H enzymes are depleted. Taken together, these results might suggest that RNase H1 is the main enzyme that restricts R-loops genome-wide during S phase, while RNase H2 might be needed outside the S phase. Furthermore, it suggests that the exclusive activity of RNase H1 in G2/M might generate some damage that cannot be repaired.

These results are striking, as RNase H2 in known to take part in many functions connected to replication, which would suggest a role for RNase H2 in R-loop removal during S phase. Importantly, R-loops are known obstacles for replication fork progression and RNase H2 movement with the replication fork may lead to their recognition and degradation (Hamperl

and Cimprich, 2014; Santos-Pereira and Aguilera, 2015). Indeed, RNase H2 is thought to associate to the replisome thanks to its PIP-box domain (Bubeck et al., 2011; Chon et al., 2013; Chon et al., 2009), and in human cells RNase H2 has been found to colocalize with replication foci (Bubeck et al., 2011). Furthermore, RNase H2 functions during Okazaki primer removal and removal of misincorporated rNTPs from the DNA (Chon et al., 2013; Rydberg and Game, 2002; Sparks et al., 2012). Importantly, RNase H2 roles during replication, which are not shared by RNase H1, are redundant with other pathways. This suggests that the sensitivity of *rnh1 rnh201* mutants to genotoxic agents might be explained by excessive genome-wide accumulation of R-loops in cells which are additionally challenged by exogenously induced replication stress, which could increase the load of replication stress to unmanageable levels. To date, there is no information on the timing of RNase H2 removal of R-loops, which, taking into account our novel data, might be independent from its interaction with the replication fork. Interestingly, an Rnh202 allele that lacks the PIP-box motif has not been found to be defective in any conditions tested so far, including R-loop removal (Lafuente-Barquero et al., in press; (Chon et al., 2013; Sparks et al., 2012)), suggesting that the interaction of RNase H2 with the replication machinery is not required for RNase H2 function.

4.6.2 R-loops must be degraded to allow repair completion

In the recent years, several studies have identified the involvement of R-loops in DSB processing, implicating the need for RNase H activity to allow efficient DSB repair (Amon and Koshland, 2016; Li et al., 2016; Ohle et al., 2016). Of note, a recent study from the Koshland group proposed a novel and largely unexplored idea: R-loop removal activities are not only necessary in order to avoid generation of replication stress, but these activities also have to take place during R-loop induced damage resolution (Amon and Koshland, 2016). The presence of unprocessed R-loops during the repair of R-loop induced DSBs could lead to inaccessibility of the DNA strand which partakes in the RNA-DNA hybrid, in a way that might inhibit resection (if it is on the 5’ strand) or strand invasion into a homologous sequence after resection of the opposite strand (if it is on the 3’ strand; Figure 23). *rnh1 rnh201* mutants increasingly accumulate Rad52 foci from late S until M

phase, indicative of DNA damage which is difficult to repair. When the R-loop load is further increased in *rnh1 rnh201* mutants, the excessive DNA damage cannot be resolved and cells arrest permanently in G2/M. This phenotype could be rescued by depleting factors involved in the BIR repair mechanism, and especially in BIR processivity. Importantly, this did not prevent DNA damage formation, but promoted damage resolution in G2/M.

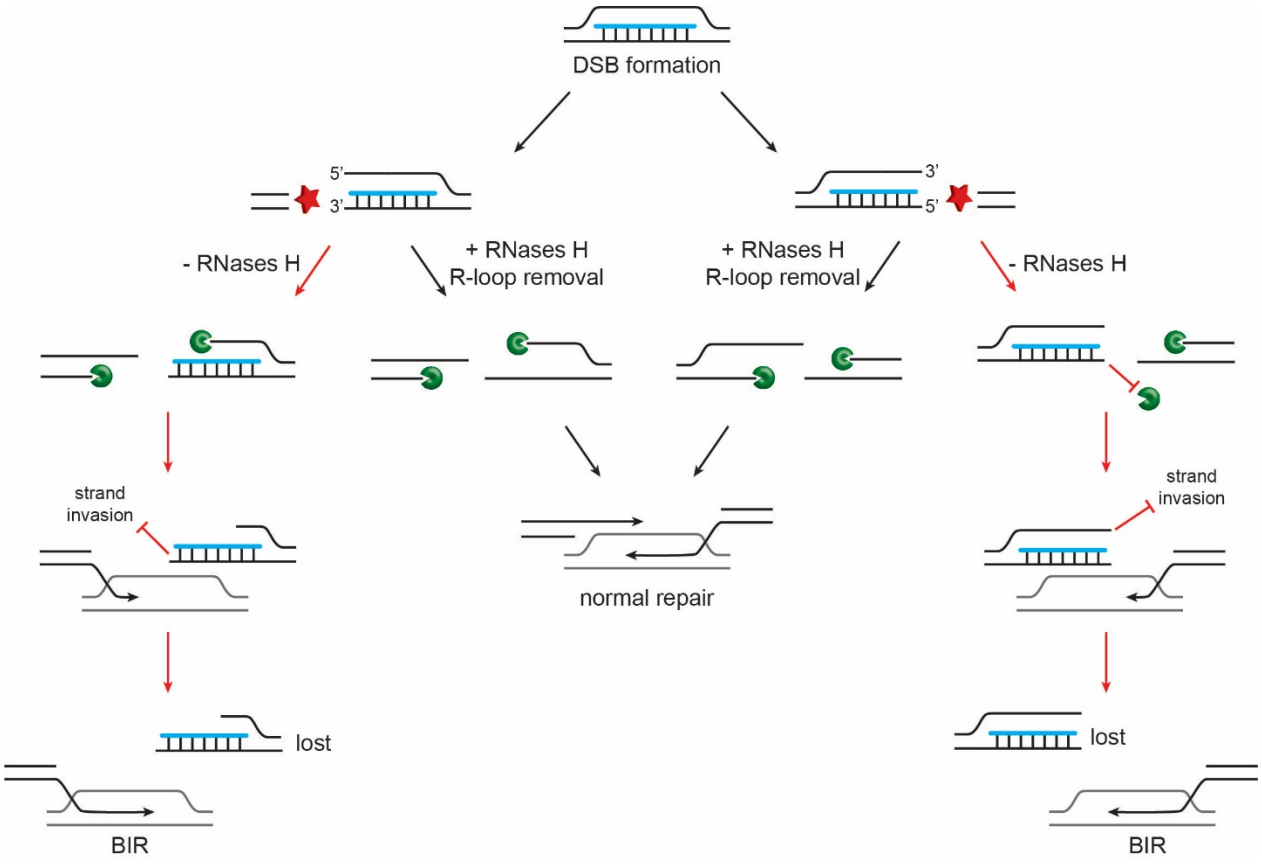

Figure 23. R-loop removal is required for efficient processing of R-loop induced DSBs.

After the generation of a DSBs at the site of a stabilized R-loop, the R-loop must be removed by RNase H activity in order to allow efficient HR-dependent repair (center). When the R-loop involves the 3' end of a break, if not removed it would cover the 3' recombinogenic DNA end, inhibiting strand invasion and HR ensue (left). When the R-loop involves the 5' end of the DSB, if not removed it may inhibit the activity of exonucleases, needed to generate a recombinogenic 3' ssDNA (right). In both cases, the chromosome part containing the unresolved R-loop would be lost and the other DSB end must be repaired by the mutagenic BIR mechanism (Deem et al., 2008; Smith et al., 2007). Modified from (Amon and Koshland, 2016).

These results suggest that the absence of RNase H activity generates damage that is difficult to repair after S phase completion. Furthermore, excessive R-loop stabilization results in the promotion of BIR-mediated repair, which is a pathway that is active when only one strand of a DSB is available. During BIR, one end of the DSB invades the homologous chromosome and replicates through it (Malkova and Ira, 2013; Malkova et al., 1996); this process can replicate entire chromosomes, and therefore could be highly detrimental for genome stability and is not the preferred repair mechanism at DSBs (Deem et al., 2008; Smith et al., 2007). Indeed, BIR activation at DSB containing stable R-loops is a source of genome instability (Amon and Koshland, 2016).

Two other studies have detected R-loop accumulation around DSBs upon DSB generation and the need for their processing (Li et al., 2016; Ohle et al., 2016). A work by the Fischer lab in *S. pombe* has identified the need for regulated action of RNAse H activity at DSBs (Ohle et al., 2016). While in the absence of RNase H1 and H2 R-loop deregulated processing led to impaired resection of DSBs, and therefore diminished recombination efficiency, when RNase H1 was overexpressed resection was excessive and led to genome instability. This work indicates that RNase H activity, by removing R-loops at DSBs, allows the correct processing of DSB ends to permit efficient HR-mediated repair (Ohle et al., 2016). An additional study in human cells has implied the need for protecting the single stranded DNA generated by resection from forming R-loops with RNAs that had been transcribed prior to DSB formation, to allow efficient HR-mediated repair (Li et al., 2016). Finally, some preliminary data from *S. cerevisiae* suggest that R-loops might be DSB repair intermediates also in this organism. When wild type cells are grown in medium containing low doses of MMS, overexpression of RNase H1 causes a slight but significant reduction of cellular viability compared to the empty vector control (Misino et al., manuscript submitted). This observation might be in line with the scenario presented in (Ohle et al., 2016). In conclusion, RNase H activity appears to be essential for efficient repair of DSBs, especially when they contain R-loops at their extremities.

By considering the requirement of RNase H enzymes in the cell cycle when cells are under replication stress and the novel data just described, we can imagine the following scenario (Figure 24). During S phase, RNase H1 is able to remove all R-loops that are potentially deleterious for genome instability, as RNase H1 expression in S phase in *rnh201* mutants

leads to survival upon replication stress induction (Figure 17A). On the contrary, RNase H2 might only play a minor role in removing R-loops in this cell cycle phase. Indeed, expression of RNase H2 only in S phase in *rnh1* mutants led to a phenotype equal to *rnh1 rnh201* (Figure 20A). In G2/M, RNase H2 might be the enzyme dedicated to the removal of R-loops in order to allow efficient repair of DSBs containing R-loops. On the contrary, RNase H1 action in this phase might be inhibited, as expression of RNase H1 exclusively in G2/M phase in *rnh201* mutants leads to high replication stress sensitivity (Figure 17A). Indeed, *rnh201* mutants display increased loss of heterozygosity (O'Connell et al., 2015). It is possible that the presence of RNase H activity after BIR has already initiated might generate a recombinogenic end that would interfere with the repair process already in act, leading to genome instability.

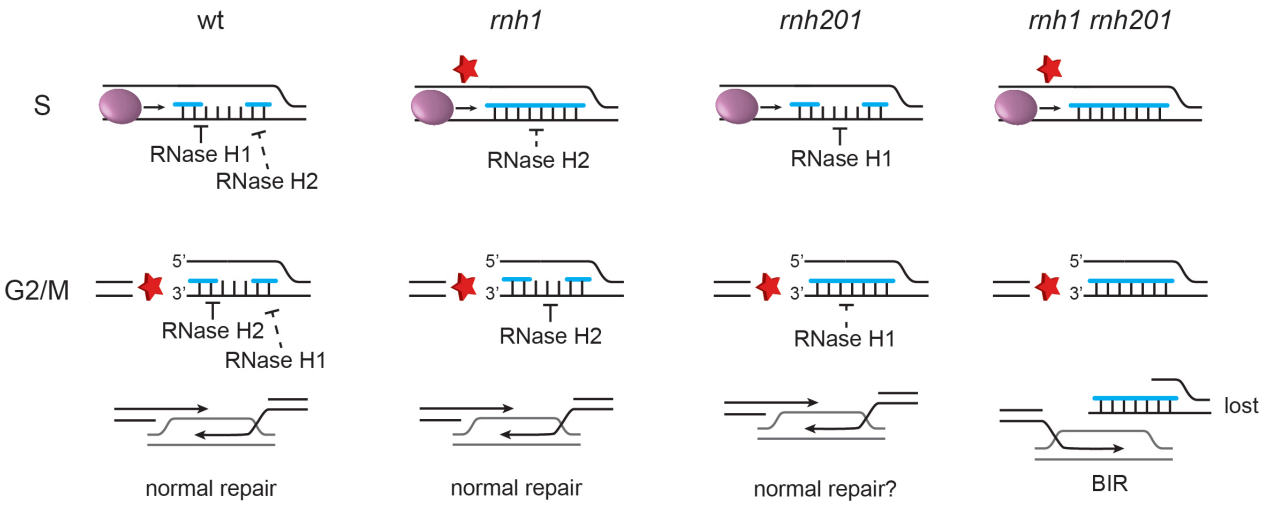

Figure 24. Possible requirement for RNase H1 and H2 function in the cell cycle.

Left: RNase H1 might provide the major RNase H activity during S phase, while RNase H2 might play a minor role. In G2, R-loops present at DSBs might be processed by RNase H2, while RNase H1 might play a minor role, or even be inhibited. In *rnh1* mutants, unprocessed R-loops might generate DSBs upon collision with the replication fork. Repair of DSBs in G2/M phase might be aided by RNase H2 removal of R-loops to allow efficient resection. In *rnh201* mutants, RNase H1 might process R-loops to prevent the generation of DSBs upon collision with the replication fork; R-loops present at DSBs might be processed by RNase H1. Right: in *rnh1 rnh201* mutants, unprocessed R-loops will cause replication-mediated DSBs, which will be difficult to repair and lead to BIR.

4.7 RNase H1 and H2 have non-overlapping functions at telomeres

The requirement for RNase H1 and H2 in pre-senescent cells appears to be strikingly different from their requirement in response to replication stress in the rest of the genome. We observed that the deletion of each RNase H enzyme has a strong effect on senescence onset, while in response to replication stress deletion of each RNase H has no effect on cell viability (Lazzaro et al., 2012). Furthermore, while in the absence of telomerase the deletion of RNase H2 leads to extremely delayed senescence onset, the deletion of RNase H1 leads to accelerated senescence, similar to RNase H1 overexpression (Figure 13). The combination of both RNases H enzymes deletions leads to a delayed senescence onset, with senescence kinetics intermediate between otherwise wild type telomerase negative strains and telomerase negative RNase H2 deficient mutants. These results suggest that RNases H enzymes play very diverse roles at telomeres during senescence and that the exclusive presence of RNase H1 during senescence has the most positive outcome, by delaying senescence onset.

The differences we detected in RNase H requirement at telomeres compared to their genome-wide requirement might be due to the fact that the consequences of R-loop accumulation at telomeres are very different to the consequences of R-loop accumulation genome-wide, even though in both cases a similar response is activated, namely the ensue of homologous recombination (Balk et al., 2013; Hamperl and Cimprich, 2014; Santos-Pereira and Aguilera, 2015). At critically short telomeres in pre-senescent cells the accumulation of R-loops has a positive outcome: the promotion of HR, leading to telomere elongation *in cis* and delay of senescence onset (Balk et al., 2013; Fallet et al., 2014; Graf et al., 2017). Instead, R-loop accumulation across the genome is deleterious, leading to hyper-recombination and genome instability (Hamperl and Cimprich, 2014; Santos-Pereira and Aguilera, 2015). Telomeres resemble one-sided DSBs, and are subjected to BIR-based recombination mechanisms (Dilley et al., 2016; Lydeard et al., 2007). While at short telomeres BIR delays senescence onset and sustains telomere maintenance in the absence of telomerase (Lydeard et al., 2007; Xu et al., 2015), and therefore is a favorable outcome, BIR-mediated repair of DSBs in the genome is highly mutagenic and can lead to genome instability and loss of heterozygosity (Deem et al., 2008; Smith et al., 2007), and therefore must be repressed. Interestingly, BIR was shown

to be the prevalent repair mechanism active at DSBs generated by R-loops in *rnh1 rnh201 S. cerevisiae* mutants (Amon and Koshland, 2016). Therefore, RNase H activity must lead to different outcomes at telomeres and genome wide.

The different roles that RNase H enzymes play at telomeres could be linked to their differential binding to long compared to short telomeres: while RNase H2 could be identified at long telomeres, but was decreased at short (Figure 11C), we could not detect RNase H1 binding to long telomeres but it was enriched at short (Figure 11G). The modest enrichment levels of RNase H1 at short telomeres as determined by ChIP might be due to transient localization of the protein. Thereby, the use of a catalytically dead RNase H1 mutant that has been previously identified (Ginno et al., 2012; Zimmer and Koshland, 2016), which can bind R-loops but cannot resolve them causing a more stable recruitment to these structures, could be useful to allow a more robust detection of RNase H1 at short telomeres. While we saw that at short telomeres RNase H2 localization is decreased due to the reduced recruitment of Rif2, this does not exclude independent localization of the enzyme by either interaction with the replication fork (PCNA) or simply by the R-loops themselves, although importantly RNase H2 binding to long telomeres was completely lost in *rif2* cells (Figure 5B).

Therefore, the two RNase H enzymes might have access to R-loops at different times or act at different steps. As proposed by the Koshland lab, processing of R-loops is not only important to inhibit replication stress and eventually the formation of DSBs, but also to repair R-loop induced damage (Amon and Koshland, 2016). Indeed, we can imagine a scenario whereby short telomeres accumulate R-loops in a way that could cause replication stress and HR as a mean to rescue telomere replication. During the repair process, the R-loop must be removed in order to allow access to exonucleases to generate a recombinogenic ssDNA that will invade another telomere. In such scenario, RNase H2 could be dedicated to the regulation of R-loops at long telomeres to avoid replication stress, but as telomeres shorten, where R-loops accumulate and HR ensues, RNase H1 might localize to telomeres and allow efficient HR. How RNase H1 might be recruited preferentially to short telomeres is discussed in the following section.

4.7.1 RPA might recruit RNase H1 to R-loops and promote is activity

Novel data indicate that human RNase H1 physically and functionally interacts with the trimeric single-stranded DNA binding protein complex RPA (Nguyen et al., 2017b). The interaction with RPA stimulates RNase H1 binding to R-loops both *in vitro* and *in vivo*, and additionally it stimulates RNase H1 catalytic activity on R-loops *in vitro*. Indeed, RPA and RNase H1 colocalize at R-loops in cells. In RNase H1 mutants that retain R-loop resolution activity *in vitro* but are compromised in RPA binding, RNase H1 fails to localize to R-loops and cannot process them *in vivo*. Furthermore, when overexpressed, mutant RNase H1 cannot rescue the R-loop mediated genome instability in R-loop accumulating mutants, whereas overexpression of wild type RNase H1 can (Nguyen et al., 2017b). These data indicate that RPA is an R-loop sensor and that the interaction between RPA and RNase H1 is important for the ability of RNase H1 to bind R-loops and to promote their degradation; interestingly, no interaction between RPA and RNase H2 has been detected in this study (Nguyen et al., 2017b), suggesting that RPA might not be required for RNase H2 recruitment to R-loops. The RPA-RNase H1 interaction is conserved in bacteria, as in *E. coli* the single-stranded DNA-binding protein (SSB) binds to RNase HI *in vivo* and stimulates its activity on R-loops *in vitro* (Petzold et al., 2015). Moreover, in *S. cerevisiae* RNase H1 was found to interact with two subunits of the RPA complex, namely Rfa1 and Rfa3, by a proteomic approach (Gavin et al., 2002).

The functional interaction between RPA and RNase H1 could therefore be a conserved mechanism in place to recruit RNase H1 to R-loops. Importantly, this interaction could be relevant for the recruitment of RNase H1 to short telomeres: R-loop stabilization at short telomeres due to local RNase H2 depletion might lead to increased recruitment of RPA to the displaced single stranded filament; indeed, RPA localizes to stabilized R-loops in human cells (Nguyen et al., 2017b). RPA binding to stabilized telomeric R-loops might recruit RNase H1 and promote its activity. Furthermore, the exonucleolytic processing of the 5’ C-strand (the one involved in the R-loop) to allow HR initiation, would lead to further RPA accumulation on the telomeric 3’ overhang, and thereby enhanced local RNase H1 recruitment/activation. Importantly, short telomeres possess long ssDNA overhangs generated by resection activities (Fallet et al., 2014)(Figure 25). This RPA-mediated RNase H1 recruitment might be required for efficient resection of the C-strand (Ohle et

al., 2016) and promotion of HR by generating a long recombinogenic single stranded DNA. In line with this, RNase H1 depletion in telomerase negative cells leads to accelerated senescence onset, which could be due to impaired HR at these telomeres. Interestingly, RPA accumulates at telomeres in ALT cancer cells and seems to be regulated by ATRX activity, as upon ATRX knockdown RPA accumulates at ALT telomeres in G2 phase, which is when TERRA foci at telomeres are stabilized (Flynn et al., 2015; O'Sullivan et al., 2014). Therefore, RPA increased presence at ALT telomeres, which may be due to increased R-loop presence, might be what allows RNase H1 binding exclusively at ALT telomeres and not at telomeres in normal cells.

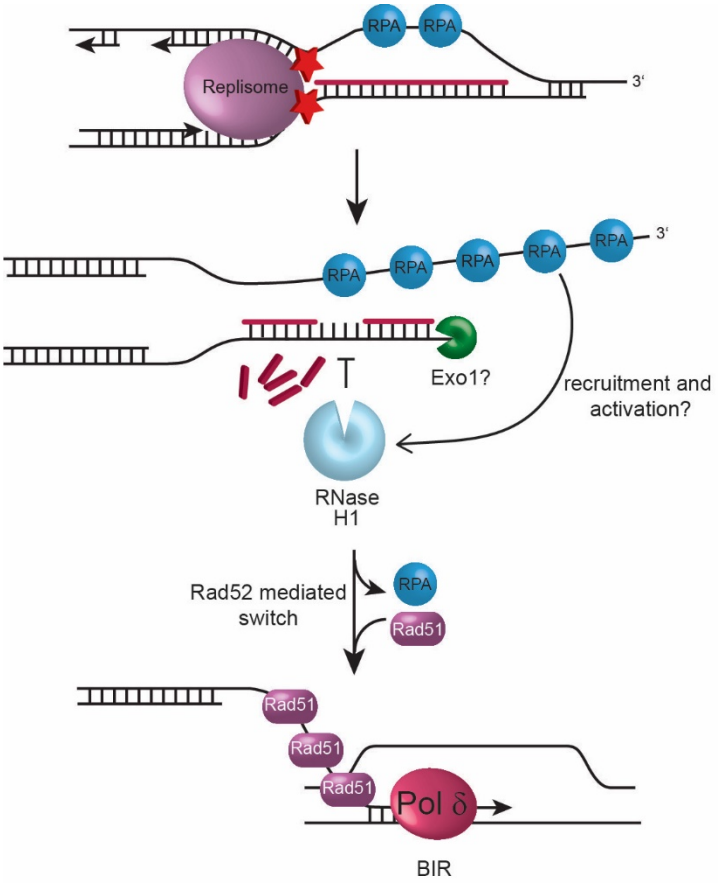

Figure 25. Possible explanation for RNase H1 recruitment to short telomeres.

The single stranded component of stabilized R-loops at short telomeres might be bound by RPA. After R-loop mediated induction of replication stress, resection of the 5' end ensues and recruits more RPA to the opposite strand. Local increased RPA concentration might promote RNase H1 recruitment and activity to remove the R-loop, thereby allowing efficient resection and subsequent BIR-mediated recombination.

We can therefore propose the following model (Figure 26). At long telomeres, RNase H2 has a major role in regulating the timing of R-loops removal, in order to avoid collisions with the replication machinery; RNase H1 might play a compensatory role if RNase H2 is impaired, which could explain why only the double mutant *rnh1 rnh201* displays increased R-loop levels (observation by A. Maicher). As telomeres shorten and RNase H2 recruitment to telomeres is reduced, RNase H1 instead localizes to telomeres; RNase H1 localization and activity might be promoted by RPA enrichment at short telomeres, and may allow efficient resection of the 5'-strand. This model would explain the different senescence kinetics of cells depleted for RNase H enzymes. In the absence of RNase H1, critically short telomeres accumulating R-loops may be impaired in the resection of the 5' strand, leading to impaired recombination and therefore faster senescence. In the absence of RNase H2, the timing of R-loop removal at long telomeres might be impaired, although RNase H1 might still be able to partially remove them. This might lead to recombination already at long telomeres and following efficient resection of the C-strand, therefore causing delayed senescence onset. In the double mutant, R-loop deregulation at long telomeres will promote early recombination, which might be resected inefficiently due to stabilization of the R-loop which might render the 5' strand less accessible to exonucleases, and therefore result in an intermediate phenotype of senescence kinetics. On the contrary, in the case of RNase H1 overexpression, degradation of telomeric R-loops at all steps will impair telomere recombination and lead to fast senescence.

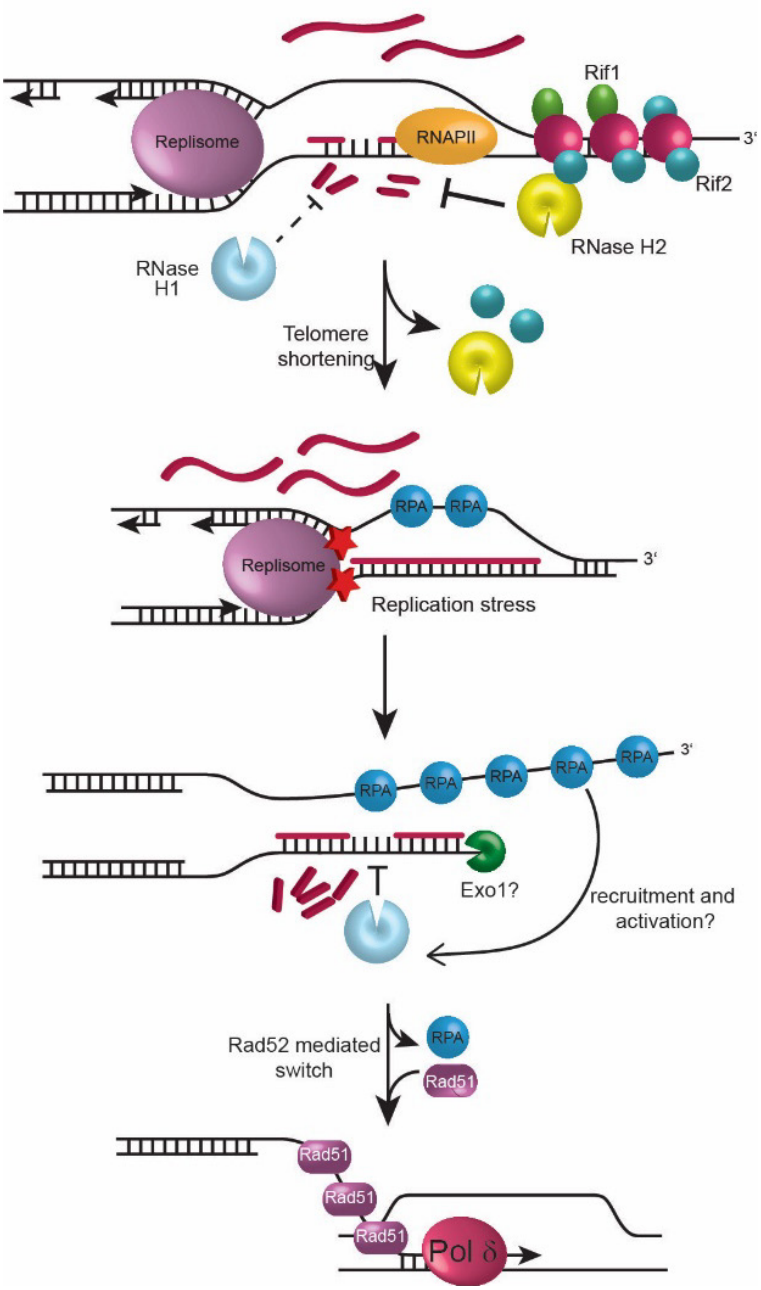

Figure 26. RNase H1 and H2 might functions at telomeres in different steps.

At long telomeres, Rif2 recruits RNase H2 to remove R-loops before the arrival of the replication fork to telomeres. RNase H1 might act at long telomeres when RNase H2 is impaired. As telomeres shorten, RNase H2 loss allows R-loop accumulation and consequent replication stress; RPA might bind to the R-loop. RNase H1 might be recruited to short telomeres by increased localization of RPA, and promote efficient 5' end resection, which initiates BIR-dependent telomere elongation.

4.7.2 Cell cycle regulation of RNase H1 and H2 action at telomeres

The results presented in this thesis suggest that during senescence RNase H1 activity is exclusively required during G2/M phases, independently of RNase H2 presence. Similarly, cells expressing RNase H2 only in S phase during senescence behave as RNase H2 depleted cells, suggesting that also RNase H2 action might be needed in other cell cycle phases. A caveat of the experimental setup using cell cycle specific promoters might be that the expression of proteins using the S phase specific construct seem to lead to degradation of the protein at the end of S phase. Because long telomeres are replicated in late S phase (McCarroll and Fangman, 1988; Raghuraman et al., 2001), which is when RNase H2 must decrease the telomeric R-loops to avoid replication stress, we cannot exclude that the phenotype of RNase H2 expression exclusively in S phase is simply due to its absence in late S phase. RNase H1 requirement outside of S phase might be explained by its proposed role in promoting resection at short telomeres, which might take place in this phase of the cell cycle.

4.8 Future perspectives

We have identified a mechanism that regulates the level of telomeric R-loops, whereby R-loop accumulation is restricted at long telomeres, where they could potentially induce DNA damage upon collision with the replication fork (Hamperl and Cimprich, 2014; Santos-Pereira and Aguilera, 2015). On the contrary, R-loops are stabilized at short telomeres, where they promote HR-mediated telomere elongation and buffer against premature senescence onset (Balk et al., 2013; Fallet et al., 2014). These findings highlight the need for a tight regulation of R-loop accumulation such that telomeric R-loops would be stabilized only when the outcome would be favorable. Indeed, the generation of a single critically short telomere in telomerase negative cells is enough to induce senescence (Abdallah et al., 2009), suggesting that the rescue of short telomeres by homologous recombination might benefit the cell survival; importantly, telomeric R-loops seem to play a pivotal role in this process (Balk et al., 2013; Graf et al., 2017; Yu et al., 2014). This mechanism might be especially important in multicellular organisms, in which accelerated telomere shortening may result in defective tissue regeneration and premature aging.

It would be interesting to map the domain of Rif2 which is required for the interaction with RNase H2. The C-terminus of Rif2 contains a domain required for the interaction with Rap1, and a Rap1 Binding Motif (RBM) is also present in the unstructured N-terminus, which is thought to bridge together two Rap1 molecules (Figure 27; (Shi et al., 2013)). In the middle of the protein is a long AAA+ domain containing Walker A and B motifs; furthermore, in the N-terminus there is a BAT domain (Blocks Addition of Telomeres), which is sufficient to inhibit telomerase action at telomeres (Kaizer et al., 2015; Shi et al., 2013). By constructing truncation mutants of Rif2 which maintain the C-terminal Rap1-binding domain to allow its localization to telomeres, it would be possible to identify the domain required for RNase H2 interaction. This would allow the creation of a Rif2 mutant defective for RNase H2 recruitment, which would be interesting to analyze relative to its effect of R-loops accumulation at telomeres and its effect on senescence kinetics.

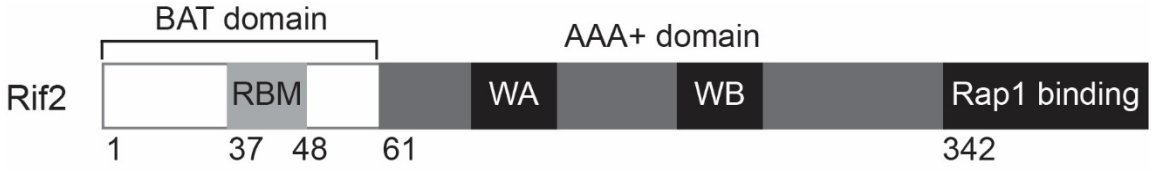

Figure 27. The Rif2 protein contains multiple domains.

Rif2 contains an unstructured N-terminus domain, which is sufficient to inhibit telomerase action at telomeres (BAT domain), and a Rap1-binding domain (RBM). The middle of the protein contains an AAA+ domain, comprising Walker A and Walker B domains, and the C-terminus contains a domain necessary for Rap1 binding. Modified from (Kaizer et al., 2015).

Several observations suggest that pre-senescent cells suffer from replication stress at telomeres (Abdallah et al., 2009; Grandin et al., 2005; Ijpma and Greider, 2003), and multiple studies have suggested that a source of replication stress at telomeres might be the accumulation of R-loops (Arora et al., 2014; Balk et al., 2013; Chawla et al., 2011; Sagie et al., 2017). It will be important to investigate in a direct manner whether the replication stress present in pre-senescent cells is due to R-loop accumulation, as the answer will allow us to explain mechanistically how telomeric R-loops promote recombination at telomeres (Balk et al., 2013). It will therefore be interesting to monitor the phosphorylation status of the replication checkpoint protein Mrc1 in pre-senescent cells upon overexpression of RNase H1 or when R-loops are allowed to accumulate in excess, as for example in *rnh1 rnh201* mutants.

Another interesting area to explore is the deeper understanding of the requirement for RNase H activity to promote efficient repair of DSBs (Amon and Koshland, 2016; Li et al., 2016; Ohle et al., 2016). It will be important to further analyze how R-loops influence DSB repair in *S. cerevisiae*, and especially if R-loops are formed upon DSB formation, as in *S. pombe* and human cells (Li et al., 2016; Ohle et al., 2016). In line with that, RNase H activity might also be important at short telomeres in order to promote efficient resection of the strand containing the RNA-DNA hybrid to initiate HR. This question might be addressed by measuring the telomeric overhang extension in RNase H mutants or upon RNase H1 overexpression, especially in pre-senescent cells. This approach might indicate whether this hypothesis is correct, and whether there is a preferential requirement for one of the RNase H enzymes in this process.

Finally, emerging evidence suggests that the uncontrolled accumulation of telomeric R-loops in human cells might cause telomere instability and might be at the basis of telomeric diseases such as IPF syndrome (Sagie et al., 2017). Importantly, telomeric R-loop accumulation has been shown to be an essential factor involved in the maintenance of ALT cancer telomeres (Arora et al., 2014), reminiscent of yeast type II survivors (Misino et al., manuscript submitted). It will be thus important in the first place to understand how R-loop levels are kept in check at telomeres in human cells, and especially if RNase H2 might play a role in this process. Furthermore, it will be important to understand how R-loops are regulated in type II survivors and by which mechanism they promote telomere maintenance via HR, in order to obtain insights into how telomeres are maintained in ALT cancer cells. In conclusion, it would be of great interest to explore the possibility of targeting R-loops or TERRA as a strategy to selectively impair the growth of ALT tumor cells and as a therapy for IPF syndrome patients.

5. Abbreviations

5-FOA	5-fluoroorotic acid
A	Adenine
aa	Amino acid
AGS	Aicardi-Goutières syndrome
AID	Auxin-inducible degron
AID	Activation-induced cytidine deaminase
ALT	Alternative lengthening of telomeres
Amp	Ampicillin
APB	ALT-associated PML bodies
ARS	Autonomously replicating sequence
BIR	Break-induced replication
bp	Base pairs
C	Cytosine
CEN	Centromeric
ChIP	Chromatin immunoprecipitation
Co-IP	Co-immunoprecipitation
CSR	Class switch recombination
CST	Cdc13-Stn1-Ten1
DKC	Dyskeratosis congenita
DNA	Deoxyribonucleic acid
DRIP	DNA-RNA immunoprecipitation
ds	Double stranded
DSB	Double strand break
E. coli	*Escherichia coli*
EV	Empty vector
FACS	Fluorescence-activated cell sorting
FLC	Flowering locus C
G	Guanine
GAL	Galactose

GFP	Green fluorescent protein
HA	Hemagglutinin
HBD	Hybrid binding domain
HIS	Histidine
HR	Homologous recombination
HTT	HeT-A, TART, TAHRE
HU	Hydroxyurea
HYG	Hygromycin
IAA	Indole-3-acetic acid
ICF	Immunodeficiency, centromeric instability and facial anomalies
IgG	Immunoglobulin G
IgH	Immunoglobulin H
IPF	Idiopathic pulmonary fibrosis
KAN	Kanamycin
kb	Kilobases
kDa	KiloDaltons
LEU	Leucine
LTR	Long terminal repeats
mDNA	Mitochondrial DNA
MMS	Methyl methanesulfonate
mRNP	Messenger ribonucleoprotein particle
MRX	Mre11-Rad50-Xrs2
NAT	Nourseothricin
NER	Nucleotide excision repair
NHEJ	Non-homologous end joining
NMD	Nonsense mediated decay
NPC	Nuclear pore complex
nt	Nucleotides
ORF	Open reading frame
PCR	Polymerase chain reaction
PD	Population doublings
PIP	PCNA-interacting protein

PML	Promyelocytic leukaemia
qPCR	Quantitative PCR
RAFF	Raffinose
rDNA	Ribosomal DNA
RED	Ribonucleotide excision defective
RNA	Ribonucleic acid
RNA pol	RNA polymerase
RNase H	Ribonuclease H
rNTP	Ribonucleoside triphosphate
rRNA	Ribosomal RNA
S. cerevisiae	*Saccharomyces cerevisiae*
S. pombe	*Schizosaccharomyces pombe*
SASP	Senescence-associated secretory phenotype
SC	Synthetic complete
SEM	Standard error of the mean
ss	Single stranded
STR	Subtelomeric repeated elements
T	Thymine
TAP	Tandem affinity purification
TERRA	Telomeric repeat containing RNA
TPE	Telomere position effect
T-Rec	Telomerase recruitment cluster
tRNA	Transfer RNA
TRP	Tryptophan
TSS	Transcription start site
URA	Uracil
YAC	Yeast artificial chromosome

6. References

Abdallah, P., Luciano, P., Runge, K.W., Lisby, M., Geli, V., Gilson, E., and Teixeira, M.T. (2009). A two-step model for senescence triggered by a single critically short telomere. Nature Cell Biology *11*, 988-993.

Addinall, S.G., Holstein, E.M., Lawless, C., Yu, M., Chapman, K., Banks, A.P., Ngo, H.P., Maringele, L., Taschuk, M., Young, A.*, et al.* (2011). Quantitative fitness analysis shows that NMD proteins and many other protein complexes suppress or enhance distinct telomere cap defects. PLoS Genetics *7*, e1001362.

Aguilera, A., and Klein, H.L. (1990). HPR1, a novel yeast gene that prevents intrachromosomal excision recombination, shows carboxy-terminal homology to the Saccharomyces cerevisiae TOP1 gene. Molecular and Cellular Biology *10*, 1439-1451.

Alder, J.K., Guo, N., Kembou, F., Parry, E.M., Anderson, C.J., Gorgy, A.I., Walsh, M.F., Sussan, T., Biswal, S., Mitzner, W.*, et al.* (2011). Telomere length is a determinant of emphysema susceptibility. American Journal of Respiratory and Critical Care Medicine *184*, 904-912.

Alter, B.P., Giri, N., Savage, S.A., and Rosenberg, P.S. (2009). Cancer in dyskeratosis congenita. Blood *113*, 6549-6557.

Alzu, A., Bermejo, R., Begnis, M., Lucca, C., Piccini, D., Carotenuto, W., Saponaro, M., Brambati, A., Cocito, A., Foiani, M.*, et al.* (2012). Senataxin associates with replication forks to protect fork integrity across RNA-polymerase-II-transcribed genes. Cell *151*, 835-846.

Amon, J.D., and Koshland, D. (2016). RNase H enables efficient repair of R-loop induced DNA damage. eLife *5*.

Anbalagan, S., Bonetti, D., Lucchini, G., and Longhese, M.P. (2011). Rif1 supports the function of the CST complex in yeast telomere capping. PLoS Genetics *7*, e1002024.

Anderson, E.M., Halsey, W.A., and Wuttke, D.S. (2002). Delineation of the high-affinity single-stranded telomeric DNA-binding domain of Saccharomyces cerevisiae Cdc13. Nucleic Acids Research *30*, 4305-4313.

Aparicio, O.M., Billington, B.L., and Gottschling, D.E. (1991). Modifiers of position effect are shared between telomeric and silent mating-type loci in S. cerevisiae. Cell *66*, 1279-1287.

Arbuckle, J.H., Medveczky, M.M., Luka, J., Hadley, S.H., Luegmayr, A., Ablashi, D., Lund, T.C., Tolar, J., De Meirleir, K., Montoya, J.G.*, et al.* (2010). The latent human herpesvirus-6A genome specifically integrates in telomeres of human chromosomes in vivo and in vitro. Proceedings of the National Academy of Sciences of the United States of America *107*, 5563-5568.

Arbuckle, J.H., and Medveczky, P.G. (2011). The molecular biology of human herpesvirus-6 latency and telomere integration. Microbes and Infection *13*, 731-741.

Armanios, M., and Blackburn, E.H. (2012). The telomere syndromes. Nature Reviews Genetics *13*, 693-704.

References

Armanios, M.Y., Chen, J.J., Cogan, J.D., Alder, J.K., Ingersoll, R.G., Markin, C., Lawson, W.E., Xie, M., Vulto, I., Phillips, J.A., 3rd*, et al.* (2007). Telomerase mutations in families with idiopathic pulmonary fibrosis. The New England Journal of Medicine *356*, 1317-1326.

Arnoult, N., Van Beneden, A., and Decottignies, A. (2012). Telomere length regulates TERRA levels through increased trimethylation of telomeric H3K9 and HP1alpha. Nature Structural & Molecular Biology *19*, 948-956.

Arora, R., Lee, Y., Wischnewski, H., Brun, C.M., Schwarz, T., and Azzalin, C.M. (2014). RNaseH1 regulates TERRA-telomeric DNA hybrids and telomere maintenance in ALT tumour cells. Nature Communications *5*, 5220.

Arudchandran, A., Cerritelli, S., Narimatsu, S., Itaya, M., Shin, D.Y., Shimada, Y., and Crouch, R.J. (2000). The absence of ribonuclease H1 or H2 alters the sensitivity of Saccharomyces cerevisiae to hydroxyurea, caffeine and ethyl methanesulphonate: implications for roles of RNases H in DNA replication and repair. Genes to Cells : devoted to molecular & cellular mechanisms *5*, 789-802.

Azzalin, C.M., and Lingner, J. (2008). Telomeres: the silence is broken. Cell Cycle *7*, 1161-1165.

Azzalin, C.M., Reichenbach, P., Khoriauli, L., Giulotto, E., and Lingner, J. (2007). Telomeric repeat containing RNA and RNA surveillance factors at mammalian chromosome ends. Science *318*, 798-801.

Baker, D.J., Childs, B.G., Durik, M., Wijers, M.E., Sieben, C.J., Zhong, J., Saltness, R.A., Jeganathan, K.B., Verzosa, G.C., Pezeshki, A*., et al.* (2016). Naturally occurring p16(Ink4a)-positive cells shorten healthy lifespan. Nature *530*, 184-189.

Baker, D.J., Wijshake, T., Tchkonia, T., LeBrasseur, N.K., Childs, B.G., van de Sluis, B., Kirkland, J.L., and van Deursen, J.M. (2011). Clearance of p16Ink4a-positive senescent cells delays ageing-associated disorders. Nature *479*, 232-236.

Balk, B., Maicher, A., Dees, M., Klermund, J., Luke-Glaser, S., Bender, K., and Luke, B. (2013). Telomeric RNA-DNA hybrids affect telomere-length dynamics and senescence. Nature Structural & Molecular Biology *20*, 1199-1205.

Bansbach, C.E., Betous, R., Lovejoy, C.A., Glick, G.G., and Cortez, D. (2009). The annealing helicase SMARCAL1 maintains genome integrity at stalled replication forks. Genes & Development *23*, 2405-2414.

Bianchi, A., and Shore, D. (2007). Early replication of short telomeres in budding yeast. Cell *128*, 1051-1062.

Biessmann, H., Champion, L.E., O'Hair, M., Ikenaga, K., Kasravi, B., and Mason, J.M. (1992). Frequent transpositions of Drosophila melanogaster HeT-A transposable elements to receding chromosome ends. The EMBO Journal *11*, 4459-4469.

Bonetti, D., Clerici, M., Anbalagan, S., Martina, M., Lucchini, G., and Longhese, M.P. (2010). Shelterin-like proteins and Yku inhibit nucleolytic processing of Saccharomyces cerevisiae telomeres. PLoS Genetics *6*, e1000966.

References

Boule, J.B., Vega, L.R., and Zakian, V.A. (2005). The yeast Pif1p helicase removes telomerase from telomeric DNA. Nature *438*, 57-61.

Boule, J.B., and Zakian, V.A. (2007). The yeast Pif1p DNA helicase preferentially unwinds RNA DNA substrates. Nucleic Acids Research *35*, 5809-5818.

Boulton, S.J., and Jackson, S.P. (1998). Components of the Ku-dependent non-homologous end-joining pathway are involved in telomeric length maintenance and telomeric silencing. The EMBO Journal *17*, 1819-1828.

Brigati, C., Kurtz, S., Balderes, D., Vidali, G., and Shore, D. (1993). An essential yeast gene encoding a TTAGGG repeat-binding protein. Molecular and Cellular Biology *13*, 1306-1314.

Bubeck, D., Reijns, M.A., Graham, S.C., Astell, K.R., Jones, E.Y., and Jackson, A.P. (2011). PCNA directs type 2 RNase H activity on DNA replication and repair substrates. Nucleic Acids Research *39*, 3652-3666.

Buser, R., Kellner, V., Melnik, A., Wilson-Zbinden, C., Schellhaas, R., Kastner, L., Piwko, W., Dees, M., Picotti, P., Maric, M.*, et al.* (2016). The Replisome-Coupled E3 Ubiquitin Ligase Rtt101Mms22 Counteracts Mrc1 Function to Tolerate Genotoxic Stress. PLoS Genetics *12*, e1005843.

Castellano-Pozo, M., Santos-Pereira, J.M., Rondon, A.G., Barroso, S., Andujar, E., Perez-Alegre, M., Garcia-Muse, T., and Aguilera, A. (2013). R loops are linked to histone h3 s10 phosphorylation and chromatin condensation. Molecular Cell *52*, 583-590.

Cenci, G., Ciapponi, L., and Gatti, M. (2005). The mechanism of telomere protection: a comparison between Drosophila and humans. Chromosoma *114*, 135-145.

Cerritelli, S.M., and Crouch, R.J. (2009). Ribonuclease H: the enzymes in eukaryotes. The FEBS Journal *276*, 1494-1505.

Cerritelli, S.M., Frolova, E.G., Feng, C., Grinberg, A., Love, P.E., and Crouch, R.J. (2003). Failure to produce mitochondrial DNA results in embryonic lethality in Rnaseh1 null mice. Molecular Cell *11*, 807-815.

Chaconas, G., and Kobryn, K. (2010). Structure, function, and evolution of linear replicons in Borrelia. Annual Review of Microbiology *64*, 185-202.

Chan, C.S., and Tye, B.K. (1983a). A family of Saccharomyces cerevisiae repetitive autonomously replicating sequences that have very similar genomic environments. Journal of Molecular Biology *168*, 505-523.

Chan, C.S., and Tye, B.K. (1983b). Organization of DNA sequences and replication origins at yeast telomeres. Cell *33*, 563-573.

Chan, Y.A., Aristizabal, M.J., Lu, P.Y., Luo, Z., Hamza, A., Kobor, M.S., Stirling, P.C., and Hieter, P. (2014). Genome-wide profiling of yeast DNA:RNA hybrid prone sites with DRIP-chip. PLoS Genetics *10*, e1004288.

Chang, J., Wang, Y., Shao, L., Laberge, R.M., Demaria, M., Campisi, J., Janakiraman, K., Sharpless, N.E., Ding, S., Feng, W.*, et al.* (2016). Clearance of senescent cells by ABT263 rejuvenates aged hematopoietic stem cells in mice. Nature Medicine *22*, 78-83.

Chang, M., Arneric, M., and Lingner, J. (2007a). Telomerase repeat addition processivity is increased at critically short telomeres in a Tel1-dependent manner in Saccharomyces cerevisiae. Genes & development *21*, 2485-2494.

Chang, M., Dittmar, J.C., and Rothstein, R. (2011). Long telomeres are preferentially extended during recombination-mediated telomere maintenance. Nature Structural & Molecular Biology *18*, 451-456.

Chang, Y.F., Imam, J.S., and Wilkinson, M.F. (2007b). The nonsense-mediated decay RNA surveillance pathway. Annual Review of Biochemistry *76*, 51-74.

Chawla, R., Redon, S., Raftopoulou, C., Wischnewski, H., Gagos, S., and Azzalin, C.M. (2011). Human UPF1 interacts with TPP1 and telomerase and sustains telomere leading-strand replication. The EMBO Journal *30*, 4047-4058.

Chen, Q., Ijpma, A., and Greider, C.W. (2001). Two survivor pathways that allow growth in the absence of telomerase are generated by distinct telomere recombination events. Molecular and Cellular Biology *21*, 1819-1827.

Childs, B.G., Durik, M., Baker, D.J., and van Deursen, J.M. (2015). Cellular senescence in aging and age-related disease: from mechanisms to therapy. Nature Medicine *21*, 1424-1435.

Chon, H., Sparks, J.L., Rychlik, M., Nowotny, M., Burgers, P.M., Crouch, R.J., and Cerritelli, S.M. (2013). RNase H2 roles in genome integrity revealed by unlinking its activities. Nucleic Acids Research *41*, 3130-3143.

Chon, H., Vassilev, A., DePamphilis, M.L., Zhao, Y., Zhang, J., Burgers, P.M., Crouch, R.J., and Cerritelli, S.M. (2009). Contributions of the two accessory subunits, RNASEH2B and RNASEH2C, to the activity and properties of the human RNase H2 complex. Nucleic Acids Research *37*, 96-110.

Churikov, D., Charifi, F., Simon, M.N., and Geli, V. (2014). Rad59-facilitated acquisition of y' elements by short telomeres delays the onset of senescence. PLoS Genetics *10*, e1004736.

Cohen, H., and Sinclair, D.A. (2001). Recombination-mediated lengthening of terminal telomeric repeats requires the Sgs1 DNA helicase. Proceedings of the National Academy of Sciences of the United States of America *98*, 3174-3179.

Cornelio, D.A., Sedam, H.N., Ferrarezi, J.A., Sampaio, N.M., and Argueso, J.L. (2017). Both R-loop removal and ribonucleotide excision repair activities of RNase H2 contribute substantially to chromosome stability. DNA Repair *52*, 110-114.

Costantino, L., and Koshland, D. (2015). The Yin and Yang of R-loop biology. Current Opinion in Cell Biology *34*, 39-45.

Counter, C.M., Meyerson, M., Eaton, E.N., and Weinberg, R.A. (1997). The catalytic subunit of yeast telomerase. Proceedings of the National Academy of Sciences of the United States of America *94*, 9202-9207.

References

Cox, K.E., Marechal, A., and Flynn, R.L. (2016). SMARCAL1 Resolves Replication Stress at ALT Telomeres. Cell Reports *14*, 1032-1040.

Cusanelli, E., Romero, C.A., and Chartrand, P. (2013). Telomeric Noncoding RNA TERRA Is Induced by Telomere Shortening to Nucleate Telomerase Molecules at Short Telomeres. Molecular Cell *51*, 780-791.

d'Adda di Fagagna, F., Reaper, P.M., Clay-Farrace, L., Fiegler, H., Carr, P., Von Zglinicki, T., Saretzki, G., Carter, N.P., and Jackson, S.P. (2003). A DNA damage checkpoint response in telomere-initiated senescence. Nature *426*, 194-198.

Danilevskaya, O.N., Lowenhaupt, K., and Pardue, M.L. (1998). Conserved subfamilies of the Drosophila HeT-A telomere-specific retrotransposon. Genetics *148*, 233-242.

de Jong, R.N., van der Vliet, P.C., and Brenkman, A.B. (2003). Adenovirus DNA replication: protein priming, jumping back and the role of the DNA binding protein DBP. Current Topics in Microbiology and Immunology *272*, 187-211.

Deem, A., Barker, K., Vanhulle, K., Downing, B., Vayl, A., and Malkova, A. (2008). Defective break-induced replication leads to half-crossovers in Saccharomyces cerevisiae. Genetics *179*, 1845-1860.

Demaria, M., Ohtani, N., Youssef, S.A., Rodier, F., Toussaint, W., Mitchell, J.R., Laberge, R.M., Vijg, J., Van Steeg, H., Dolle, M.E.*, et al.* (2014). An essential role for senescent cells in optimal wound healing through secretion of PDGF-AA. Developmental Cell *31*, 722-733.

Denchi, E.L., and de Lange, T. (2007). Protection of telomeres through independent control of ATM and ATR by TRF2 and POT1. Nature *448*, 1068-1071.

Deng, Z., Norseen, J., Wiedmer, A., Riethman, H., and Lieberman, P.M. (2009). TERRA RNA binding to TRF2 facilitates heterochromatin formation and ORC recruitment at telomeres. Molecular Cell *35*, 403-413.

Deng, Z., Wang, Z., Stong, N., Plasschaert, R., Moczan, A., Chen, H.S., Hu, S., Wikramasinghe, P., Davuluri, R.V., Bartolomei, M.S.*, et al.* (2012). A role for CTCF and cohesin in subtelomere chromatin organization, TERRA transcription, and telomere end protection. The EMBO Journal *31*, 4165-4178.

Dilley, R.L., Verma, P., Cho, N.W., Winters, H.D., Wondisford, A.R., and Greenberg, R.A. (2016). Break-induced telomere synthesis underlies alternative telomere maintenance. Nature *539*, 54-58.

Dimri, G.P., Lee, X., Basile, G., Acosta, M., Scott, G., Roskelley, C., Medrano, E.E., Linskens, M., Rubelj, I., Pereira-Smith, O.*, et al.* (1995). A biomarker that identifies senescent human cells in culture and in aging skin in vivo. Proceedings of the National Academy of Sciences of the United States of America *92*, 9363-9367.

Dionne, I., and Wellinger, R.J. (1998). Processing of telomeric DNA ends requires the passage of a replication fork. Nucleic Acids Research *26*, 5365-5371.

Dokal, I. (2011). Dyskeratosis congenita. Hematology Am Soc Hematol Educ Program *2011*, 480-486.

References

Doksani, Y., Wu, J.Y., de Lange, T., and Zhuang, X. (2013). Super-Resolution Fluorescence Imaging of Telomeres Reveals TRF2-Dependent T-loop Formation. Cell *155*, 345-356.

Dungrawala, H., Rose, K.L., Bhat, K.P., Mohni, K.N., Glick, G.G., Couch, F.B., and Cortez, D. (2015). The Replication Checkpoint Prevents Two Types of Fork Collapse without Regulating Replisome Stability. Molecular Cell *59*, 998-1010.

Duquette, M.L., Handa, P., Vincent, J.A., Taylor, A.F., and Maizels, N. (2004). Intracellular transcription of G-rich DNAs induces formation of G-loops, novel structures containing G4 DNA. Genes & Development *18*, 1618-1629.

Eder, P.S., Walder, R.Y., and Walder, J.A. (1993). Substrate specificity of human RNase H1 and its role in excision repair of ribose residues misincorporated in DNA. Biochimie *75*, 123-126.

El Hage, A., French, S.L., Beyer, A.L., and Tollervey, D. (2010). Loss of Topoisomerase I leads to R-loop-mediated transcriptional blocks during ribosomal RNA synthesis. Genes & Development *24*, 1546-1558.

El Hage, A., Webb, S., Kerr, A., and Tollervey, D. (2014). Genome-wide distribution of RNA-DNA hybrids identifies RNase H targets in tRNA genes, retrotransposons and mitochondria. PLoS Genetics *10*, e1004716.

Elledge, S.J., and Davis, R.W. (1990). Two genes differentially regulated in the cell cycle and by DNA-damaging agents encode alternative regulatory subunits of ribonucleotide reductase. Genes & Development *4*, 740-751.

Episkopou, H., Draskovic, I., Van Beneden, A., Tilman, G., Mattiussi, M., Gobin, M., Arnoult, N., Londono-Vallejo, A., and Decottignies, A. (2014). Alternative Lengthening of Telomeres is characterized by reduced compaction of telomeric chromatin. Nucleic Acids Research *42*, 4391-4405.

Epshtein, A., Potenski, C.J., and Klein, H.L. (2016). Increased Spontaneous Recombination in RNase H2-Deficient Cells Arises From Multiple Contiguous rNMPs and Not From Single rNMP Residues Incorporated by DNA Polymerase Epsilon. Microbial Cell *3*, 248-254.

Fallet, E., Jolivet, P., Soudet, J., Lisby, M., Gilson, E., and Teixeira, M.T. (2014). Length-dependent processing of telomeres in the absence of telomerase. Nucleic Acids Research *42*, 3648-3665.

Faure, V., Coulon, S., Hardy, J., and Geli, V. (2010). Cdc13 and telomerase bind through different mechanisms at the lagging- and leading-strand telomeres. Molecular Cell *38*, 842-852.

Feng, J., Funk, W.D., Wang, S.S., Weinrich, S.L., Avilion, A.A., Chiu, C.P., Adams, R.R., Chang, E., Allsopp, R.C., Yu, J.*, et al.* (1995). The RNA component of human telomerase. Science *269*, 1236-1241.

Ferdows, M.S., and Barbour, A.G. (1989). Megabase-sized linear DNA in the bacterium Borrelia burgdorferi, the Lyme disease agent. Proceedings of the National Academy of Sciences of the United States of America *86*, 5969-5973.

Flynn, R.L., Centore, R.C., O'Sullivan, R.J., Rai, R., Tse, A., Songyang, Z., Chang, S., Karlseder, J., and Zou, L. (2011). TERRA and hnRNPA1 orchestrate an RPA-to-POT1 switch on telomeric single-stranded DNA. Nature *471*, 532-536.

Flynn, R.L., Cox, K.E., Jeitany, M., Wakimoto, H., Bryll, A.R., Ganem, N.J., Bersani, F., Pineda, J.R., Suva, M.L., Benes, C.H.*, et al.* (2015). Alternative lengthening of telomeres renders cancer cells hypersensitive to ATR inhibitors. Science *347*, 273-277.

Frank, C.J., Hyde, M., and Greider, C.W. (2006). Regulation of telomere elongation by the cyclin-dependent kinase CDK1. Molecular Cell *24*, 423-432.

Fu, X.H., Duan, Y.M., Liu, Y.T., Cai, C., Meng, F.L., and Zhou, J.Q. (2014). Telomere recombination preferentially occurs at short telomeres in telomerase-null type II survivors. PloS One *9*, e90644.

Fuller, A.M., Cook, E.G., Kelley, K.J., and Pardue, M.L. (2010). Gag proteins of Drosophila telomeric retrotransposons: collaborative targeting to chromosome ends. Genetics *184*, 629-636.

Gallardo, M., Luna, R., Erdjument-Bromage, H., Tempst, P., and Aguilera, A. (2003). Nab2p and the Thp1p-Sac3p complex functionally interact at the interface between transcription and mRNA metabolism. The Journal of Biological Chemistry *278*, 24225-24232.

Gan, W., Guan, Z., Liu, J., Gui, T., Shen, K., Manley, J.L., and Li, X. (2011). R-loop-mediated genomic instability is caused by impairment of replication fork progression. Genes & Development *25*, 2041-2056.

Gao, H., Cervantes, R.B., Mandell, E.K., Otero, J.H., and Lundblad, V. (2007). RPA-like proteins mediate yeast telomere function. Nature Structural & Molecular Biology *14*, 208-214.

Garcia-Benitez, F., Gaillard, H., and Aguilera, A. (2017). Physical proximity of chromatin to nuclear pores prevents harmful R loop accumulation contributing to maintain genome stability. Proceedings of the National Academy of Sciences of the United States of America *114*, 10942-10947.

Garcia-Cao, M., O'Sullivan, R., Peters, A.H., Jenuwein, T., and Blasco, M.A. (2004). Epigenetic regulation of telomere length in mammalian cells by the Suv39h1 and Suv39h2 histone methyltransferases. Nature Genetics *36*, 94-99.

Garcia-Pichardo, D., Canas, J.C., Garcia-Rubio, M.L., Gomez-Gonzalez, B., Rondon, A.G., and Aguilera, A. (2017). Histone Mutants Separate R Loop Formation from Genome Instability Induction. Molecular Cell *66*, 597-609 e595.

Garvik, B., Carson, M., and Hartwell, L. (1995). Single-stranded DNA arising at telomeres in cdc13 mutants may constitute a specific signal for the RAD9 checkpoint. Molecular and Cellular Biology *15*, 6128-6138.

Gavin, A.C., Bosche, M., Krause, R., Grandi, P., Marzioch, M., Bauer, A., Schultz, J., Rick, J.M., Michon, A.M., Cruciat, C.M.*, et al.* (2002). Functional organization of the yeast proteome by systematic analysis of protein complexes. Nature *415*, 141-147.

George, J.A., DeBaryshe, P.G., Traverse, K.L., Celniker, S.E., and Pardue, M.L. (2006). Genomic organization of the Drosophila telomere retrotransposable elements. Genome Research *16*, 1231-1240.

Gilson, E., Roberge, M., Giraldo, R., Rhodes, D., and Gasser, S.M. (1993). Distortion of the DNA double helix by RAP1 at silencers and multiple telomeric binding sites. Journal of Molecular Biology *231*, 293-310.

Ginno, P.A., Lott, P.L., Christensen, H.C., Korf, I., and Chedin, F. (2012). R-loop formation is a distinctive characteristic of unmethylated human CpG island promoters. Molecular Cell *45*, 814-825.

Gomez-Gonzalez, B., Garcia-Rubio, M., Bermejo, R., Gaillard, H., Shirahige, K., Marin, A., Foiani, M., and Aguilera, A. (2011). Genome-wide function of THO/TREX in active genes prevents R-loop-dependent replication obstacles. The EMBO Journal *30*, 3106-3119.

Gonzalez-Aguilera, C., Tous, C., Gomez-Gonzalez, B., Huertas, P., Luna, R., and Aguilera, A. (2008). The THP1-SAC3-SUS1-CDC31 complex works in transcription elongation-mRNA export preventing RNA-mediated genome instability. Molecular Biology of the Cell *19*, 4310-4318.

Gotta, M., Laroche, T., Formenton, A., Maillet, L., Scherthan, H., and Gasser, S.M. (1996). The clustering of telomeres and colocalization with Rap1, Sir3, and Sir4 proteins in wild-type Saccharomyces cerevisiae. The Journal of Cell Biology *134*, 1349-1363.

Gottschling, D.E., Aparicio, O.M., Billington, B.L., and Zakian, V.A. (1990). Position effect at S. cerevisiae telomeres: reversible repression of Pol II transcription. Cell *63*, 751-762.

Graf, M., Bonetti, D., Lockhart, A., Serhal, K., Kellner, V., Maicher, A., Jolivet, P., Teixeira, M.T., and Luke, B. (2017). Telomere Length Determines TERRA and R-Loop Regulation through the Cell Cycle. Cell *170*, 72-85 e14.

Grandin, N., Bailly, A., and Charbonneau, M. (2005). Activation of Mrc1, a mediator of the replication checkpoint, by telomere erosion. Biology of the Cell *97*, 799-814.

Grandin, N., Damon, C., and Charbonneau, M. (2001). Ten1 functions in telomere end protection and length regulation in association with Stn1 and Cdc13. The EMBO Journal *20*, 1173-1183.

Gravel, S., Larrivee, M., Labrecque, P., and Wellinger, R.J. (1998). Yeast Ku as a regulator of chromosomal DNA end structure. Science *280*, 741-744.

Greenwood, J., and Cooper, J.P. (2012). Non-coding telomeric and subtelomeric transcripts are differentially regulated by telomeric and heterochromatin assembly factors in fission yeast. Nucleic Acids Research *40*, 2956-2963.

Griffith, J.D., Comeau, L., Rosenfield, S., Stansel, R.M., Bianchi, A., Moss, H., and de Lange, T. (1999). Mammalian Telomeres End in a Large Duplex Loop. Cell *97*, 503-514.

Grossi, S., Puglisi, A., Dmitriev, P.V., Lopes, M., and Shore, D. (2004). Pol12, the B subunit of DNA polymerase alpha, functions in both telomere capping and length regulation. Genes & Development *18*, 992-1006.

Hamperl, S., and Cimprich, K.A. (2014). The contribution of co-transcriptional RNA:DNA hybrid structures to DNA damage and genome instability. DNA Repair *19*, 84-94.

Harley, C.B., Futcher, A.B., and Greider, C.W. (1990). Telomeres shorten during ageing of human fibroblasts. Nature *345*, 458-460.

Hayflick, L. (1965). The Limited in Vitro Lifetime of Human Diploid Cell Strains. Experimental Cell Research *37*, 614-636.

Hecht, A., Strahl-Bolsinger, S., and Grunstein, M. (1996). Spreading of transcriptional repressor SIR3 from telomeric heterochromatin. Nature *383*, 92-96.

Henson, J.D., and Reddel, R.R. (2010). Assaying and investigating Alternative Lengthening of Telomeres activity in human cells and cancers. FEBS Letters *584*, 3800-3811.

Hirano, Y., Fukunaga, K., and Sugimoto, K. (2009). Rif1 and rif2 inhibit localization of tel1 to DNA ends. Molecular Cell *33*, 312-322.

Holohan, B., Wright, W.E., and Shay, J.W. (2014). Cell biology of disease: Telomeropathies: an emerging spectrum disorder. The Journal of Cell Biology *205*, 289-299.

Hombauer, H., Srivatsan, A., Putnam, C.D., and Kolodner, R.D. (2011). Mismatch repair, but not heteroduplex rejection, is temporally coupled to DNA replication. Science *334*, 1713-1716.

Huang, C.H., Lin, Y.S., Yang, Y.L., Huang, S.W., and Chen, C.W. (1998). The telomeres of Streptomyces chromosomes contain conserved palindromic sequences with potential to form complex secondary structures. Molecular Microbiology *28*, 905-916.

Huang, C.H., Tsai, H.H., Tsay, Y.G., Chien, Y.N., Wang, S.L., Cheng, M.Y., Ke, C.H., and Chen, C.W. (2007). The telomere system of the Streptomyces linear plasmid SCP1 represents a novel class. Molecular Microbiology *63*, 1710-1718.

Huang, S.N., Williams, J.S., Arana, M.E., Kunkel, T.A., and Pommier, Y. (2017). Topoisomerase I-mediated cleavage at unrepaired ribonucleotides generates DNA double-strand breaks. The EMBO Journal *36*, 361-373.

Huertas, P., and Aguilera, A. (2003). Cotranscriptionally Formed DNA:RNA Hybrids Mediate Transcription Elongation Impairment and Transcription-Associated Recombination. Molecular Cell *12*, 711-721.

Hughes, T.R., Weilbaecher, R.G., Walterscheid, M., and Lundblad, V. (2000). Identification of the single-strand telomeric DNA binding domain of the Saccharomyces cerevisiae Cdc13 protein. Proceedings of the National Academy of Sciences of the United States of America *97*, 6457-6462.

Iglesias, N., Redon, S., Pfeiffer, V., Dees, M., Lingner, J., and Luke, B. (2011). Subtelomeric repetitive elements determine TERRA regulation by Rap1/Rif and Rap1/Sir complexes in yeast. EMBO Reports *12*, 587-593.

Ijpma, A.S., and Greider, C.W. (2003). Short telomeres induce a DNA damage response in Saccharomyces cerevisiae. Molecular Biology of the Cell *14*, 987-1001.

Imai, S., Armstrong, C.M., Kaeberlein, M., and Guarente, L. (2000). Transcriptional silencing and longevity protein Sir2 is an NAD-dependent histone deacetylase. Nature *403*, 795-800.

Itoh, T., and Tomizawa, J. (1980). Formation of an RNA primer for initiation of replication of ColE1 DNA by ribonuclease H. Proceedings of the National Academy of Sciences of the United States of America *77*, 2450-2454.

Ivessa, A.S., Zhou, J.Q., Schulz, V.P., Monson, E.K., and Zakian, V.A. (2002). Saccharomyces Rrm3p, a 5' to 3' DNA helicase that promotes replication fork progression through telomeric and subtelomeric DNA. Genes & Development *16*, 1383-1396.

Janke, C., Magiera, M.M., Rathfelder, N., Taxis, C., Reber, S., Maekawa, H., Moreno-Borchart, A., Doenges, G., Schwob, E., Schiebel, E.*, et al.* (2004). A versatile toolbox for PCR-based tagging of yeast genes: new fluorescent proteins, more markers and promoter substitution cassettes. Yeast *21*, 947-962.

Jeong, H.S., Backlund, P.S., Chen, H.C., Karavanov, A.A., and Crouch, R.J. (2004). RNase H2 of Saccharomyces cerevisiae is a complex of three proteins. Nucleic Acids Research *32*, 407-414.

Johnson, F.B., Marciniak, R.A., McVey, M., Stewart, S.A., Hahn, W.C., and Guarente, L. (2001). The Saccharomyces cerevisiae WRN homolog Sgs1p participates in telomere maintenance in cells lacking telomerase. The EMBO Journal *20*, 905-913.

Kaizer, H., Connelly, C.J., Bettridge, K., Viggiani, C., and Greider, C.W. (2015). Regulation of Telomere Length Requires a Conserved N-Terminal Domain of Rif2 in Saccharomyces cerevisiae. Genetics *201*, 573-586.

Karras, G.I., and Jentsch, S. (2010). The RAD6 DNA damage tolerance pathway operates uncoupled from the replication fork and is functional beyond S phase. Cell *141*, 255-267.

Kaul, Z., Cesare, A.J., Huschtscha, L.I., Neumann, A.A., and Reddel, R.R. (2012). Five dysfunctional telomeres predict onset of senescence in human cells. EMBO Reports *13*, 52-59.

Kim, N.W., Piatyszek, M.A., Prowse, K.R., Harley, C.B., West, M.D., Ho, P.L., Coviello, G.M., Wright, W.E., Weinrich, S.L., and Shay, J.W. (1994). Specific association of human telomerase activity with immortal cells and cancer. Science *266*, 2011-2015.

Koering, C.E., Fourel, G., Binet-Brasselet, E., Laroche, T., Klein, F., and Gilson, E. (2000). Identification of high affinity Tbf1p-binding sites within the budding yeast genome. Nucleic Acids Research *28*, 2519-2526.

Larcher, M.V., Pasquier, E., MacDonald, R.S., and Wellinger, R.J. (2016). Ku Binding on Telomeres Occurs at Sites Distal from the Physical Chromosome Ends. PLoS Genetics *12*, e1006479.

Larrivee, M., LeBel, C., and Wellinger, R.J. (2004). The generation of proper constitutive G-tails on yeast telomeres is dependent on the MRX complex. Genes & Development *18*, 1391-1396.

Larrivee, M., and Wellinger, R.J. (2006). Telomerase- and capping-independent yeast survivors with alternate telomere states. Nature Cell Biology *8*, 741-747.

Lazzaro, F., Novarina, D., Amara, F., Watt, D.L., Stone, J.E., Costanzo, V., Burgers, P.M., Kunkel, T.A., Plevani, P., and Muzi-Falconi, M. (2012). RNase H and postreplication repair protect cells from ribonucleotides incorporated in DNA. Molecular Cell *45*, 99-110.

Le, S., Moore, J.K., Haber, J.E., and Greider, C.W. (1999). RAD50 and RAD51 define two pathways that collaborate to maintain telomeres in the absence of telomerase. Genetics *152*, 143-152.

Lendvay, T.S., Morris, D.K., Sah, J., Balasubramanian, B., and Lundblad, V. (1996). Senescence mutants of Saccharomyces cerevisiae with a defect in telomere replication identify three additional EST genes. Genetics *144*, 1399-1412.

Li, L., Germain, D.R., Poon, H.Y., Hildebrandt, M.R., Monckton, E.A., McDonald, D., Hendzel, M.J., and Godbout, R. (2016). DEAD Box 1 Facilitates Removal of RNA and Homologous Recombination at DNA Double-Strand Breaks. Molecular and Cellular Biology *36*, 2794-2810.

Li, X., and Manley, J.L. (2005). Inactivation of the SR protein splicing factor ASF/SF2 results in genomic instability. Cell *122*, 365-378.

Lian, H.Y., Robertson, E.D., Hiraga, S., Alvino, G.M., Collingwood, D., McCune, H.J., Sridhar, A., Brewer, B.J., Raghuraman, M.K., and Donaldson, A.D. (2011). The effect of Ku on telomere replication time is mediated by telomere length but is independent of histone tail acetylation. Molecular Biology of the Cell *22*, 1753-1765.

Lieber, M.R. (2010). The mechanism of double-strand DNA break repair by the nonhomologous DNA end-joining pathway. Annual Review of Biochemistry *79*, 181-211.

Lim, Y.W., Sanz, L.A., Xu, X., Hartono, S.R., and Chedin, F. (2015). Genome-wide DNA hypomethylation and RNA:DNA hybrid accumulation in Aicardi-Goutieres syndrome. eLife *4*.

Lindahl, T. (1993). Instability and decay of the primary structure of DNA. Nature *362*, 709-715.

Lingner, J., Hughes, T.R., Shevchenko, A., Mann, M., Lundblad, V., and Cech, T.R. (1997). Reverse transcriptase motifs in the catalytic subunit of telomerase. Science *276*, 561-567.

Liu, C.C., Gopalakrishnan, V., Poon, L.F., Yan, T., and Li, S. (2013). Cdk1 regulates the temporal recruitment of telomerase and CST complex for telomere replication. Molecular and Cellular Biology.

Liu, L.F., and Wang, J.C. (1987). Supercoiling of the DNA template during transcription. Proceedings of the National Academy of Sciences of the United States of America *84*, 7024-7027.

Liu, Y., Sanoff, H.K., Cho, H., Burd, C.E., Torrice, C., Ibrahim, J.G., Thomas, N.E., and Sharpless, N.E. (2009). Expression of p16(INK4a) in peripheral blood T-cells is a biomarker of human aging. Aging Cell *8*, 439-448.

Louis, E.J., and Vershinin, A.V. (2005). Chromosome ends: different sequences may provide conserved functions. BioEssays : news and reviews in molecular, cellular and developmental biology *27*, 685-697.

Lovejoy, C.A., Li, W., Reisenweber, S., Thongthip, S., Bruno, J., de Lange, T., De, S., Petrini, J.H., Sung, P.A., Jasin, M*., et al.* (2012). Loss of ATRX, genome instability, and an altered DNA damage

response are hallmarks of the alternative lengthening of telomeres pathway. PLoS Genetics *8*, e1002772.

Luke, B., and Lingner, J. (2009). TERRA: telomeric repeat-containing RNA. The EMBO Journal *28*, 2503-2510.

Luke, B., Panza, A., Redon, S., Iglesias, N., Li, Z., and Lingner, J. (2008). The Rat1p 5' to 3' exonuclease degrades telomeric repeat-containing RNA and promotes telomere elongation in Saccharomyces cerevisiae. Molecular Cell *32*, 465-477.

Lundblad, V., and Blackburn, E.H. (1993). An alternative pathway for yeast telomere maintenance rescues est1- senescence. Cell *73*, 347-360.

Lundblad, V., and Szostak, J.W. (1989). A mutant with a defect in telomere elongation leads to senescence in yeast. Cell *57*, 633-643.

Lydeard, J.R., Jain, S., Yamaguchi, M., and Haber, J.E. (2007). Break-induced replication and telomerase-independent telomere maintenance require Pol32. Nature *448*, 820-823.

Maicher, A., Kastner, L., Dees, M., and Luke, B. (2012). Deregulated telomere transcription causes replication-dependent telomere shortening and promotes cellular senescence. Nucleic Acids Research *40*, 6649-6659.

Malkova, A., and Ira, G. (2013). Break-induced replication: functions and molecular mechanism. Current Opinion in Genetics & Development.

Malkova, A., Ivanov, E.L., and Haber, J.E. (1996). Double-strand break repair in the absence of RAD51 in yeast: a possible role for break-induced DNA replication. Proceedings of the National Academy of Sciences of the United States of America *93*, 7131-7136.

Marcand, S., Brevet, V., and Gilson, E. (1999). Progressive cis-inhibition of telomerase upon telomere elongation. The EMBO Journal *18*, 3509-3519.

Marcand, S., Gilson, E., and Shore, D. (1997). A protein-counting mechanism for telomere length regulation in yeast. Science *275*, 986-990.

Marcand, S., Pardo, B., Gratias, A., Cahun, S., and Callebaut, I. (2008). Multiple pathways inhibit NHEJ at telomeres. Genes & Development *22*, 1153-1158.

Martin, S.G., Laroche, T., Suka, N., Grunstein, M., and Gasser, S.M. (1999). Relocalization of telomeric Ku and SIR proteins in response to DNA strand breaks in yeast. Cell *97*, 621-633.

McCarroll, R.M., and Fangman, W.L. (1988). Time of replication of yeast centromeres and telomeres. Cell *54*, 505-513.

McGee, J.S., Phillips, J.A., Chan, A., Sabourin, M., Paeschke, K., and Zakian, V.A. (2010). Reduced Rif2 and lack of Mec1 target short telomeres for elongation rather than double-strand break repair. Nature Structural & Molecular Biology *17*, 1438-1445.

Michishita, E., McCord, R.A., Berber, E., Kioi, M., Padilla-Nash, H., Damian, M., Cheung, P., Kusumoto, R., Kawahara, T.L., Barrett, J.C.*, et al.* (2008). SIRT6 is a histone H3 lysine 9 deacetylase that modulates telomeric chromatin. Nature *452*, 492-496.

Mikhailovsky, S., Belenkaya, T., and Georgiev, P. (1999). Broken chromosomal ends can be elongated by conversion in Drosophila melanogaster. Chromosoma *108*, 114-120.

Miller, K.M., Rog, O., and Cooper, J.P. (2006). Semi-conservative DNA replication through telomeres requires Taz1. Nature *440*, 824-828.

Mischo, H.E., Gomez-Gonzalez, B., Grzechnik, P., Rondon, A.G., Wei, W., Steinmetz, L., Aguilera, A., and Proudfoot, N.J. (2011). Yeast Sen1 helicase protects the genome from transcription-associated instability. Molecular Cell *41*, 21-32.

Mitchell, J.R., Wood, E., and Collins, K. (1999). A telomerase component is defective in the human disease dyskeratosis congenita. Nature *402*, 551-555.

Moravec, M., Wischnewski, H., Bah, A., Hu, Y., Liu, N., Lafranchi, L., King, M.C., and Azzalin, C.M. (2016). TERRA promotes telomerase-mediated telomere elongation in Schizosaccharomyces pombe. EMBO Reports.

Morawska, M., and Ulrich, H.D. (2013). An expanded tool kit for the auxin-inducible degron system in budding yeast. Yeast *30*, 341-351.

Moretti, P., Freeman, K., Coodly, L., and Shore, D. (1994). Evidence that a complex of SIR proteins interacts with the silencer and telomere-binding protein RAP1. Genes & Development *8*, 2257-2269.

Mozdy, A.D., and Cech, T.R. (2006). Low abundance of telomerase in yeast: implications for telomerase haploinsufficiency. RNA *12*, 1721-1737.

Munoz-Espin, D., Canamero, M., Maraver, A., Gomez-Lopez, G., Contreras, J., Murillo-Cuesta, S., Rodriguez-Baeza, A., Varela-Nieto, I., Ruberte, J., Collado, M.*, et al.* (2013). Programmed cell senescence during mammalian embryonic development. Cell *155*, 1104-1118.

Nergadze, S.G., Farnung, B.O., Wischnewski, H., Khoriauli, L., Vitelli, V., Chawla, R., Giulotto, E., and Azzalin, C.M. (2009). CpG-island promoters drive transcription of human telomeres. RNA *15*, 2186-2194.

Nguyen, D.T., Voon, H.P.J., Xella, B., Scott, C., Clynes, D., Babbs, C., Ayyub, H., Kerry, J., Sharpe, J.A., Sloane-Stanley, J.A.*, et al.* (2017a). The chromatin remodelling factor ATRX suppresses R-loops in transcribed telomeric repeats. EMBO Reports *18*, 914-928.

Nguyen, H.D., Yadav, T., Giri, S., Saez, B., Graubert, T.A., and Zou, L. (2017b). Functions of Replication Protein A as a Sensor of R Loops and a Regulator of RNaseH1. Molecular Cell *65*, 832-847 e834.

Nguyen, T.A., Tak, Y.S., Lee, C.H., Kang, Y.H., Cho, I.T., and Seo, Y.S. (2011). Analysis of subunit assembly and function of the Saccharomyces cerevisiae RNase H2 complex. The FEBS Journal *278*, 4927-4942.

Nowotny, M., Cerritelli, S.M., Ghirlando, R., Gaidamakov, S.A., Crouch, R.J., and Yang, W. (2008). Specific recognition of RNA/DNA hybrid and enhancement of human RNase H1 activity by HBD. The EMBO Journal *27*, 1172-1181.

O'Connell, K., Jinks-Robertson, S., and Petes, T.D. (2015). Elevated Genome-Wide Instability in Yeast Mutants Lacking RNase H Activity. Genetics *201*, 963-975.

O'Sullivan, R.J., Arnoult, N., Lackner, D.H., Oganesian, L., Haggblom, C., Corpet, A., Almouzni, G., and Karlseder, J. (2014). Rapid induction of alternative lengthening of telomeres by depletion of the histone chaperone ASF1. Nature Structural & Molecular Biology *21*, 167-174.

Ohle, C., Tesorero, R., Schermann, G., Dobrev, N., Sinning, I., and Fischer, T. (2016). Transient RNA-DNA Hybrids Are Required for Efficient Double-Strand Break Repair. Cell *167*, 1001-1013 e1007.

Okano, M., Bell, D.W., Haber, D.A., and Li, E. (1999). DNA methyltransferases Dnmt3a and Dnmt3b are essential for de novo methylation and mammalian development. Cell *99*, 247-257.

Palladino, F., Laroche, T., Gilson, E., Axelrod, A., Pillus, L., and Gasser, S.M. (1993). SIR3 and SIR4 proteins are required for the positioning and integrity of yeast telomeres. Cell *75*, 543-555.

Palm, W., and de Lange, T. (2008). How shelterin protects mammalian telomeres. Annual Review of Genetics *42*, 301-334.

Parajuli, S., Teasley, D.C., Murali, B., Jackson, J., Vindigni, A., and Stewart, S.A. (2017). Human ribonuclease H1 resolves R-loops and thereby enables progression of the DNA replication fork. The Journal of Biological Chemistry *292*, 15216-15224.

Pardue, M.L., and DeBaryshe, P.G. (2008). Drosophila telomeres: A variation on the telomerase theme. Fly *2*, 101-110.

Parry, E.M., Alder, J.K., Lee, S.S., Phillips, J.A., 3rd, Loyd, J.E., Duggal, P., and Armanios, M. (2011). Decreased dyskerin levels as a mechanism of telomere shortening in X-linked dyskeratosis congenita. Journal of Medical Genetics *48*, 327-333.

Paulsen, R.D., Soni, D.V., Wollman, R., Hahn, A.T., Yee, M.C., Guan, A., Hesley, J.A., Miller, S.C., Cromwell, E.F., Solow-Cordero, D.E.*, et al.* (2009). A genome-wide siRNA screen reveals diverse cellular processes and pathways that mediate genome stability. Molecular Cell *35*, 228-239.

Pellegrini, L. (2012). The Pol alpha-primase complex. Sub-cellular Biochemistry *62*, 157-169.

Petzold, C., Marceau, A.H., Miller, K.H., Marqusee, S., and Keck, J.L. (2015). Interaction with Single-stranded DNA-binding Protein Stimulates Escherichia coli Ribonuclease HI Enzymatic Activity. The Journal of Biological Chemistry *290*, 14626-14636.

Pfeiffer, V., Crittin, J., Grolimund, L., and Lingner, J. (2013). The THO complex component Thp2 counteracts telomeric R-loops and telomere shortening. The EMBO Journal.

Pfeiffer, V., and Lingner, J. (2012). TERRA promotes telomere shortening through exonuclease 1-mediated resection of chromosome ends. PLoS Genetics *8*, e1002747.

Phillips, D.D., Garboczi, D.N., Singh, K., Hu, Z., Leppla, S.H., and Leysath, C.E. (2013). The sub-nanomolar binding of DNA-RNA hybrids by the single-chain Fv fragment of antibody S9.6. Journal of molecular recognition : JMR *26*, 376-381.

Phillips, J.A., Chan, A., Paeschke, K., and Zakian, V.A. (2015). The pif1 helicase, a negative regulator of telomerase, acts preferentially at long telomeres. PLoS Genetics *11*, e1005186.

Porro, A., Feuerhahn, S., Delafontaine, J., Riethman, H., Rougemont, J., and Lingner, J. (2014). Functional characterization of the TERRA transcriptome at damaged telomeres. Nature Communications *5*, 5379.

Porro, A., Feuerhahn, S., Reichenbach, P., and Lingner, J. (2010). Molecular dissection of telomeric repeat-containing RNA biogenesis unveils the presence of distinct and multiple regulatory pathways. Molecular and Cellular Biology *30*, 4808-4817.

Qi, H., and Zakian, V.A. (2000). The Saccharomyces telomere-binding protein Cdc13p interacts with both the catalytic subunit of DNA polymerase alpha and the telomerase-associated est1 protein. Genes & Development *14*, 1777-1788.

Raghuraman, M.K., Winzeler, E.A., Collingwood, D., Hunt, S., Wodicka, L., Conway, A., Lockhart, D.J., Davis, R.W., Brewer, B.J., and Fangman, W.L. (2001). Replication dynamics of the yeast genome. Science *294*, 115-121.

Rashkova, S., Karam, S.E., Kellum, R., and Pardue, M.L. (2002). Gag proteins of the two Drosophila telomeric retrotransposons are targeted to chromosome ends. The Journal of Cell Biology *159*, 397-402.

Redon, S., Reichenbach, P., and Lingner, J. (2010). The non-coding RNA TERRA is a natural ligand and direct inhibitor of human telomerase. Nucleic Acids Research *38*, 5797-5806.

Rice, G., Patrick, T., Parmar, R., Taylor, C.F., Aeby, A., Aicardi, J., Artuch, R., Montalto, S.A., Bacino, C.A., Barroso, B.*, et al.* (2007). Clinical and molecular phenotype of Aicardi-Goutieres syndrome. American Journal of Human Genetics *81*, 713-725.

Roberts, R.W., and Crothers, D.M. (1992). Stability and properties of double and triple helices: dramatic effects of RNA or DNA backbone composition. Science *258*, 1463-1466.

Roos, C.M., Zhang, B., Palmer, A.K., Ogrodnik, M.B., Pirtskhalava, T., Thalji, N.M., Hagler, M., Jurk, D., Smith, L.A., Casaclang-Verzosa, G.*, et al.* (2016). Chronic senolytic treatment alleviates established vasomotor dysfunction in aged or atherosclerotic mice. Aging Cell *15*, 973-977.

Roy, D., and Lieber, M.R. (2009). G clustering is important for the initiation of transcription-induced R-loops in vitro, whereas high G density without clustering is sufficient thereafter. Molecular and Cellular Biology *29*, 3124-3133.

Roy, D., Yu, K., and Lieber, M.R. (2008). Mechanism of R-loop formation at immunoglobulin class switch sequences. Molecular and Cellular Biology *28*, 50-60.

Roy, D., Zhang, Z., Lu, Z., Hsieh, C.L., and Lieber, M.R. (2010). Competition between the RNA transcript and the nontemplate DNA strand during R-loop formation in vitro: a nick can serve as a strong R-loop initiation site. Molecular and Cellular Biology *30*, 146-159.

Roy, R., Meier, B., McAinsh, A.D., Feldmann, H.M., and Jackson, S.P. (2004). Separation-of-function mutants of yeast Ku80 reveal a Yku80p-Sir4p interaction involved in telomeric silencing. The Journal of Biological Chemistry *279*, 86-94.

Rydberg, B., and Game, J. (2002). Excision of misincorporated ribonucleotides in DNA by RNase H (type 2) and FEN-1 in cell-free extracts. Proceedings of the National Academy of Sciences of the United States of America *99*, 16654-16659.

Sabourin, M., Tuzon, C.T., and Zakian, V.A. (2007). Telomerase and Tel1p preferentially associate with short telomeres in S. cerevisiae. Molecular Cell *27*, 550-561.

Sagie, S., Toubiana, S., Hartono, S.R., Katzir, H., Tzur-Gilat, A., Havazelet, S., Francastel, C., Velasco, G., Chedin, F., and Selig, S. (2017). Telomeres in ICF syndrome cells are vulnerable to DNA damage due to elevated DNA:RNA hybrids. Nature Communications *8*, 14015.

San Filippo, J., Sung, P., and Klein, H. (2008). Mechanism of eukaryotic homologous recombination. Annual Review of Biochemistry *77*, 229-257.

Sandell, L.L., and Zakian, V.A. (1993). Loss of a yeast telomere: arrest, recovery, and chromosome loss. Cell *75*, 729-739.

Santos-Pereira, J.M., and Aguilera, A. (2015). R loops: new modulators of genome dynamics and function. Nature Reviews Genetics *16*, 583-597.

Santos-Pereira, J.M., Herrero, A.B., Garcia-Rubio, M.L., Marin, A., Moreno, S., and Aguilera, A. (2013). The Npl3 hnRNP prevents R-loop-mediated transcription-replication conflicts and genome instability. Genes & Development *27*, 2445-2458.

Schober, H., Ferreira, H., Kalck, V., Gehlen, L.R., and Gasser, S.M. (2009). Yeast telomerase and the SUN domain protein Mps3 anchor telomeres and repress subtelomeric recombination. Genes & Development *23*, 928-938.

Schoeftner, S., and Blasco, M.A. (2008). Developmentally regulated transcription of mammalian telomeres by DNA-dependent RNA polymerase II. Nature Cell Biology *10*, 228-236.

Schramke, V., Luciano, P., Brevet, V., Guillot, S., Corda, Y., Longhese, M.P., Gilson, E., and Geli, V. (2004). RPA regulates telomerase action by providing Est1p access to chromosome ends. Nature Genetics *36*, 46-54.

Sfeir, A., Kosiyatrakul, S.T., Hockemeyer, D., MacRae, S.L., Karlseder, J., Schildkraut, C.L., and de Lange, T. (2009). Mammalian telomeres resemble fragile sites and require TRF1 for efficient replication. Cell *138*, 90-103.

Shi, T., Bunker, R.D., Mattarocci, S., Ribeyre, C., Faty, M., Gut, H., Scrima, A., Rass, U., Rubin, S.M., Shore, D*., et al.* (2013). Rif1 and Rif2 shape telomere function and architecture through multivalent Rap1 interactions. Cell *153*, 1340-1353.

Shore, D., and Nasmyth, K. (1987). Purification and cloning of a DNA binding protein from yeast that binds to both silencer and activator elements. Cell *51*, 721-732.

Siegel, R.L., Miller, K.D., and Jemal, A. (2015). Cancer Statistics, 2015. CA: a cancer journal for clinicians *65*, 5-29.

Singer, M.S., and Gottschling, D.E. (1994). TLC1: template RNA component of Saccharomyces cerevisiae telomerase. Science *266*, 404-409.

References

Skourti-Stathaki, K., Kamieniarz-Gdula, K., and Proudfoot, N.J. (2014). R-loops induce repressive chromatin marks over mammalian gene terminators. Nature *516*, 436-439.

Skourti-Stathaki, K., Proudfoot, N.J., and Gromak, N. (2011). Human senataxin resolves RNA/DNA hybrids formed at transcriptional pause sites to promote Xrn2-dependent termination. Molecular Cell *42*, 794-805.

Smith, C.E., Llorente, B., and Symington, L.S. (2007). Template switching during break-induced replication. Nature *447*, 102-105.

Sollier, J., Stork, C.T., Garcia-Rubio, M.L., Paulsen, R.D., Aguilera, A., and Cimprich, K.A. (2014). Transcription-coupled nucleotide excision repair factors promote R-loop-induced genome instability. Molecular Cell *56*, 777-785.

Soudet, J., Jolivet, P., and Teixeira, M.T. (2014). Elucidation of the DNA End-Replication Problem in Saccharomyces cerevisiae. Molecular Cell *53*, 954-964.

Sparks, J.L., Chon, H., Cerritelli, S.M., Kunkel, T.A., Johansson, E., Crouch, R.J., and Burgers, P.M. (2012). RNase H2-initiated ribonucleotide excision repair. Molecular Cell *47*, 980-986.

Sridhar, A., Kedziora, S., and Donaldson, A.D. (2014). At short telomeres Tel1 directs early replication and phosphorylates Rif1. PLoS Genetics *10*, e1004691.

Steinert, S., Shay, J.W., and Wright, W.E. (2004). Modification of subtelomeric DNA. Molecular and Cellular Biology *24*, 4571-4580.

Strahl-Bolsinger, S., Hecht, A., Luo, K., and Grunstein, M. (1997). SIR2 and SIR4 interactions differ in core and extended telomeric heterochromatin in yeast. Genes & Development *11*, 83-93.

Stuckey, R., Garcia-Rodriguez, N., Aguilera, A., and Wellinger, R.E. (2015). Role for RNA:DNA hybrids in origin-independent replication priming in a eukaryotic system. Proceedings of the National Academy of Sciences of the United States of America *112*, 5779-5784.

Sun, Q., Csorba, T., Skourti-Stathaki, K., Proudfoot, N.J., and Dean, C. (2013). R-loop stabilization represses antisense transcription at the Arabidopsis FLC locus. Science *340*, 619-621.

Taddei, A., Hediger, F., Neumann, F.R., Bauer, C., and Gasser, S.M. (2004). Separation of silencing from perinuclear anchoring functions in yeast Ku80, Sir4 and Esc1 proteins. The EMBO Journal *23*, 1301-1312.

Taddei, A., Van Houwe, G., Nagai, S., Erb, I., van Nimwegen, E., and Gasser, S.M. (2009). The functional importance of telomere clustering: global changes in gene expression result from SIR factor dispersion. Genome Research *19*, 611-625.

Taggart, A.K., Teng, S.C., and Zakian, V.A. (2002). Est1p as a cell cycle-regulated activator of telomere-bound telomerase. Science *297*, 1023-1026.

Takata, H., Tanaka, Y., and Matsuura, A. (2005). Late S phase-specific recruitment of Mre11 complex triggers hierarchical assembly of telomere replication proteins in Saccharomyces cerevisiae. Molecular Cell *17*, 573-583.

Teixeira, M.T., Arneric, M., Sperisen, P., and Lingner, J. (2004). Telomere length homeostasis is achieved via a switch between telomerase- extendible and -nonextendible states. Cell *117*, 323-335.

Teng, S.C., Chang, J., McCowan, B., and Zakian, V.A. (2000). Telomerase-independent lengthening of yeast telomeres occurs by an abrupt Rad50p-dependent, Rif-inhibited recombinational process. Molecular Cell *6*, 947-952.

Teng, S.C., and Zakian, V.A. (1999). Telomere-telomere recombination is an efficient bypass pathway for telomere maintenance in Saccharomyces cerevisiae. Molecular and Cellular Biology *19*, 8083-8093.

Traktman, P., and Boyle, K. (2004). Methods for analysis of poxvirus DNA replication. Methods in Molecular Biology *269*, 169-186.

Tsakiri, K.D., Cronkhite, J.T., Kuan, P.J., Xing, C., Raghu, G., Weissler, J.C., Rosenblatt, R.L., Shay, J.W., and Garcia, C.K. (2007). Adult-onset pulmonary fibrosis caused by mutations in telomerase. Proceedings of the National Academy of Sciences of the United States of America *104*, 7552-7557.

Tseng, S.F., Lin, J.J., and Teng, S.C. (2006). The telomerase-recruitment domain of the telomere binding protein Cdc13 is regulated by Mec1p/Tel1p-dependent phosphorylation. Nucleic Acids Research *34*, 6327-6336.

Tuduri, S., Crabbe, L., Conti, C., Tourriere, H., Holtgreve-Grez, H., Jauch, A., Pantesco, V., De Vos, J., Thomas, A., Theillet, C.*, et al.* (2009). Topoisomerase I suppresses genomic instability by preventing interference between replication and transcription. Nature Cell Biology *11*, 1315-1324.

Vodenicharov, M.D., Laterreur, N., and Wellinger, R.J. (2010). Telomere capping in non-dividing yeast cells requires Yku and Rap1. The EMBO Journal *29*, 3007-3019.

Vulliamy, T.J., Knight, S.W., Mason, P.J., and Dokal, I. (2001). Very short telomeres in the peripheral blood of patients with X-linked and autosomal dyskeratosis congenita. Blood Cells, Molecules & Diseases *27*, 353-357.

Wahba, L., Amon, J.D., Koshland, D., and Vuica-Ross, M. (2011). RNase H and multiple RNA biogenesis factors cooperate to prevent RNA:DNA hybrids from generating genome instability. Molecular Cell *44*, 978-988.

Wahba, L., Costantino, L., Tan, F.J., Zimmer, A., and Koshland, D. (2016). S1-DRIP-seq identifies high expression and polyA tracts as major contributors to R-loop formation. Genes & Development *30*, 1327-1338.

Wahba, L., Gore, S.K., and Koshland, D. (2013). The homologous recombination machinery modulates the formation of RNA-DNA hybrids and associated chromosome instability. eLife *2*, e00505.

Walmsley, R.W., Chan, C.S., Tye, B.K., and Petes, T.D. (1984). Unusual DNA sequences associated with the ends of yeast chromosomes. Nature *310*, 157-160.

Wang, Z., Deng, Z., Dahmane, N., Tsai, K., Wang, P., Williams, D.R., Kossenkov, A.V., Showe, L.C., Zhang, R., Huang, Q.*, et al.* (2015). Telomeric repeat-containing RNA (TERRA) constitutes

a nucleoprotein component of extracellular inflammatory exosomes. Proceedings of the National Academy of Sciences of the United States of America *112*, E6293-6300.

Watson, J.D. (1972). Origin of concatemeric T7 DNA. Nature: New biology *239*, 197-201.

Weinert, T.A., and Hartwell, L.H. (1993). Cell cycle arrest of cdc mutants and specificity of the RAD9 checkpoint. Genetics *134*, 63-80.

Wellinger, R.E., Prado, F., and Aguilera, A. (2006). Replication fork progression is impaired by transcription in hyperrecombinant yeast cells lacking a functional THO complex. Molecular and Cellular Biology *26*, 3327-3334.

Wellinger, R.J., Wolf, A.J., and Zakian, V.A. (1993). Saccharomyces telomeres acquire single-strand TG1-3 tails late in S phase. Cell *72*, 51-60.

Wellinger, R.J., and Zakian, V.A. (2012). Everything you ever wanted to know about Saccharomyces cerevisiae telomeres: beginning to end. Genetics *191*, 1073-1105.

Westover, K.D., Bushnell, D.A., and Kornberg, R.D. (2004). Structural basis of transcription: separation of RNA from DNA by RNA polymerase II. Science *303*, 1014-1016.

Wotton, D., and Shore, D. (1997). A novel Rap1p-interacting factor, Rif2p, cooperates with Rif1p to regulate telomere length in Saccharomyces cerevisiae. Genes & Development *11*, 748-760.

Wright, J.H., Gottschling, D.E., and Zakian, V.A. (1992). Saccharomyces telomeres assume a non-nucleosomal chromatin structure. Genes & Development *6*, 197-210.

Xu, B., and Clayton, D.A. (1996). RNA-DNA hybrid formation at the human mitochondrial heavy-strand origin ceases at replication start sites: an implication for RNA-DNA hybrids serving as primers. The EMBO Journal *15*, 3135-3143.

Xu, G.L., Bestor, T.H., Bourc'his, D., Hsieh, C.L., Tommerup, N., Bugge, M., Hulten, M., Qu, X., Russo, J.J., and Viegas-Pequignot, E. (1999). Chromosome instability and immunodeficiency syndrome caused by mutations in a DNA methyltransferase gene. Nature *402*, 187-191.

Xu, Z., Fallet, E., Paoletti, C., Fehrmann, S., Charvin, G., and Teixeira, M.T. (2015). Two routes to senescence revealed by real-time analysis of telomerase-negative single lineages. Nature Communications *6*, 7680.

Yang, Y., McBride, K.M., Hensley, S., Lu, Y., Chedin, F., and Bedford, M.T. (2014). Arginine methylation facilitates the recruitment of TOP3B to chromatin to prevent R loop accumulation. Molecular Cell *53*, 484-497.

Yehezkel, S., Segev, Y., Viegas-Pequignot, E., Skorecki, K., and Selig, S. (2008). Hypomethylation of subtelomeric regions in ICF syndrome is associated with abnormally short telomeres and enhanced transcription from telomeric regions. Human Molecular Genetics *17*, 2776-2789.

Yehezkel, S., Shaked, R., Sagie, S., Berkovitz, R., Shachar-Bener, H., Segev, Y., and Selig, S. (2013). Characterization and rescue of telomeric abnormalities in ICF syndrome type I fibroblasts. Frontiers in Oncology *3*, 35.

Yu, T.Y., Kao, Y.W., and Lin, J.J. (2014). Telomeric transcripts stimulate telomere recombination to suppress senescence in cells lacking telomerase. Proceedings of the National Academy of Sciences of the United States of America *111*, 3377-3382.

Zaidi, I.W., Rabut, G., Poveda, A., Scheel, H., Malmstrom, J., Ulrich, H., Hofmann, K., Pasero, P., Peter, M., and Luke, B. (2008). Rtt101 and Mms1 in budding yeast form a CUL4(DDB1)-like ubiquitin ligase that promotes replication through damaged DNA. EMBO Reports *9*, 1034-1040.

Zimmer, A.D., and Koshland, D. (2016). Differential roles of the RNases H in preventing chromosome instability. Proceedings of the National Academy of Sciences of the United States of America *113*, 12220-12225.

Acknowledgements

I am thankful to Prof. Dr. Michael Knop for evaluating my PhD thesis and for being my first supervisor.

I would also like to thank PD Dr. Karsten Rippe and Prof. Dr. Bernd Bukau for being part of my thesis defense committee.

Additional thanks go to Prof. Dr. Massimo Lopes and Prof. Dr. René Ketting, for being part of my thesis advisory committee. I am grateful to Massimo for the valuable suggestion to use the cell cycle specific construct to investigate RNase H enzymes functions.

Special thanks go to Brian, first of all for giving me the opportunity to work in your lab, and also for the great project that I could contribute to. Thank you for the full-time supply of enthusiasm, positivity and support. I'm looking forward to continue working under your supervision!

I would like to thank all present and former members of the Luke lab for the great time spent together. Bettina, André, Lisa, Rebecca, Martina, Julia, René, Katharina, Vanessa K., Marco, Sarah, Steffi, Olga, Lara, Tina, Diego, Stefano, Matthias, Fabio, Simone, Vanessa P. and Natalie, thank you!

Special thanks go to Lara, Katharina, Vanessa, Tina and Olga for making the time in Mainz so fun and amazing!

I would like to thank Matteo for accompanying me throughout these years and for being part of my German adventure. Thank you for always being by my side.

Finally, I would like to thank my family for the never ending support and motivation, and my friends Alessandra, Chiara, Bea and Alessandro for always being there, even from far away.